**Royal Military Academy**

Signal and Image Centre

Brussels — Belgium

# Scatterometer Algorithm Review

Test Plan

Technical report no: RMA-SIC-020201

X. Neyt, P. Pettiaux, M. De Smet and M. Acheroy

May 7, 2003

ESA Study Manager: P. Lecomte
EUROPEAN SPACE AGENCY CONTRACT REPORT
The study was performed under ESA contract: 15183/01/I-LG.
Responsibility for contents resides in the author or organisation that prepared it.

# Contents

# Chapter 1

# Reference documents

[1] X. Neyt, P. Pettiaux, M. De Smet, and M. Acheroy. Scatterometer algorithm review for gyro-less operation. Technical Report RMA-SIC-011109, Royal Military Academy, December 2001.

# Part I

# Prototype test plan

# Chapter 2

# Introduction

This part describes the verification tests conducted on the prototype. The aim of these tests is to validate the prototype either against the existing wind scatterometer processor and its simulator, either against known reference sites such as the rain forest.

Altough the existing wind scatterometer processor will be used as reference, it should be noted that due to design and implementation differences, the results of both software might not be identical. Eventual differences shall be justified.

The testing of the prototype software is organized in two parts:

- internal tests, aiming at comparing internal results of the prototype agains internal results obtained from the existing wind scatterometer processor in general, and more precisely from the satellite simulator software.
- end-to-end tests, performed by comparing final products of the reference software and of the prototype. These tests will essentially confirm the correctness of the processing in the nominal cases.

It should further be noted that tests can only be performed where a reference is available. Be it the output of the existing software, or known ground true values.

# Chapter 3

# Test and validation data

## 3.1 Introduction

This chapter summarizes the data used for the testing and the validation of the prototype processor. For simplicity, each data set will be assigned a *short name* for later reference. The orbit number is taken at the ascending node crossing time.

## 3.2 Data acquired in Yaw Steering Mode

The yaw-steering mode is considered as having been perfectly obeyed by de spacecraft during acquisition. For these data sets, reference UWI files are made available for comparison purposes.

The following data set is considered as nominal.

| Short name | Orbit # | Time of first packet |
|---|---|---|
| YSM1 | 21704 | 15-JUN-1999 06:12:51.105 |
| YSM2 | 21705 | 15-JUN-1999 08:15:42.197 |
| YSM3 | 21706 | 15-JUN-1999 09:52:59.573 |
| YSM4 | 21707 | 15-JUN-1999 11:40:42.135 |
| YSM5 | 21708 | 15-JUN-1999 13:08:54.119 |
| YSM6 | 21709 | 15-JUN-1999 14:46:37.964 |
| YSM7 | 21710 | 15-JUN-1999 16:24:53.570 |
| YSM8 | 21711 | 15-JUN-1999 18:03:44.878 |
| YSM9 | 21712 | 15-JUN-1999 19:43:05.487 |

Table 3.1: Data acquired in YSM

Since the products in the YSM1 data set are discontinuous, this data set had to be discarted for some of the tests, for technical reasons.

The following datasets were also acquired in YSM, but exhibit specific artefacts.

| Short name | Orbit # | Time of first packet |
|---|---|---|
| KP | 19724 | 27-JAN-1999 22:31:06.046 |
| iqimbalance | 23897 | 15-NOV-1999 11:34:14.501 |
| arcing | 27352 | 13-JUL-2000 20:00:22.063 |
| calibration | 21134 | 06-MAY-1999 10:48:42.287 |

Table 3.2: Data acquired in YSM – data set with specific artefacts

## 3.3 Data acquired in Fine Pointing Mode

The find pointing mode is considered as having been perfectly obeyed by the spacecraft during the acquisition of these orbits.

| Short name | Orbit # | Time of first packet |
|---|---|---|
| FPM1 | 26714 | 30-MAY-2000 06:12:50.038 |
| FPM2 | 26715 | 30-MAY-2000 08:15:40.126 |
| FPM3 | 26716 | 30-MAY-2000 09:53:42.750 |
| FPM4 | 26717 | 30-MAY-2000 11:40:39.921 |
| FPM5 | 26718 | 30-MAY-2000 13:08:54.171 |
| FPM6 | 26719 | 30-MAY-2000 14:46:36.947 |
| FPM7 | 26720 | 30-MAY-2000 16:24:45.583 |
| FPM8 | 26721 | 30-MAY-2000 18:03:42.039 |
| FPM9 | 26722 | 30-MAY-2000 19:45:56.894 |

Table 3.3: Data acquired in FPM

## 3.4 Data acquired in Zero Gyro Mode

| Short name | Orbit # | Time of first packet |
|---|---|---|
| ZGM1 | 32727 | 24-JUL-2001 08:09:13.942 |
| ZGM2 | 32729 | 24-JUL-2001 11:30:10.749 |
| ZGM3 | 32726 | 24-JUL-2001 06:12:11.301 |
| ZGM4 | 32728 | 24-JUL-2001 09:53:43.266 |
| ZGM5 | 32730 | 24-JUL-2001 13:08:15.991 |
| ZGM6 | 32732 | 24-JUL-2001 16:24:09.198 |
| ZGM7 | 32733 | 24-JUL-2001 18:03:12.100 |
| ZGM8 | 32734 | 24-JUL-2001 19:42:26.893 |

Table 3.4: Data acquired in ZGM

Data acquired over the Brazilian rain forest.

| Short name | Orbit # | Time of first packet |
|---|---|---|
| RFGS1 | 32738 | 25-JUL-2001 02:18:57.636 |
| RFGS2 | 32795 | 29-JUL-2001 01:53:12.037 |
| RFGS5 | 32752 | 26-JUL-2001 01:47:13.061 |
| RFGS6 | 32781 | 28-JUL-2001 02:24:25.022 |
| RFKS1 | 32731 | 24-JUL-2001 14:46:00.193 |
| RFKS2 | 32745 | 25-JUL-2001 14:15:17.563 |
| RFKS3 | 32774 | 27-JUL-2001 14:51:34.812 |
| RFKS4 | 32788 | 28-JUL-2001 14:20:53.034 |

Table 3.5: Data acquired in ZGM over the rain forest

# Chapter 4

# Internal tests

## 4.1 Introduction

These tests are meant to test the prototype internal functions (satellite simulator, wind extraction). For convenience reasons, these tests are performed using as much as possible the nominal processor input and output interfaces.

These tests being performed against look-up tables obtained from the SSS, the same configuration as the SSS should be used for the prototype, as far as possible. In particular, the same state vectors should be used.

## 4.2 Normalization coefficient comparison

### 4.2.1 Test objective

Verify the computation of the normalization coefficient. This also verifies the computation of some aspects of the acquisition geometry (incidence angle, range).

### 4.2.2 Test procedure

The test will consist in comparing the normalization coefficient table issued by the satellite simulator with value obtained from the prototype.

In order to have comparable results, the yaw angle estimation routines were disabled in the prototype.

### 4.2.3 Success criterions

The results should be the same. A difference of TBD % is acceptable.

Eventual differences might be due to

- different approximations used in solving the range equation
- difference between the state vectors used for the computation of the LUT and the actual state vectors used by the prototype

### 4.2.4 Test data

This test will require the following data

- orbit state vectors of the selected orbit(s)
- the normalization coefficient LUT corresponding to the selected orbit(s)
- other auxiliary data (antenna mounting angles, antenna pattern, ...)

### 4.2.5 Results

The figure 4.1 shows the normalization factors computed by the prototype processor and the normalization factor from the LUT used by the original processor. The small differences noticeable for the Mid-beam around the peak values of the normalization factor are probably due to a difference in the antenna pattern used to compute the normalization factor. The across-track cut shows a good agreement. There is however a discrepancy at near-range for the Fore and Aft beams.

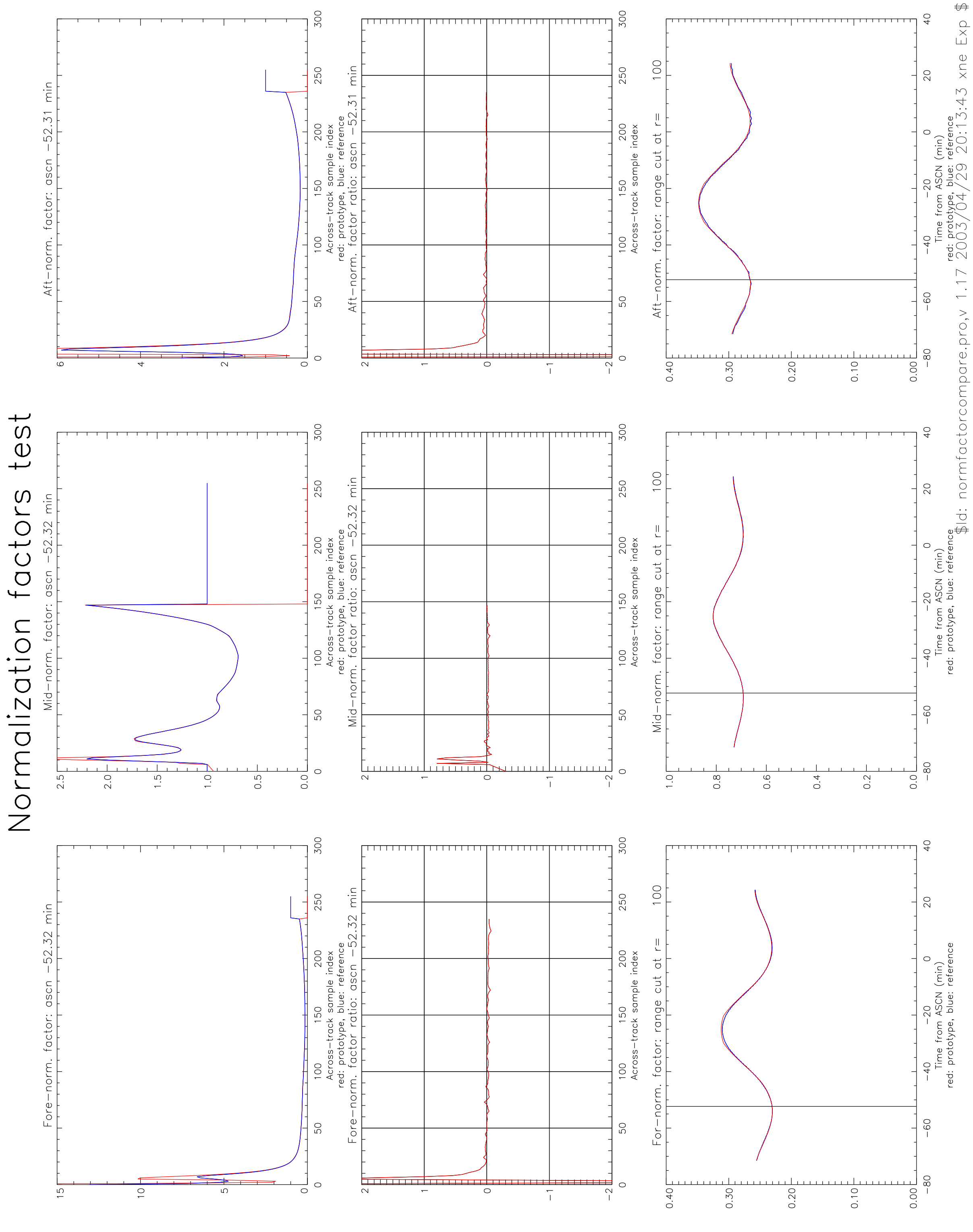


Figure 4.1: Normalization factor comparison graph

## 4.3 Residual Doppler phase comparison

### 4.3.1 Test objective

Verify the computation of the on-ground residual Doppler compensation. This also verifies some aspects of the acquisition geometry (target location on the Earth, relative velocity of the spacecraft wrt the Earth target). It also checks that the on-board Doppler compensation is correctly taken into account.

### 4.3.2 Test procedure

The test will be performed by comparing the phase look-up-table used in the current ground processor with the computations performed using the prototype.

In order to have comparable results, the yaw angle estimation routines were disabled in the prototype.

### 4.3.3 Success criterions

The results should be the same. A difference of TBD $(rad)$ is acceptable.

Larger differences might be due to

- a difference in the computation of the on-board Doppler frequency shift, where the prototype uses the actual value returned by the spacecraft.
- difference between the state vectors used for the computation of the LUT and the actual state vectors

### 4.3.4 Test data

This test will require the following data

- orbit state vectors of the selected orbit(s)
- the on-ground Doppler phase compensation LUT corresponding to the selected orbit(s)
- other auxiliary data (antenna mounting angles, ...)

### 4.3.5 Results

The figure 4.2 shows the residual Doppler phase respectively computed by the prototype processor and obtained from the LUT used in the original processor. It should be noted that constant phase differences result in a unit-norm phase rotation applied to the signal. This unit-norm phase rotation has no impact on the actual signal power. Hence a constant phase difference across-track is acceptable. Moreover, the same reasoning leads to the conclusion that the along-track continuity of the Doppler phase is incidental. This explains the strange behaviour of the reference residual Doppler phase between -40 and -20 min from ASCN.

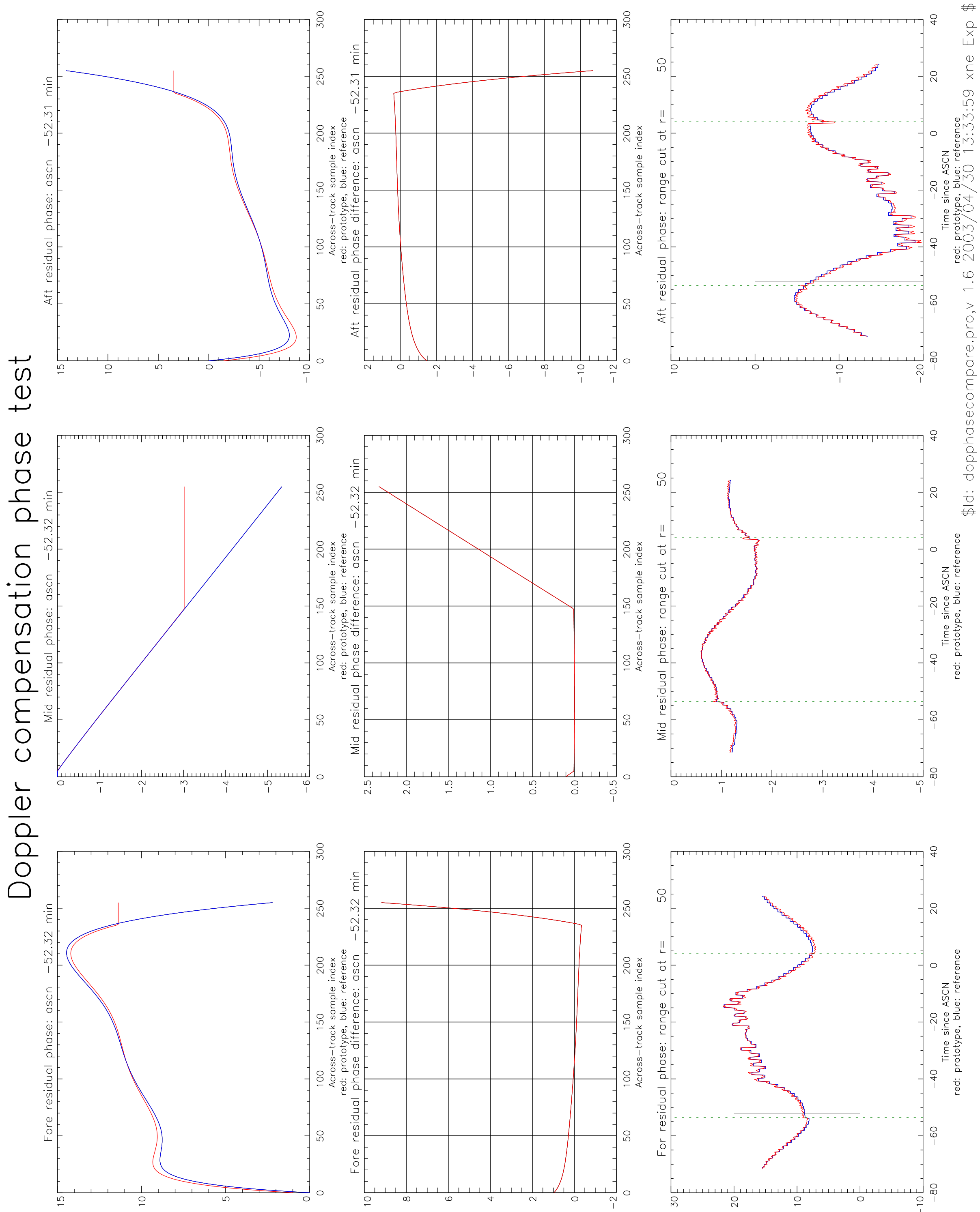


Figure 4.2: Residual Doppler phase comparison graph

## 4.4 CMOD4 Wind extraction routine

### 4.4.1 Test objective

Verify the correctness of the wind solutions provided by the wind extraction routines.

### 4.4.2 Test procedure

The wind amplitude and direction will be extracted from $\sigma^o$ values comming from the reference UWI files. The obtained wind solutions will be compared to the wind solutions found in the same reference UWI file.

The wind solutions that is closest in direction to the reference wind will be considered for the comparison. The comparison points will be

- the wind direction
- the wind speed
- the euclidean distance from the CMOD4-model

### 4.4.3 Success criterions

The test will succeed if the euclidean distance of the extracted winds is smaller that the euclidean distance of the reference winds. Positive differences between the euclidean distance of respectively the reference winds and the extracted winds smaller than the step precision of the iterative extraction algorithm are also acceptable.

### 4.4.4 Test data

The following test data was considered

- the data from orbits acquired in YSM (YSM1 trough YSM9)

### 4.4.5 Results

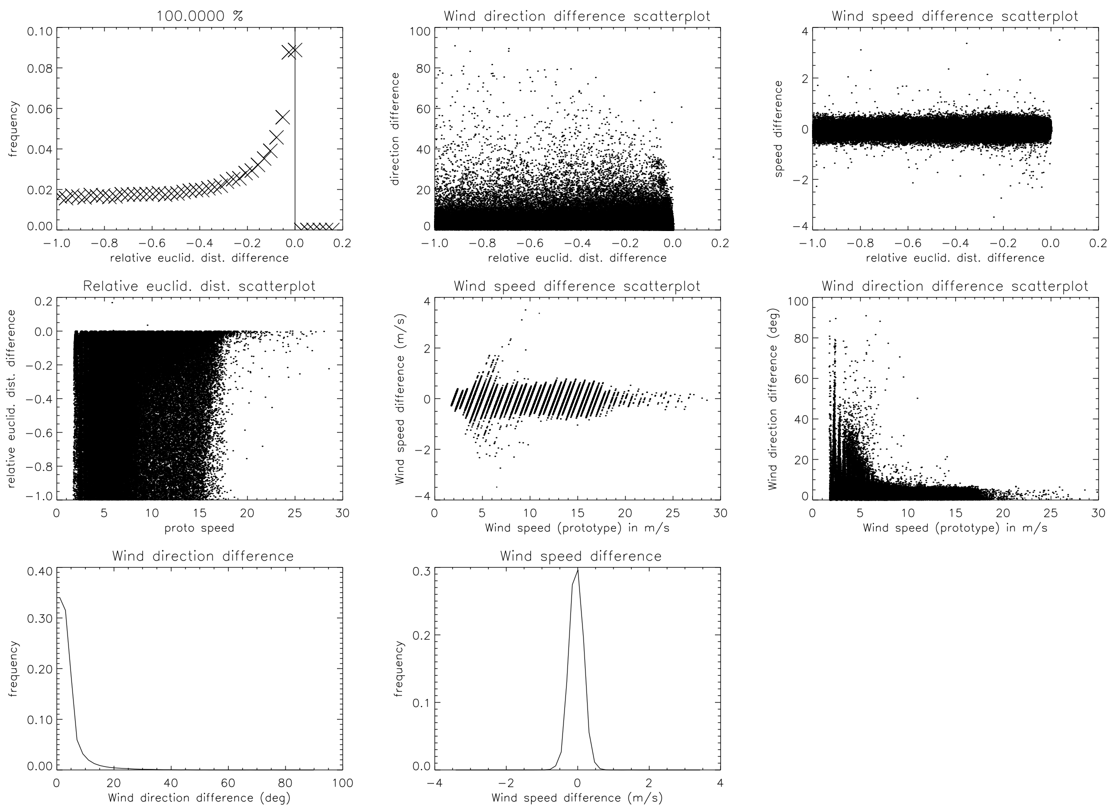


Figure 4.3: Report for the wind extraction

The graphs are plotted in function of the *relative* euclidean distance difference defined as $\frac{\Delta\varepsilon}{\varepsilon_{ref}}$. Since the ratio betwee the euclidean distance of the reference winds and of the extracted winds can be up to an order of magnitude, the relative euclidean distance can be as high as 1.

The relative euclidean distance is mostly negative, confirming the efficiency of the precision wind extraction.

# Chapter 5

# End-to-end tests

## 5.1 Introduction

These tests are to be run with a full-featured processing chain. This will generally require the availability of

- the necessary input data (source packets), preferably in the EWIC format
- auxiliary data such as the orbit state vectors, the ADC-related LUT, the antenna-pattern related LUT, calibration information where applicable
- output data (UWI files)

When comparisons are to be performed between the prototype and the current processor, these data shall be the same. Unless explicitely mentionned, these data are nominal data. In particular, the input data is to have been acquired in nominal Yaw Steering Mode.

## 5.2 Yaw estimation test

### 5.2.1 Test objective

Validate the yaw estimation routines.

### 5.2.2 Test procedure

The prototype will process nominal (YSM) orbits and non-nominal orbits with known yaw (FPM). The estimated yaw angle will be compared with theoretical yaw.

### 5.2.3 Success criterions

The results should be the same. An angular difference of TBD degree is acceptable.
Large differences might be due to

- intrinsic limitation of the yaw-estimation routines, wich is known to be less-performant at large yaw angles
- pathologic behaviour of the backscattering coefficients, for instance in the presence of strong scatterers
- non-perfect yaw attitude of the spacecraft. This error however is supposed to be much smaller than item #1. Moreover, this error can be accounted for provided the real attitude data is available,

It is therefore suggested to adjust the acceptable difference to the yaw angle deviation. For large yaw angles, the acceptable difference should be larger than for small yaw angles. Moreover, the comparison is probably only meaningful over sea and should probably only be performed there.

### 5.2.4 Test data

The following test data will be considered

- one orbit acquired in YSM (YSM5)
- eight orbits acquired in FPM (FPM1–FPM8).

### 5.2.5 Results

#### 5.2.5.1 YSM orbit

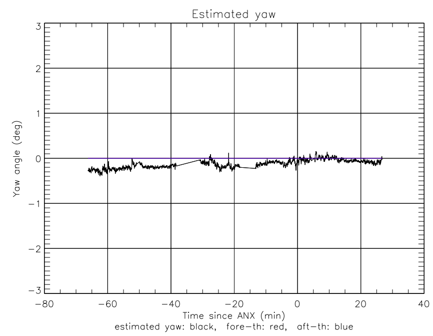


Figure 5.1: Report for YSM5

#### 5.2.5.2 FPM orbits

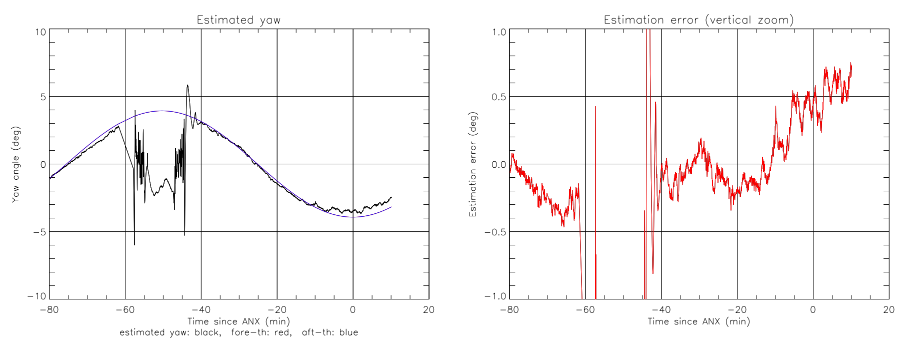


Figure 5.2: Report for FPM1

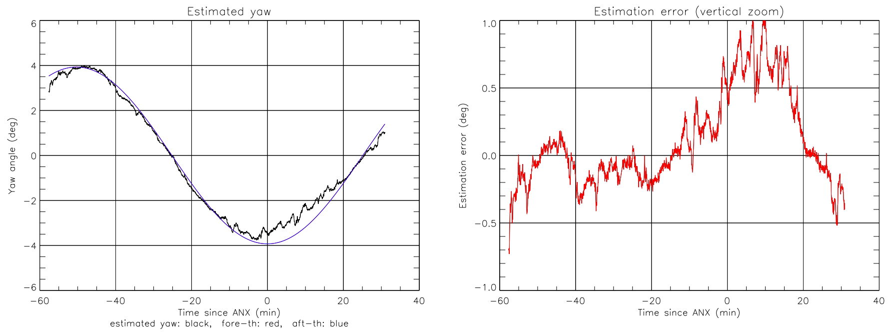


Figure 5.3: Report for FPM2

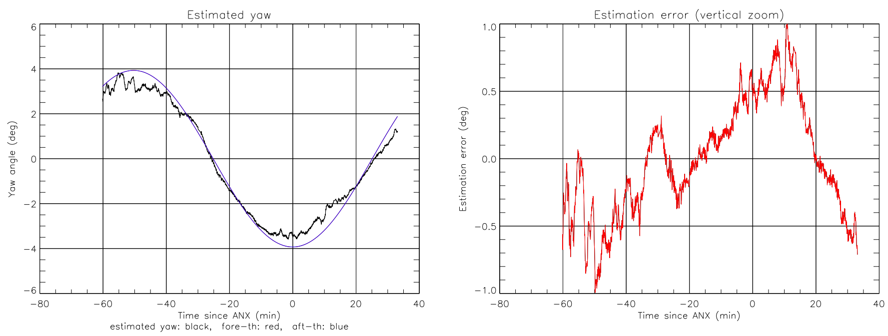


Figure 5.4: Report for FPM3

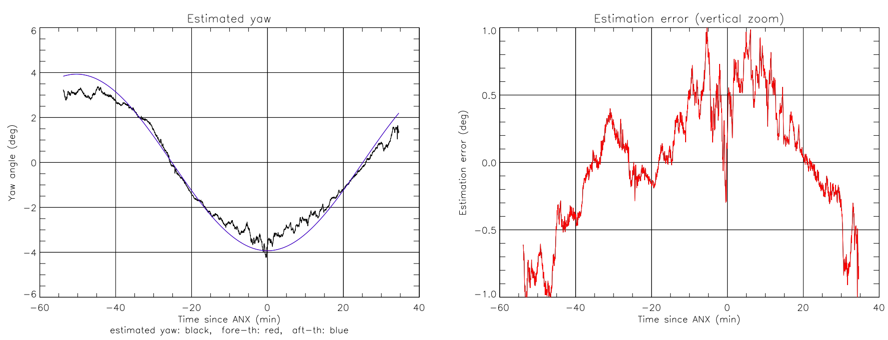


Figure 5.5: Report for FPM4

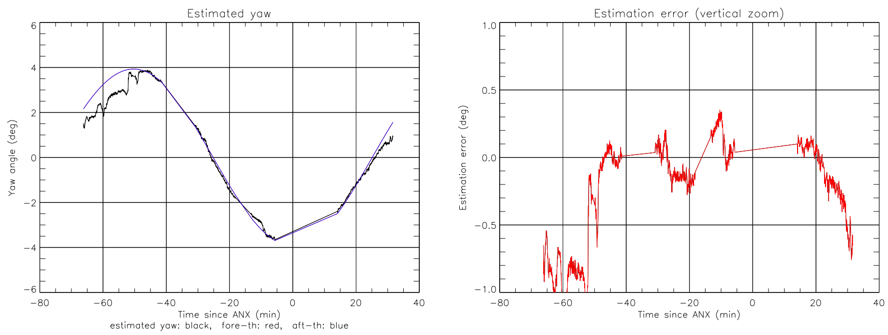


Figure 5.6: Report for FPM5

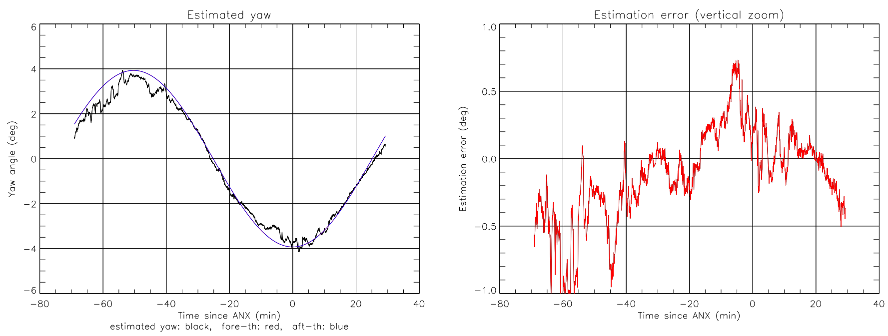


Figure 5.7: Report for FPM6

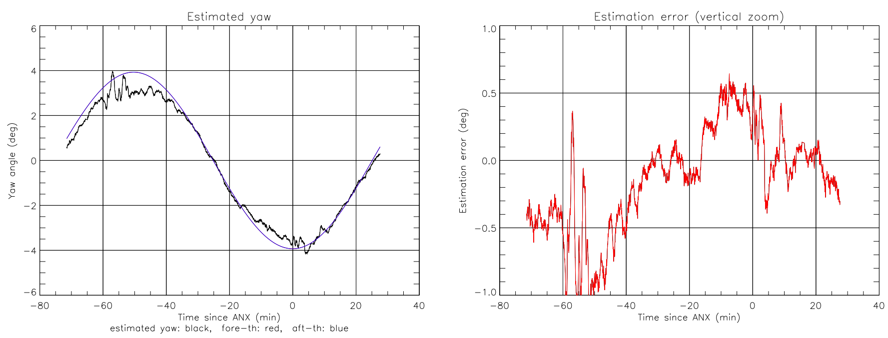


Figure 5.8: Report for FPM7

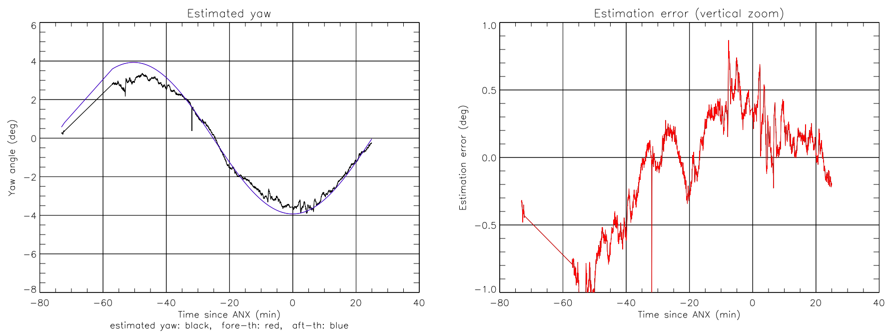


Figure 5.9: Report for FPM8

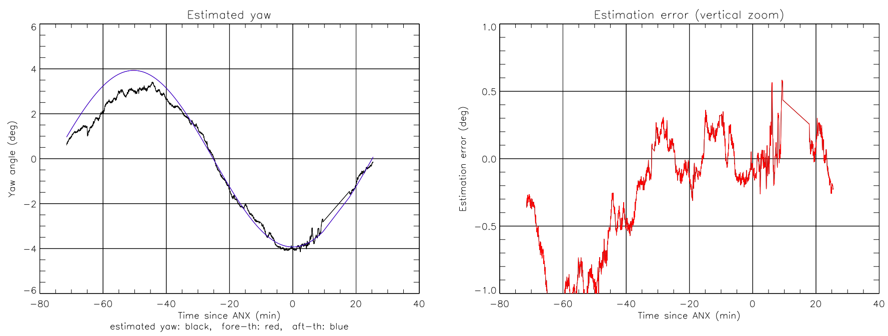


Figure 5.10: Report for FPM9

The graphs shows a good agreement between the theoretical value and the estimated value, as long as the yaw angle is small (smaller than 2 or 3 deg). For larger values, the yaw angle is underestimated.

## 5.3 Internal calibration monitoring comparison

### 5.3.1 Test objective

Assess the correctness of the internal calibration monitoring routines.

### 5.3.2 Test procedure

Compare the value of the internal calibration monitoring between the prototype and the current wind scatterometer processor. The comparison will be performed on data from a nominal orbit.

### 5.3.3 Success criterions

The value should be identical within TBD %. Larger differences might be due to a different along-track power averaging.

### 5.3.4 Test data

The following test data will be considered

- one orbit acquired in YSM (YSM5)

### 5.3.5 Results

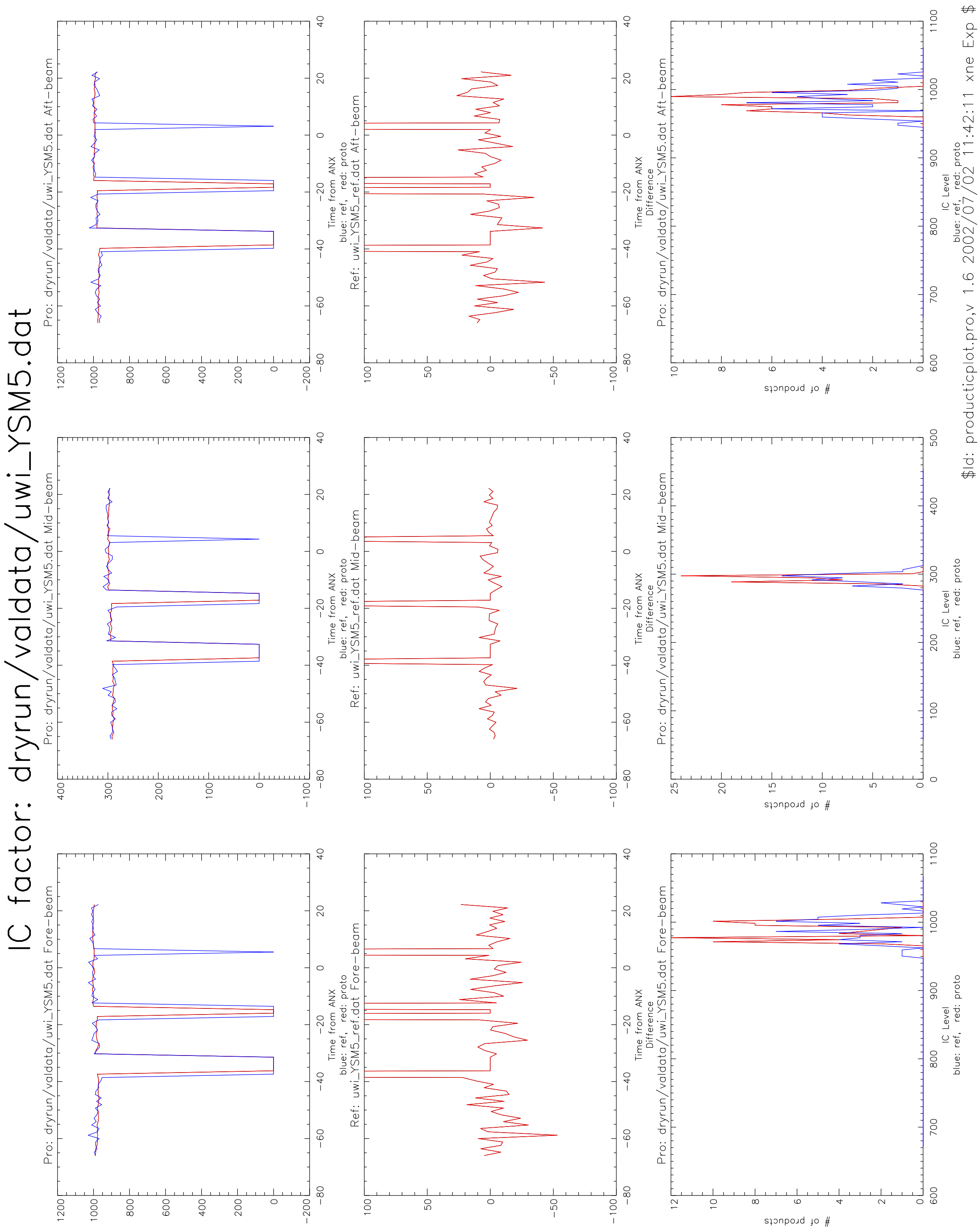


Figure 5.11: Report for YSM5

The Internal Calibration level reported by the prototype at UWI product level is computed as the average between the Internal Calibration level of all the valid nodes composing the product. The Internal Calibration level reported in the reference UWI product is probably the Internal calibration level of one of the nodes of the product. This explains that the Internal Calibration level reported by the prototype is smoother than the one obtained from the reference UWI file. This also explains the differences observed around data gaps. The prototype product will report a non-zero Internal Calibration level if at least one node out of the 361 nodes composing one product was valid.

## 5.4 Noise power monitoring comparison

### 5.4.1 Test objective

Assess the correctness of the noise power monitoring routines.

### 5.4.2 Test procedure

Compare the value of the noise power between the prototype and the current wind scatterometer processor. The comparison will be performed on data from a nominal orbit.

### 5.4.3 Success criterions

The value should be identical within TBD %.

### 5.4.4 Test data

The following test data will be considered

- one orbit acquired in YSM (YSM5)

### 5.4.5 Results

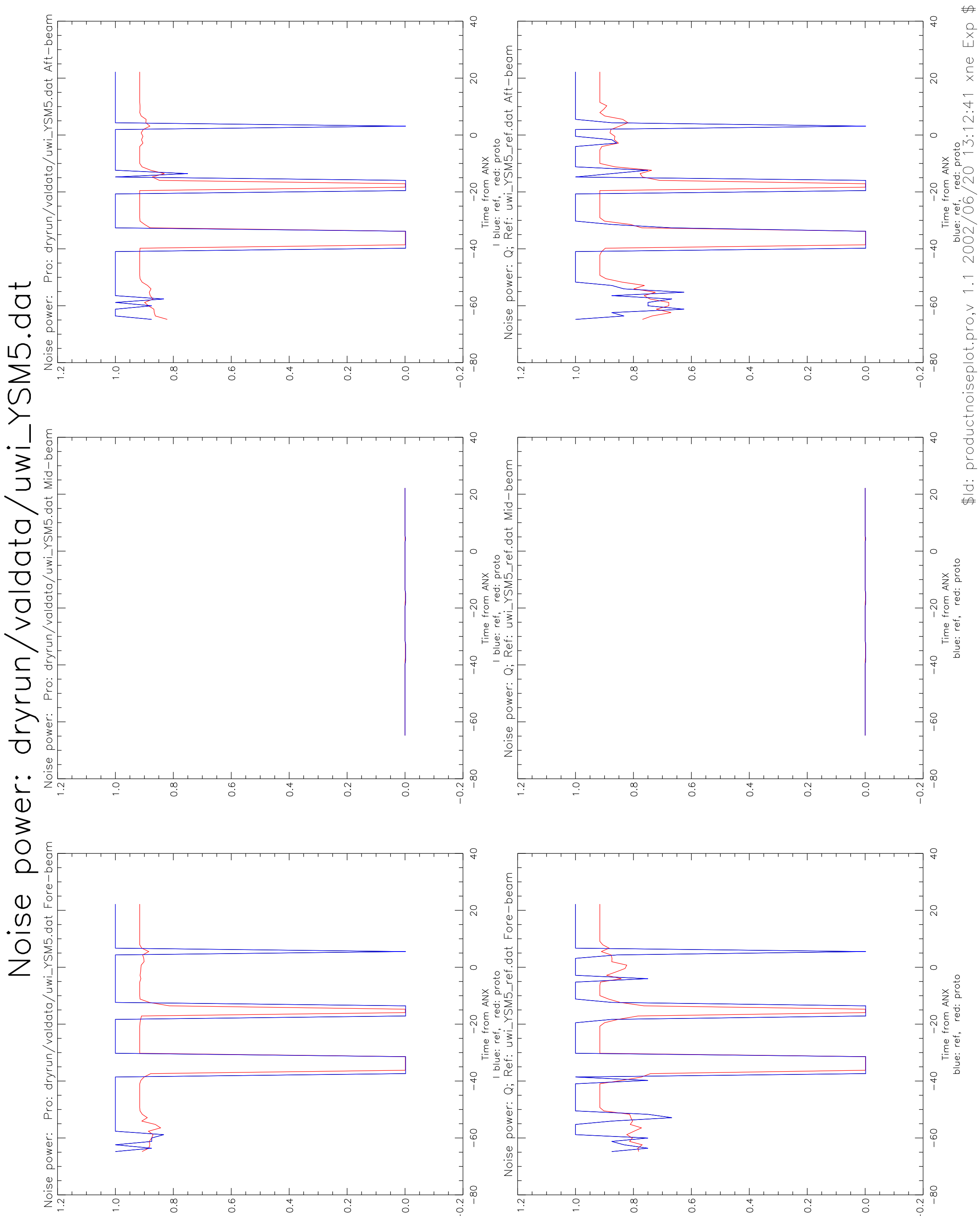


Figure 5.12: Report for YSM5

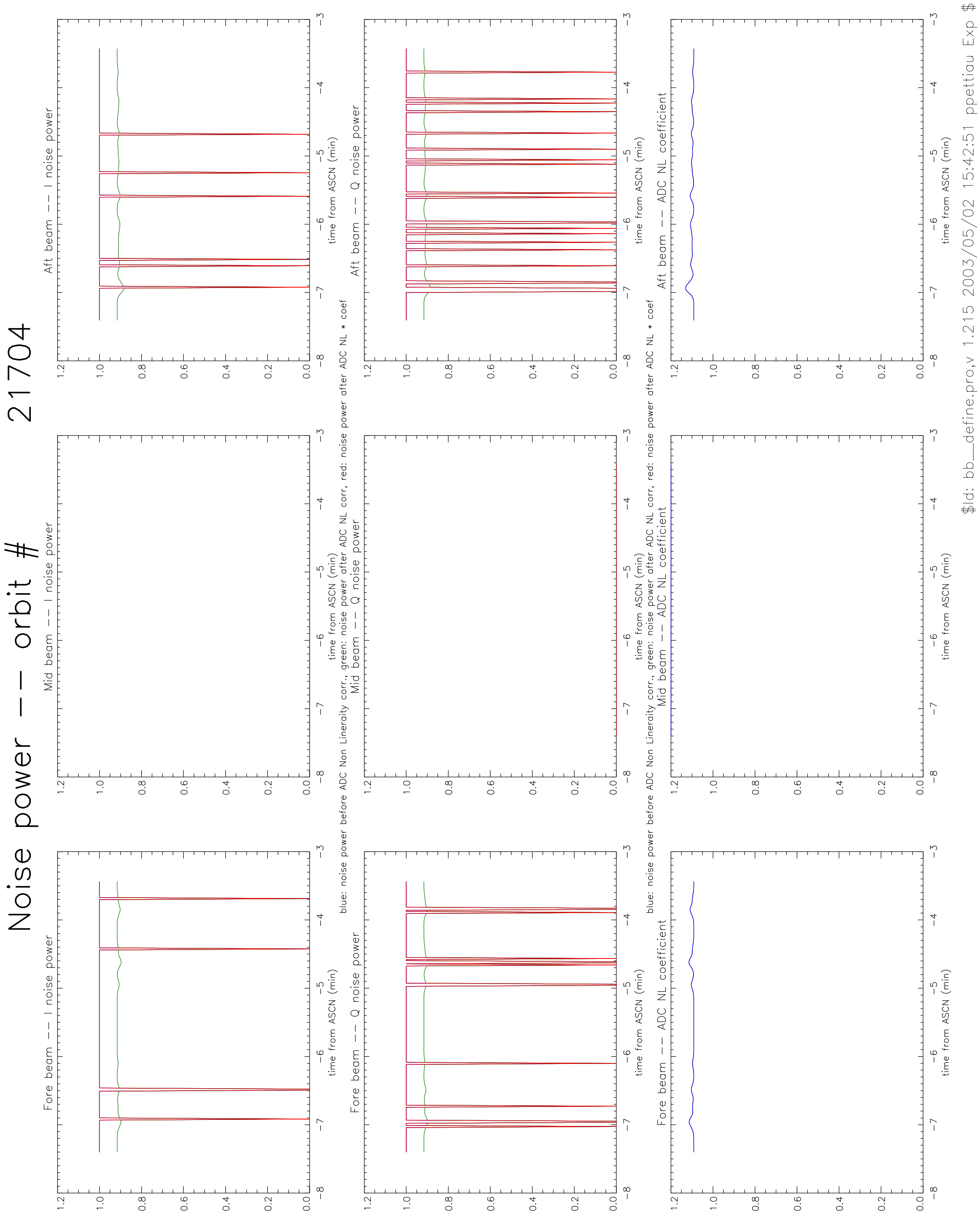


Figure 5.13: Detailed view of the noise power

A noise power level difference between the reference UWI file and the prototype can be seen on figure 5.12. This difference is due to the fact that the noise power is compensed for the non linearity of the on-board ADC. The corresponding compensation coefficient is plotted in the lower graphs of figure 5.13. The green line on the upper graphs of figure 5.13 are plots of the noise power after ADC non-linearity compensation. A coupling between the I and the Q channels can be noticed. That coupling comes from the fact that the compensation coefficient used for both channels is obtained from the total noise power ($I+Q$). The — invisible blue line — uncorrected noise power is equal to the corrected noise power multiplied by the ADC non-linearity correction coefficient.

## 5.5 Noise power flag comparison

### 5.5.1 Test objective

Assess the correctness of the noise power flagging routines.

### 5.5.2 Test procedure

Compare the value of the noise power flag between the prototype and the current wind scatterometer processor. The comparison will be performed on data from a nominal orbit.

### 5.5.3 Success criterions

The value should be identical.

### 5.5.4 Test data

The following test data will be considered

- one orbit of data, exhibiting noise power artefact (iqimbalance)

### 5.5.5 Results

| | UTC time of flagged products |
|---|---|
| Prototype | 15-NOV-1999 12:37:24.651 |
| Reference | 15-NOV-1999 12:37:24.651 |

Table 5.1: UTC time of the flagged UWI products

In the reference product, the per-product flag is set if and only if the central node is flagged. For the prototype product, the per-product flag is set if the mean noise power over the product is outside the threshold.

The figure 5.14 shows a plot around the time of the flagged reference product, of the values of the flags in more details.

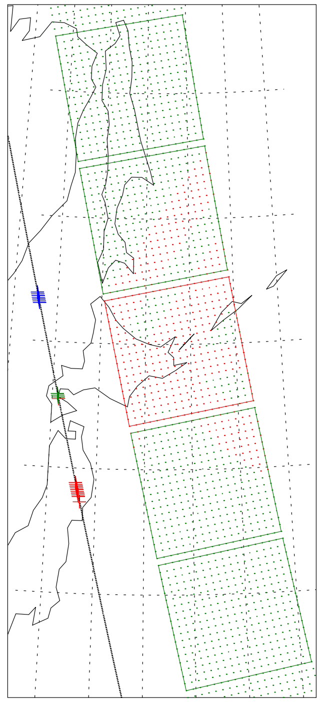


Figure 5.14: Plot of the noise power (I/Q imbalance) flags of the prototype products around the time of interest. The large red/green rectangles indicate, from the flag in the UWI product wether there was a noise power event inside the $19 \times 19$ nodes bloc. The red/green crosses indicate, from the ASPS 2.0 product wether there was a noise power event inside each of the nodes and the black line with red/green/blue (resp. fore/mid/aft beam) crosses indicate wether there was a noise power event inside one of the source packet.

## 5.6 Spectrum monitoring comparison

### 5.6.1 Test objective

Assess the correctness of the doppler compensation routines.

### 5.6.2 Test procedure

The values of the spectrum Center of Gravity will be compared between the current wind scatterometer processor and the prototype.

In order to be able to perform a meaningful comparison, the yaw estimation routine should be disabled in the prototype.

### 5.6.3 Success criterions

The value should be identical within TBD %.

Differences might be due to to the fact that a different Doppler frequency shift estimation algorithm was used.

### 5.6.4 Test data

The following test data will be considered

- the orbits acquired in YSM (YSM1 trough YSM9)

### 5.6.5 Results

The results for the other orbits are presented in appendix A.

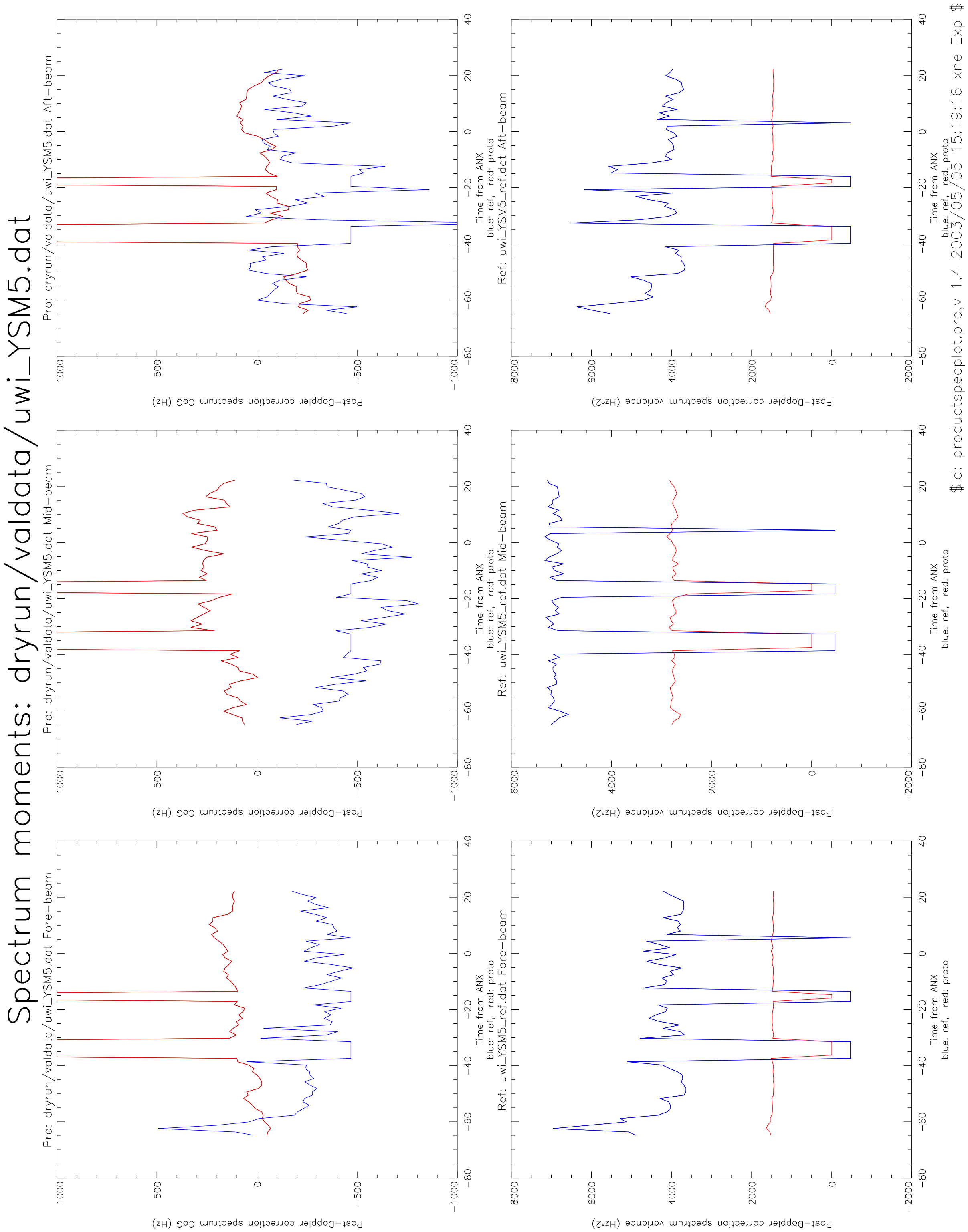


Figure 5.15: Report for YSM5

## 5.7 Arcing flag comparison

### 5.7.1 Test objective

Assess the correctness of the arcing-detection routines.

### 5.7.2 Test procedure

The value of the arcing flag will be compared between the current wind scatterometer processor and the prototype.

### 5.7.3 Success criterions

The value should be identical within TBD %.
Differences might be due to small differences in the node-sample appurtenance computation.

### 5.7.4 Test data

The following test data was considered

- one orbit of data, exhibiting arcing artefacts (arcing)

### 5.7.5 Results

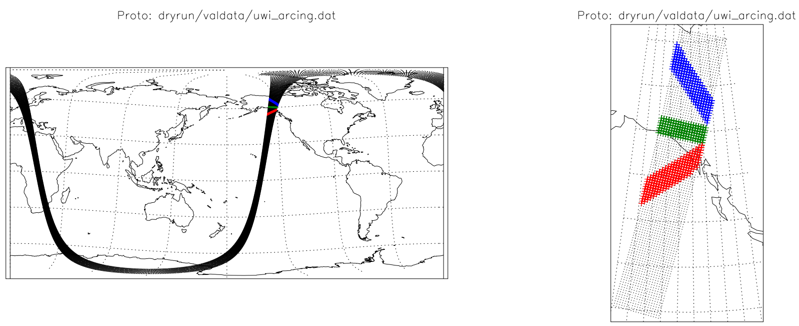


Figure 5.16: Prototype – report of arcing flag (whole orbit left, zoom at incident location right)

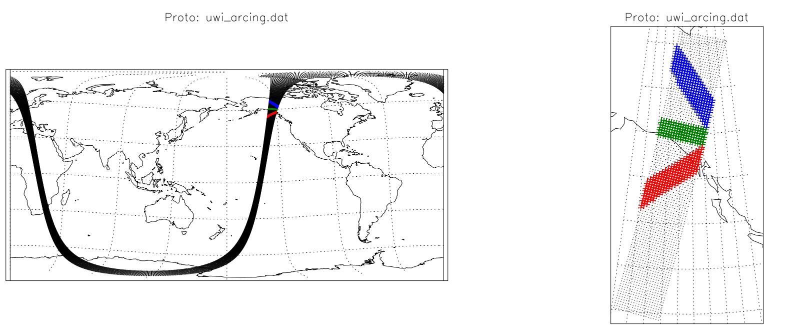


Figure 5.17: Reference – report of arcing flag (whole orbit left, zoom at incident location right)

## 5.8 Kp comparison

### 5.8.1 Test objective

Assess the correctness of the $k_p$ computation routines.

### 5.8.2 Test procedure

The values of $k_p$ will be compared between the current wind scatterometer processor and the prototype.

In order to be able to perform a meaningful comparison, the computation of $k_p$ with the current wind scatterometer processor should be done using the "statistical" method.

### 5.8.3 Success criterions

The value should be identical within TBD %.

### 5.8.4 Test data

The following test data will be considered

- the orbits specifically processed in the corresponding mode

### 5.8.5 Results

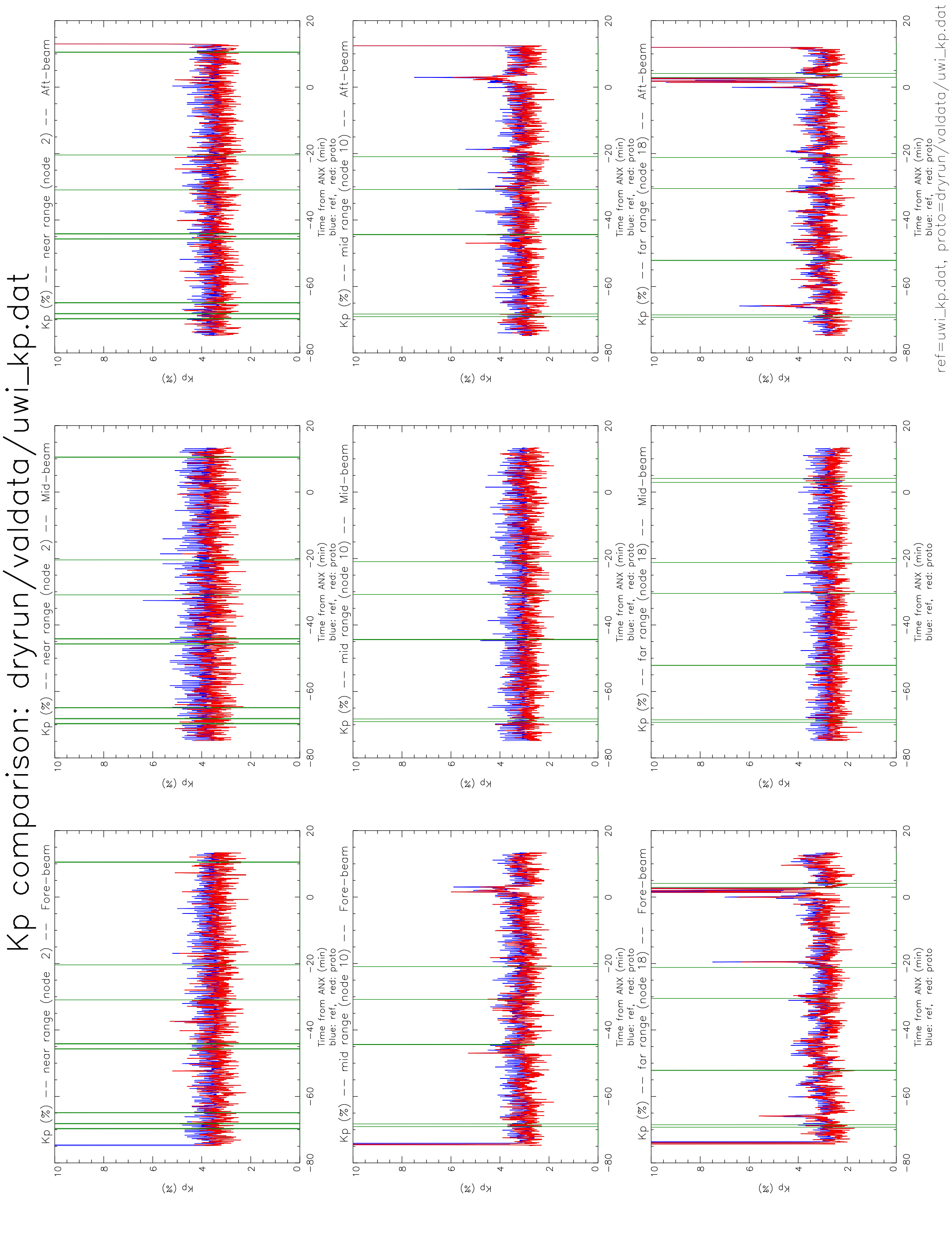


Figure 5.18: Report for KP

## 5.9 Calibration packets rejection

### 5.9.1 Test objective

Assess the correct rejection of calibration source packets.

### 5.9.2 Test procedure

An EWIC file containing calibration source packet will be processed. The output should exhibit blank nodes and blank products where calibration packets were found.

### 5.9.3 Success criterions

The output should exhibit blank nodes and blank products where calibration packets were found.

### 5.9.4 Test data

The following test data will be considered

- the orbit partially acquired in calibration mode (calibration)

### 5.9.5 Results

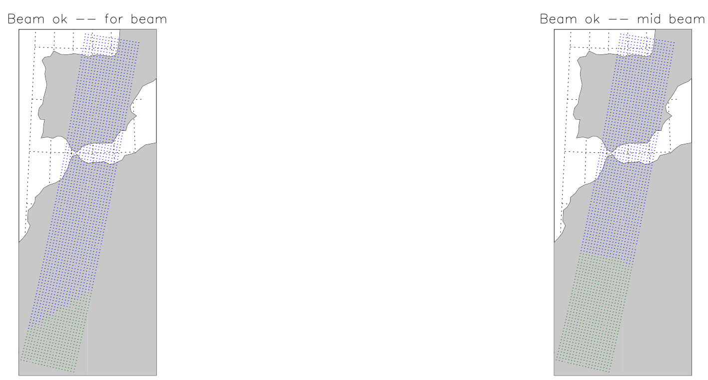


Figure 5.19: Beam ok flag for the Fore (left) and Mid (right) beams (green means the flag is not set)

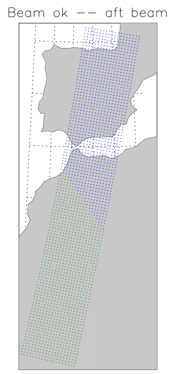

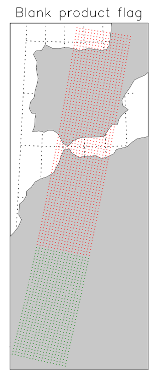


Figure 5.20: Beam ok flag for the Aft (left) beam (green means the flag is set) and blank product flag (right) — red means the flag is set.

As the graphs show and confirmed by debugging output from the prototype processor, the calibration packets are rejected.

## 5.10 Land/Sea flag comparison

### 5.10.1 Test objective

Assess the correctness of the land/sea determination routine.

### 5.10.2 Test procedure

Compare the Land/Sea flag at the nodes, both wrt the current wind scatterometer processor and wrt some other TBD reference.

### 5.10.3 Success criterions

The flag should match the reference. When compared with the flags generated by the current wind scatterometer, small differences might appear around land/sea transitions due to the different algorithm used.

### 5.10.4 Test data

The following test data will be considered

- one orbit acquired in YSM (YSM5)

### 5.10.5 Results

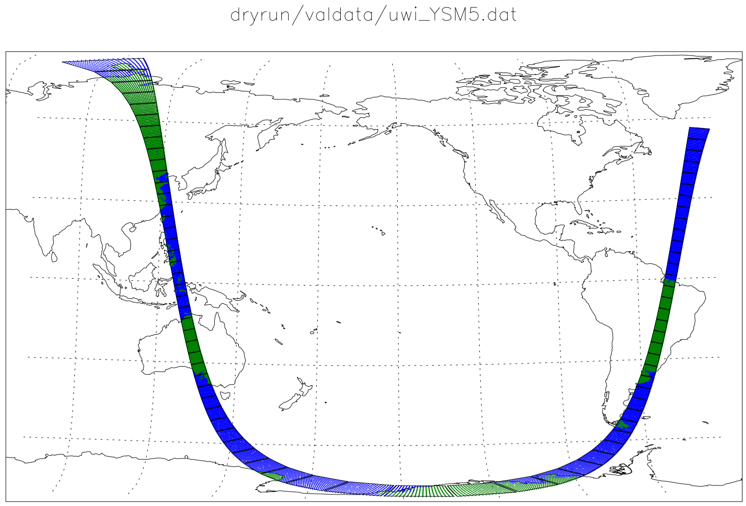


Figure 5.21: Land/sea flag for the considered orbit

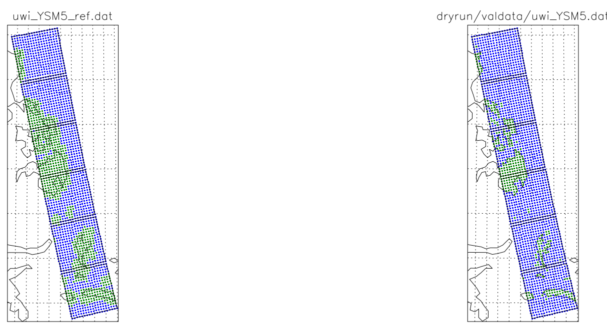


Figure 5.22: Zoom in over an area (right: prototype, left: reference)

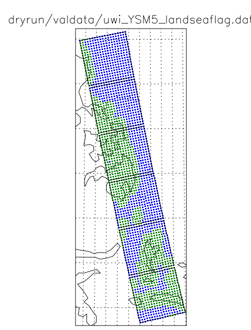


Figure 5.23: Land/sea flag assigned according to the percentage of land-samples contributing to the considered node. A node is flagged "land" if more than 15% of the samples that contribute to it are over land.

In its default mode, the prototype processor flags a node as land if the center of the node is over land. It can be configured to flag a node as land if a certain fraction of the contributing samples are over land.

## 5.11 Node location comparison

### 5.11.1 Test objective

Assess the correctness of the node-location determination routines. This will also verify some aspects of the acquisition geometry determination.

### 5.11.2 Test procedure

Compare the location of the nodes. The location of the nodes will be obtained from the output products. The test should be performed both with the yaw estimation routines enabled and disabled.

### 5.11.3 Success criterions

The location of the nodes should be identical. A difference of TBD km is acceptable.
Larger differences might be due to

- Small differences in the definition of the node location
- Quantization effects of the latitude/longitude value due to the insufficient resolution.

### 5.11.4 Test data

The following test data was considered

- the orbits acquired in YSM (YSM1 trough YSM9)
- the orbits acquired in ZGM (ZGM1 trough ZGM8)

### 5.11.5 Results

#### 5.11.5.1 YSM orbits

The results for the other orbits are presented in appendix B.

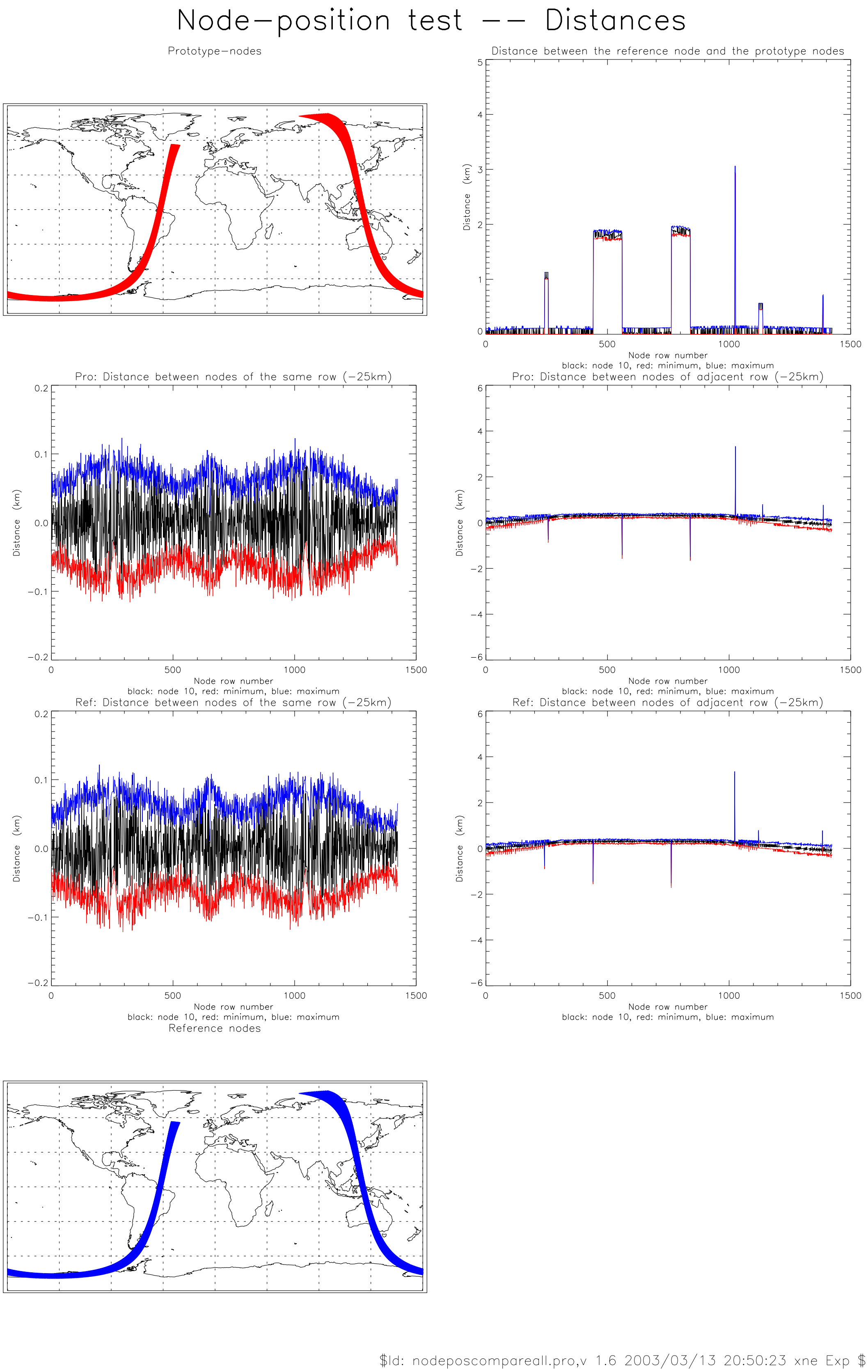


Figure 5.24: Report for YSM5

#### 5.11.5.2 ZGM orbits

The results for the other orbits are presented in appendix B.

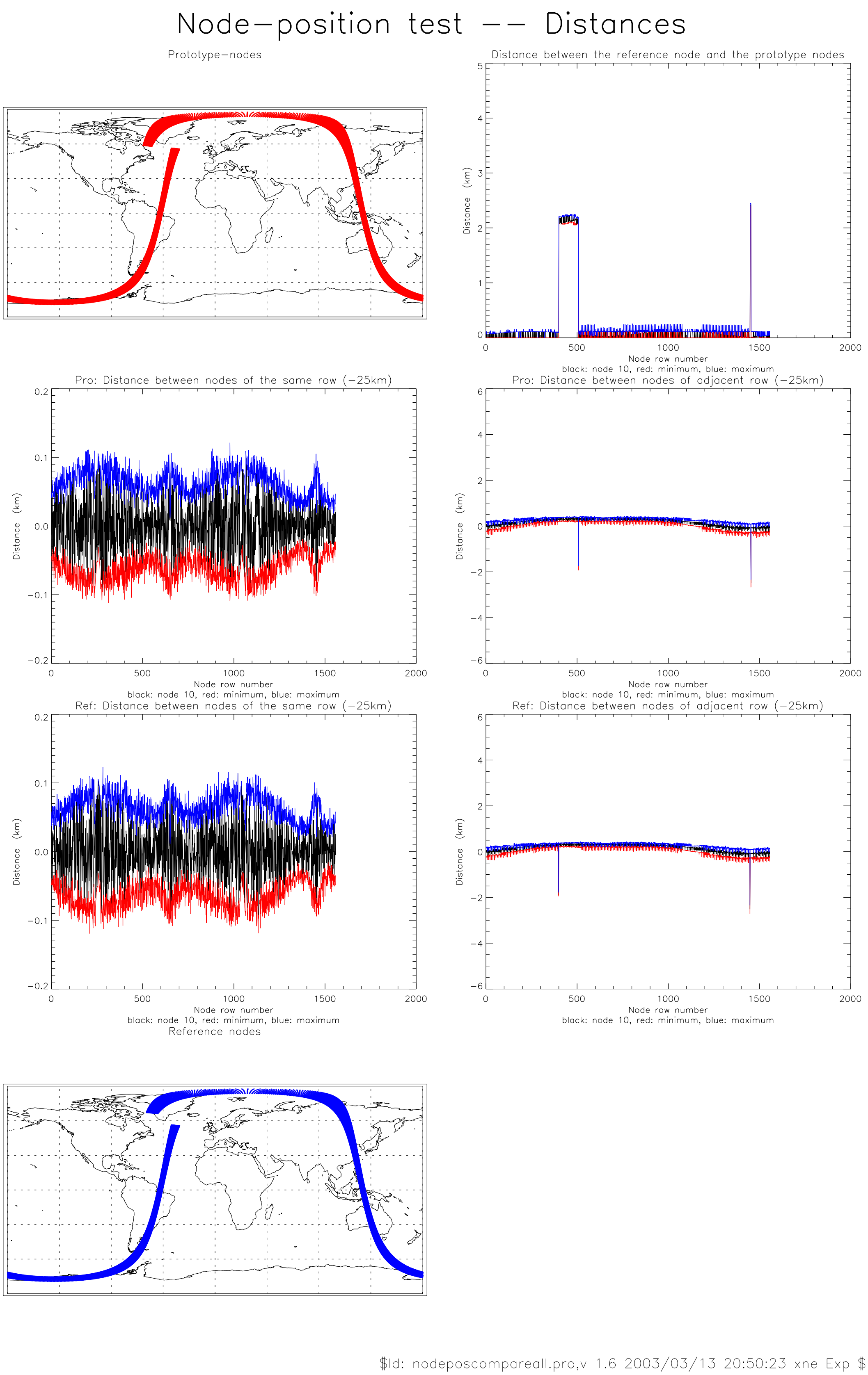


Figure 5.25: Report for ZGM5

Both graphs show that the node position difference is around 100m. This corresponds to the resolution at which the latitude and longitude of the nodes is given in the output products. The larger differences that can be seen within data gaps are due to a difference in reference position to which the node row is anchored. Within data gaps, the reference processor anchors the node rows to the first source packet available after the data gap, while the prototype processor anchors the node rows relatively to the last source packet available before the data gap. Since, by definition, there are no data within data gaps, the position of the nodes within these data gaps is of less importance.

## 5.12 Angle comparison

### 5.12.1 Test objective

Assess the correctness of the angle determination routines. This will also verify some aspects of the acquisition geometry determination.

### 5.12.2 Test procedure

Compare the incidence angle and the look angle at the node center and the subsatellite heading. These angles will be obtained from the output products. The test should be performed both with the yaw estimation routines enabled and disabled.

### 5.12.3 Success criterions

The incidence angle and the look angle should be identical. A difference of TBD deg is acceptable. Larger differences might be due to

- nearly empty nodes, in particular if there are no source packets contributing to the center of the node

### 5.12.4 Test data

The following test data were considered

- orbits acquired in YSM (YSM1 trough YSM9)

### 5.12.5 Results

The results for the other orbits are presented in appendix C.

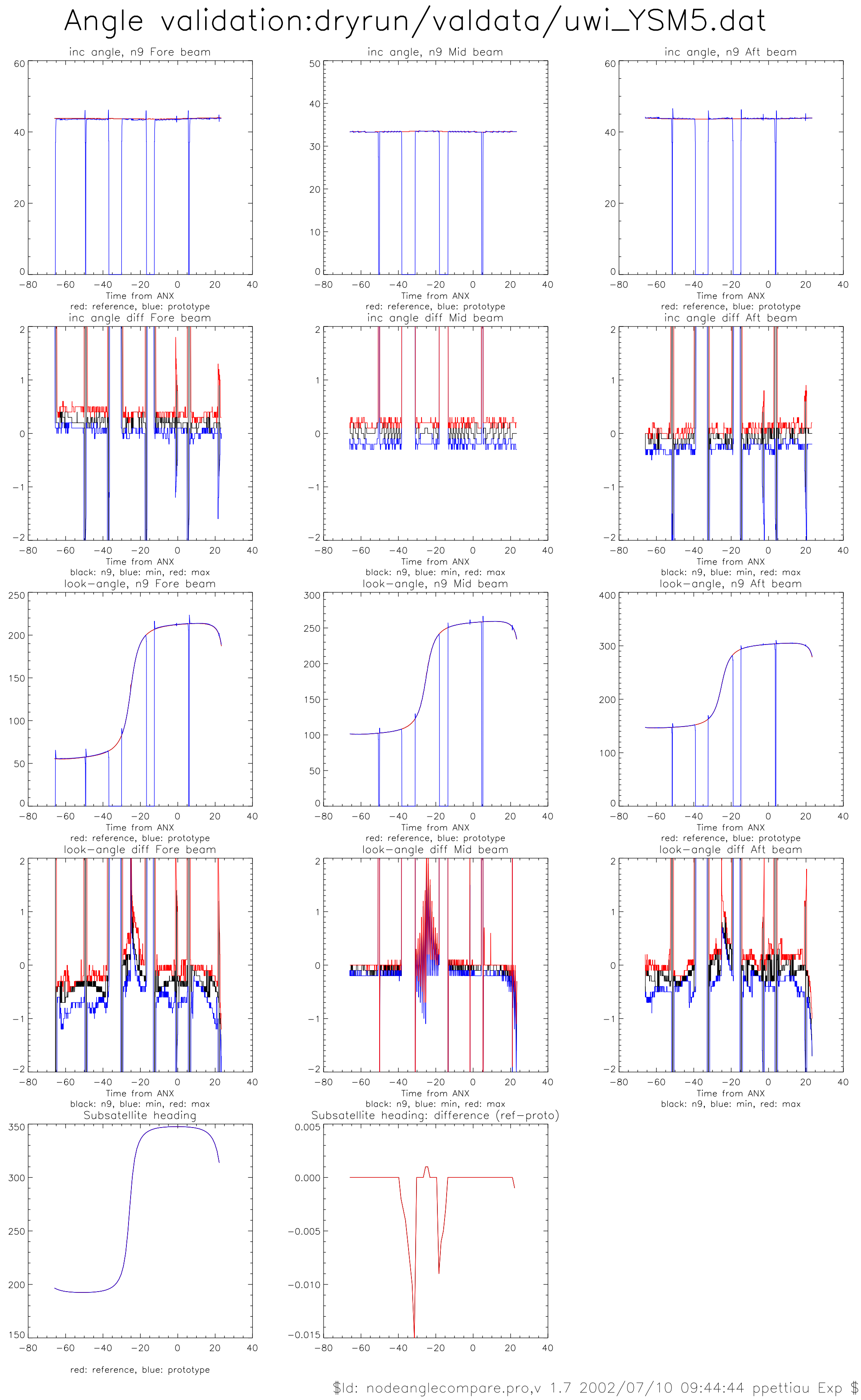


Figure 5.26: Report for YSM5

The difference in incidence angles lies withing $\pm 0.5^o$. Due to a varying yaw angle, the incidence angle at a node cannot be computed in advance. In stead, it is assigned as the incidence angle of the sample closest to the center of the node. This explains why the incidence angle is not defined within data gaps. It also explains the larger differences around the edges of the data gaps, where there are no samples near the center of the node.

The same remarks apply to the look angle and the the subsatellite heading, altough the heading is less variable and hence the differences are less noticeable.

## 5.13 Sigma 0 – nominal case

### 5.13.1 Test objective

Verify the radiometric performance of the prototype in nominal case.

### 5.13.2 Test procedure

The comparison of the $\sigma^o$will be performed along an orbit (or a piece of an orbit). This orbit might contain both wave gaps and larger gaps. Along that orbit, the spacecraft should be in Yaw Steering Mode.

### 5.13.3 Success criterions

The $\sigma^o$ value should be within TBD dB of the reference value. Larger differences might be allowed when the yaw is automatically estimated.

Larger differences might be measured near the large gaps due to the fact that the large gaps are bridged differently.

### 5.13.4 Test data

The following test data was considered

- the data from orbits acquired in YSM (YSM1 trough YSM9)

### 5.13.5 Results

The results for the other orbits are presented in appendix D.

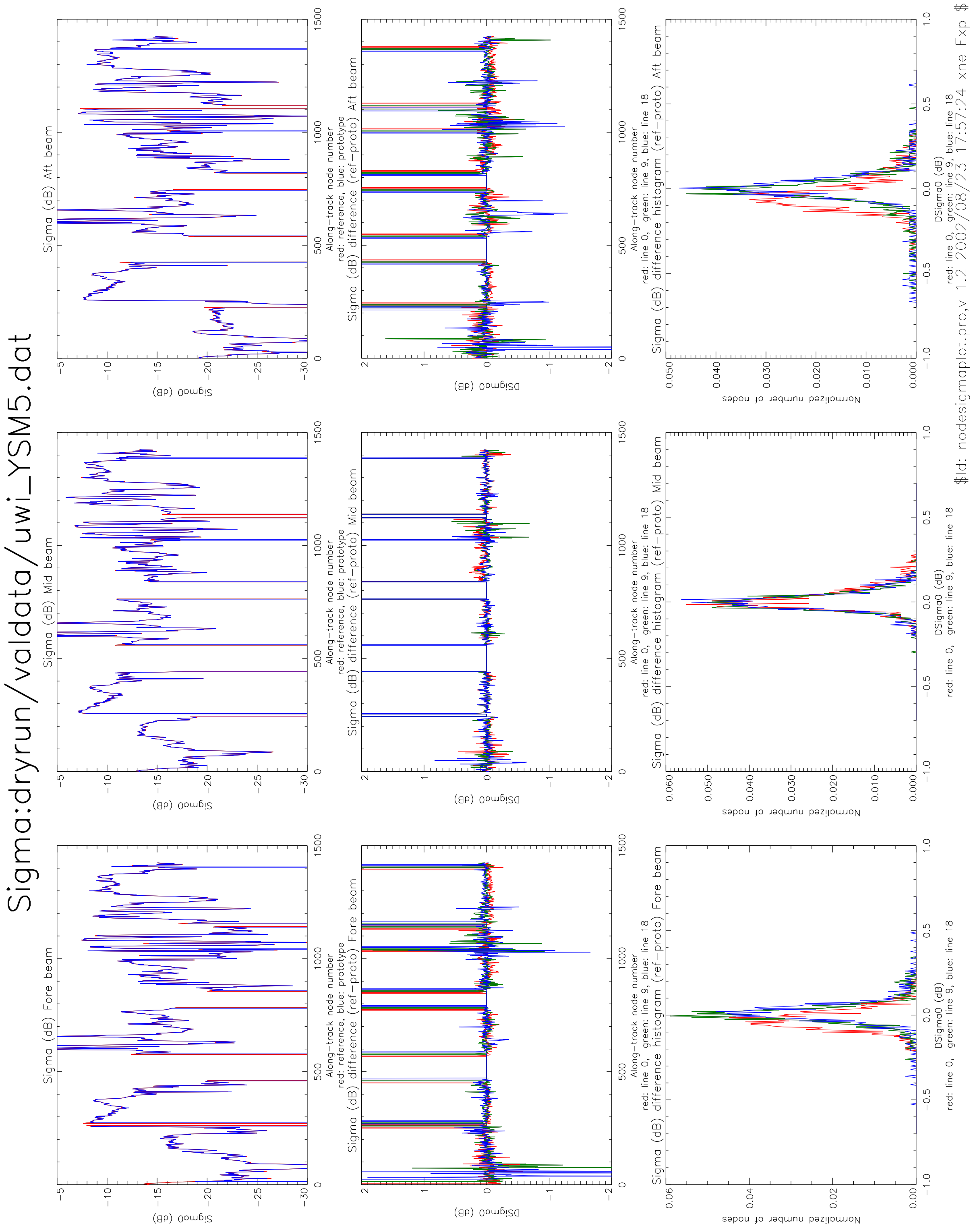


Figure 5.27: Report for YSM5

The graph below presents the biases between the reference $\sigma^o$ and the one obtained using the prototype processor. The biases are obtained by averaging the differences along one orbit for each node-number.

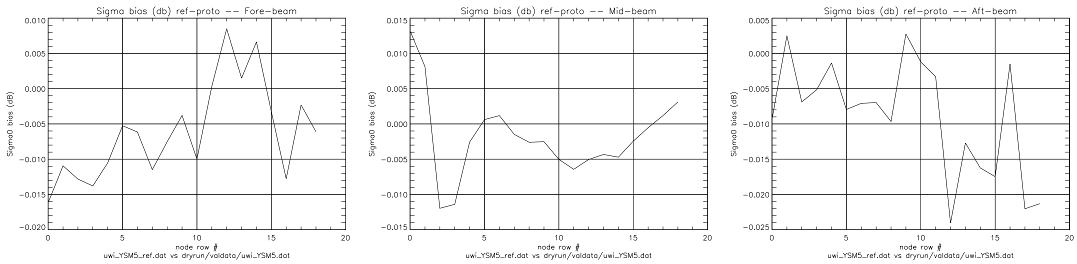


Figure 5.28: Bias for YSM5

## 5.14 Sigma 0 comparison over land

### 5.14.1 Test objective

Assess the performance of the processor in non-nominal case (non-yaw steering mode).

### 5.14.2 Test procedure

Orbits acquired in FPM and ZGM will be tested. The reference value will be the $\sigma^o$ value obtained from an orbit in YSM using the current wind scatterometer processor. Since the comparison will be performed on data acquired at different times, the comparison is meaningless over sea.

### 5.14.3 Test data

This test will require in addition to the already mentionned data, the following data

- one or several EWIC file containing data acquired in FPM, ZGM.
- the corresponding UWI files containing the node $\sigma^o$ values, obtained using the current processor with data acquired in YSM over the same area on ground.

### 5.14.4 Results

#### 5.14.4.1 Comparison of YSM and FPM orbits

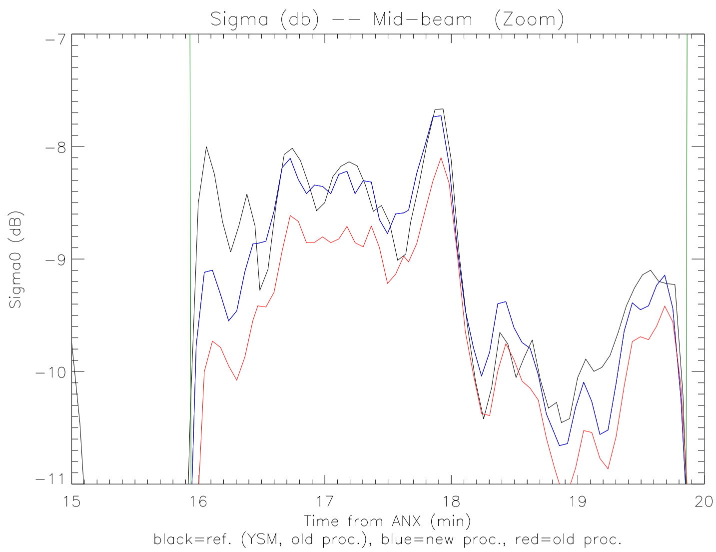


Figure 5.29: Comparison of an FPM orbit processed with and without yaw estimation.

Figure 5.29 shows a comparison of the along-track Mid-beam $\sigma^0$ value over land between YSM-data, and FPM data, these having been processed with and without yaw-related corrections. As can be seen the yaw estimation allows to gain a correct estimate of the true $\sigma^0$ (in blue) to be compared with the incorrect value obtained without performing any yaw-related correction (in red). Moreover, the new estimate is closer to the geophysical signature. This is due to the correct compensation of the residual Doppler frequency shift, which centers the received spectrum inside the pass-band of the on-ground low-pass processing filter.

#### 5.14.4.2 FPM orbits

The results for the other orbits are presented in appendix E.

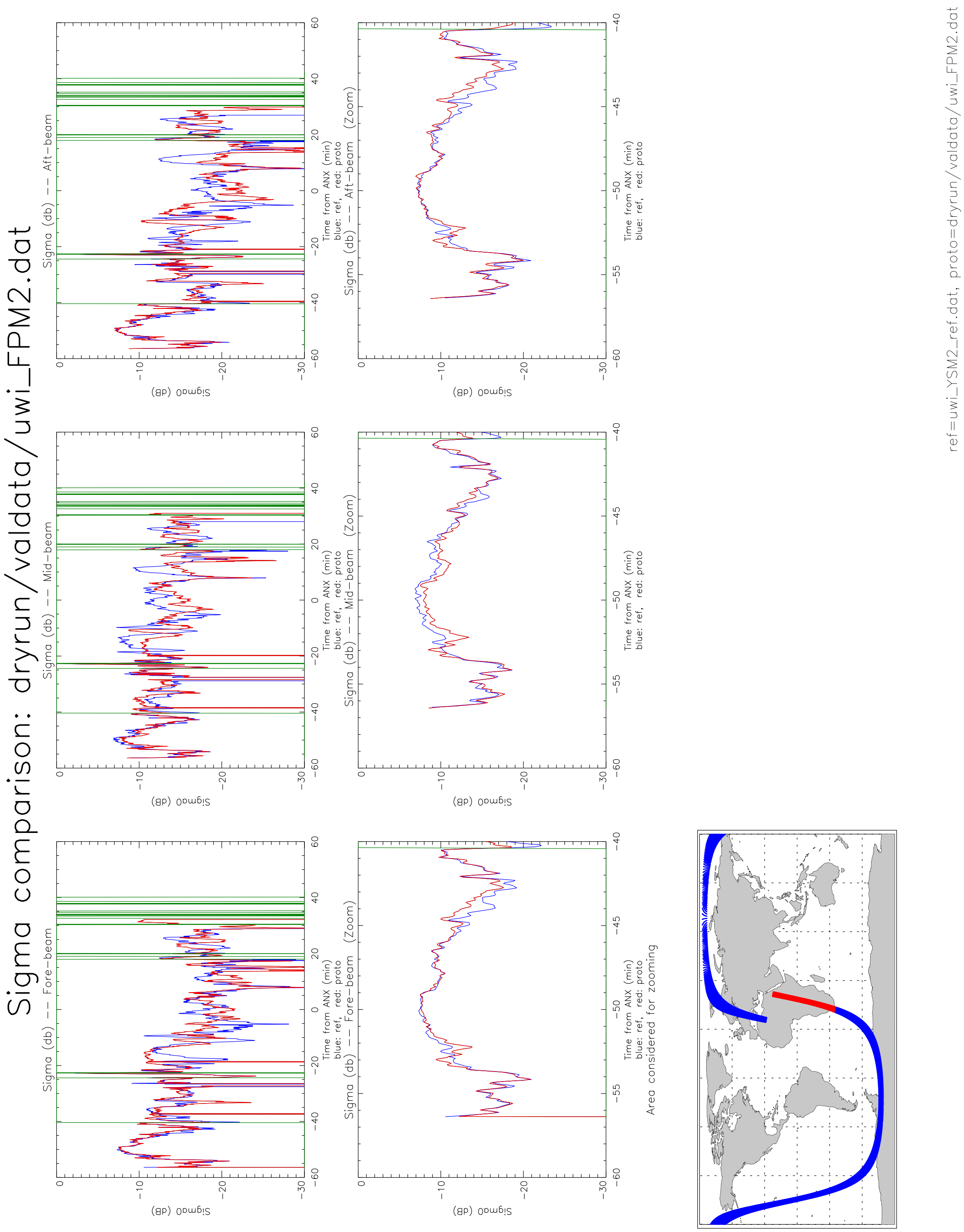


Figure 5.30: Report for YSM2/FPM2 comparison

#### 5.14.4.3 ZGM orbits

The results for the other orbits are presented in appendix E.

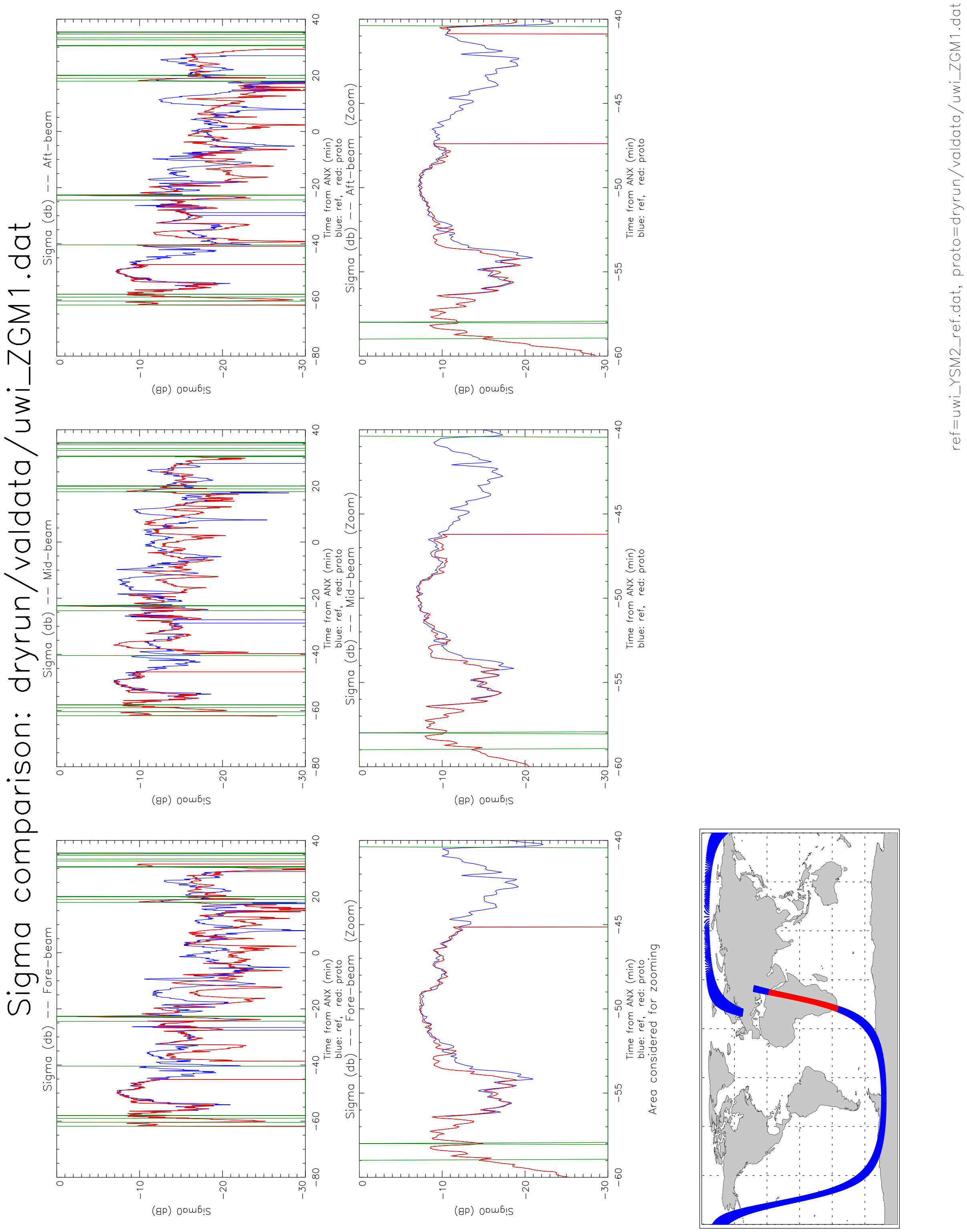


Figure 5.31: Report for YSM2/ZGM1 comparison

## 5.15 Radiometric validation

### 5.15.1 Test objective

Assess the radiometric performance of the processor in non-nominal case (non-yaw steering mode).

### 5.15.2 Test procedure

The $\gamma^o$ will be computed over the rain forest. This value should be independent of the incidence angle and hence the $\gamma^o$ value should be constant.

A histogram of the $\gamma^o$ will be computed and its center and maximum values computed.

To assess the performance of the yaw correction, the comparison is performed with and without yaw estimation.

### 5.15.3 Success criterions

The histograms should be independent of the beam considered. The standard deviation of the histogram obtained on data computed using yaw estimation should also be smaller. Moreover, the $\gamma^o$ should be independent of the incidence angle.

### 5.15.4 Test data

This test will require in addition to the already mentionned data, The following tests data were considered

- data acquired in ZGM over the rainforest (RFKS and RFGS)

### 5.15.5 Results

#### 5.15.5.1 Yaw angle evolution

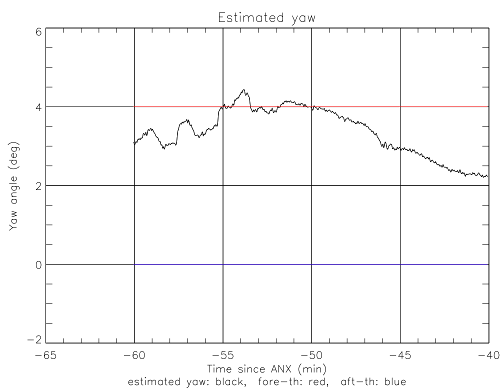


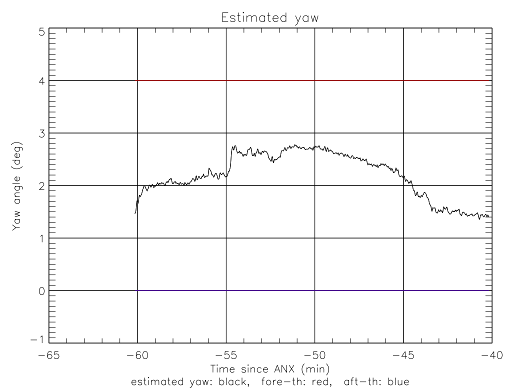


Figure 5.32: Report for RFKS1 and RFKS2

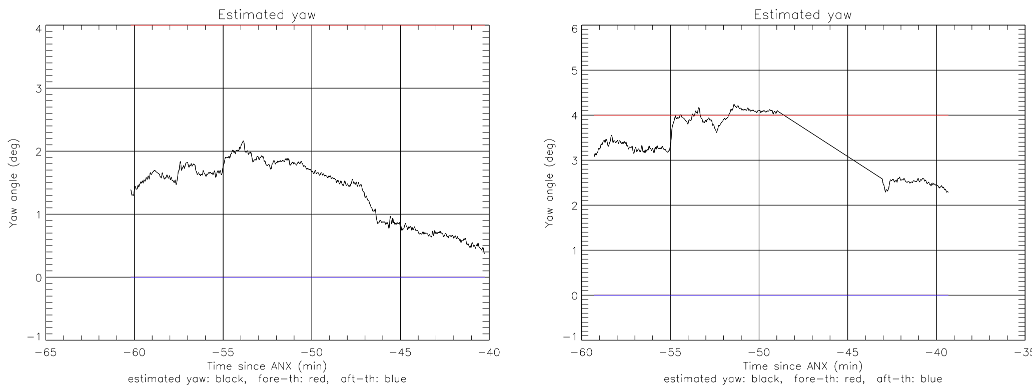


Figure 5.33: Report for RFKS3 and RFKS4

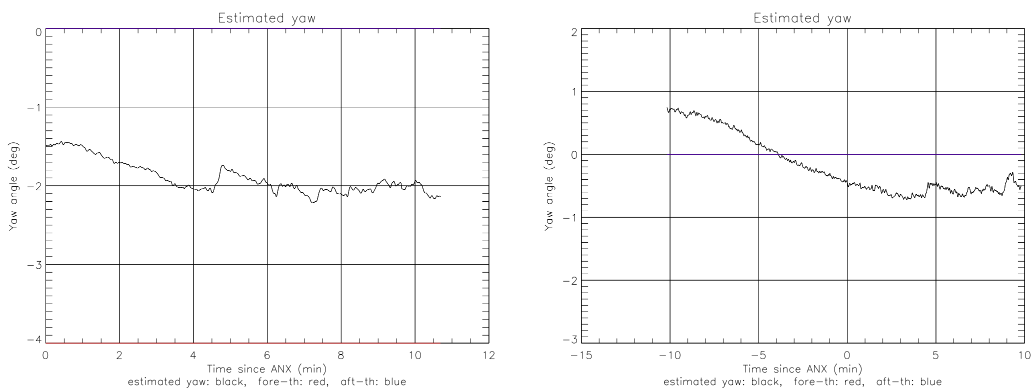


Figure 5.34: Report for RFGS1 and RFGS2

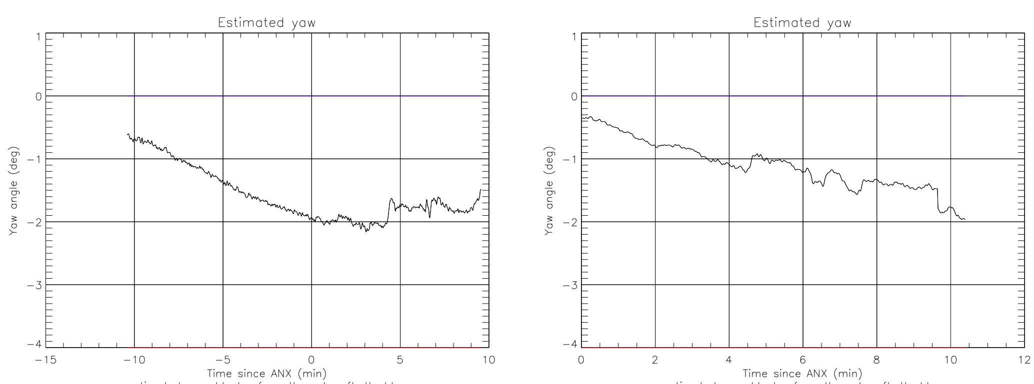


Figure 5.35: Report for RFGS5 and RFGS6

#### 5.15.5.2 Histogram comparison

The two figures below show a comparison of the $\gamma^0$ histogram obtained over the rainforest with (upper graphs) and without (lower graphs) yaw angle estimation and correction.

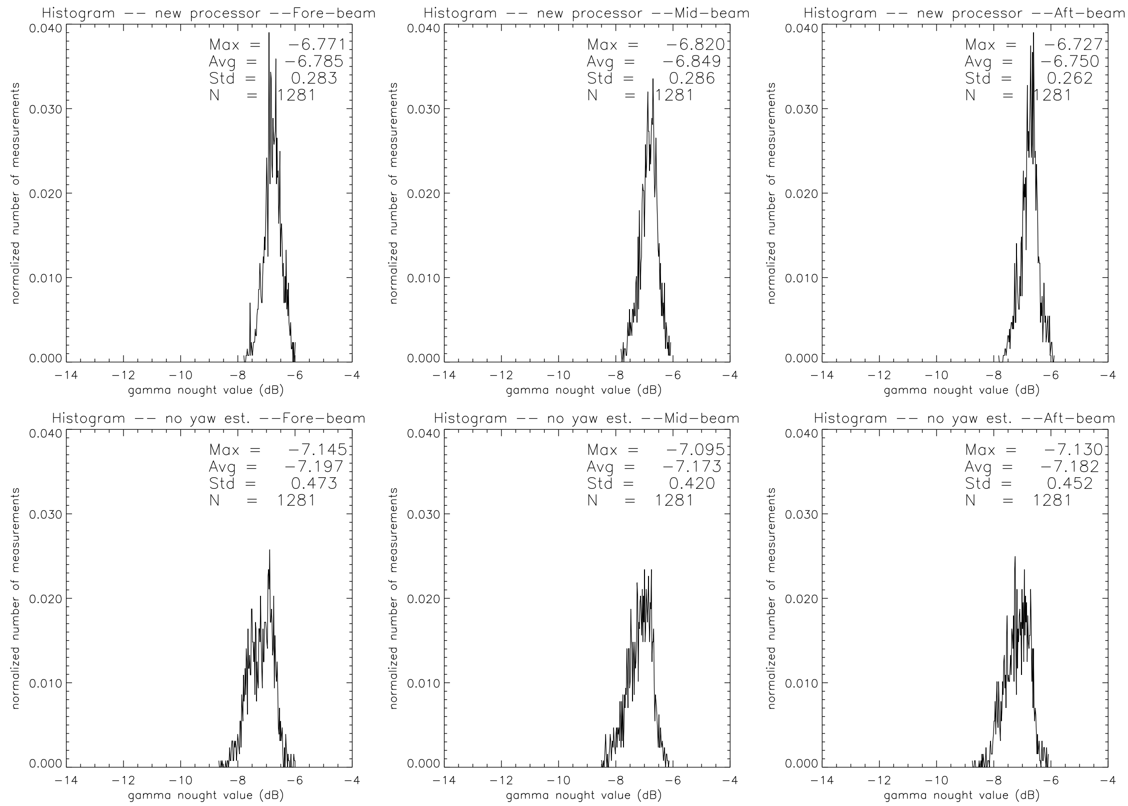


Figure 5.36: $\gamma^0$ histogram for the ascending passes

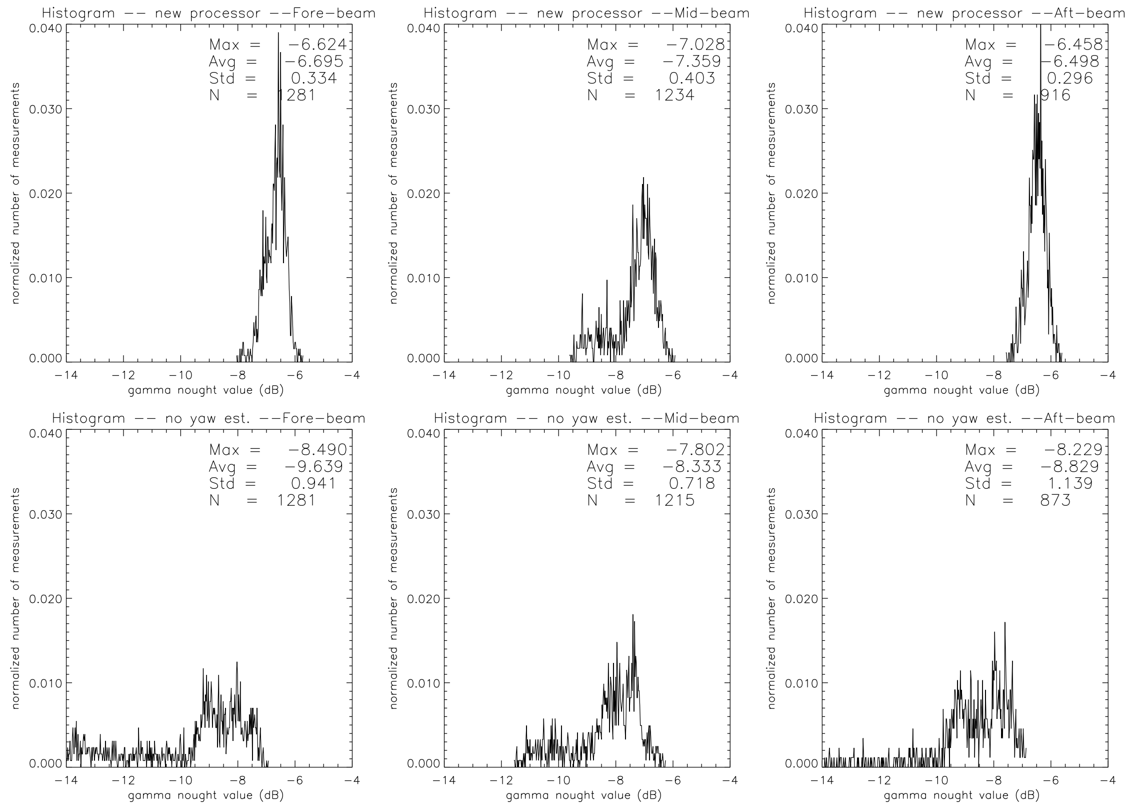


Figure 5.37: $\gamma^0$ histogram for the descending passes

The mean of the histograms obtained with correction is consistently higher than the mean of the histograms obtained without correction. This indicates that the spectrum of the returned echo is indeed better centered within the pass-band of the low-pass filter when the yaw angle correction is performed. Moreover, the spread of the histograms obtained with yaw angle correction is much smaller than that obtained without yaw angle correction. This again shows the effectivity of the yaw angle correction.

### 5.15.5.3 Histogram and antenna pattern

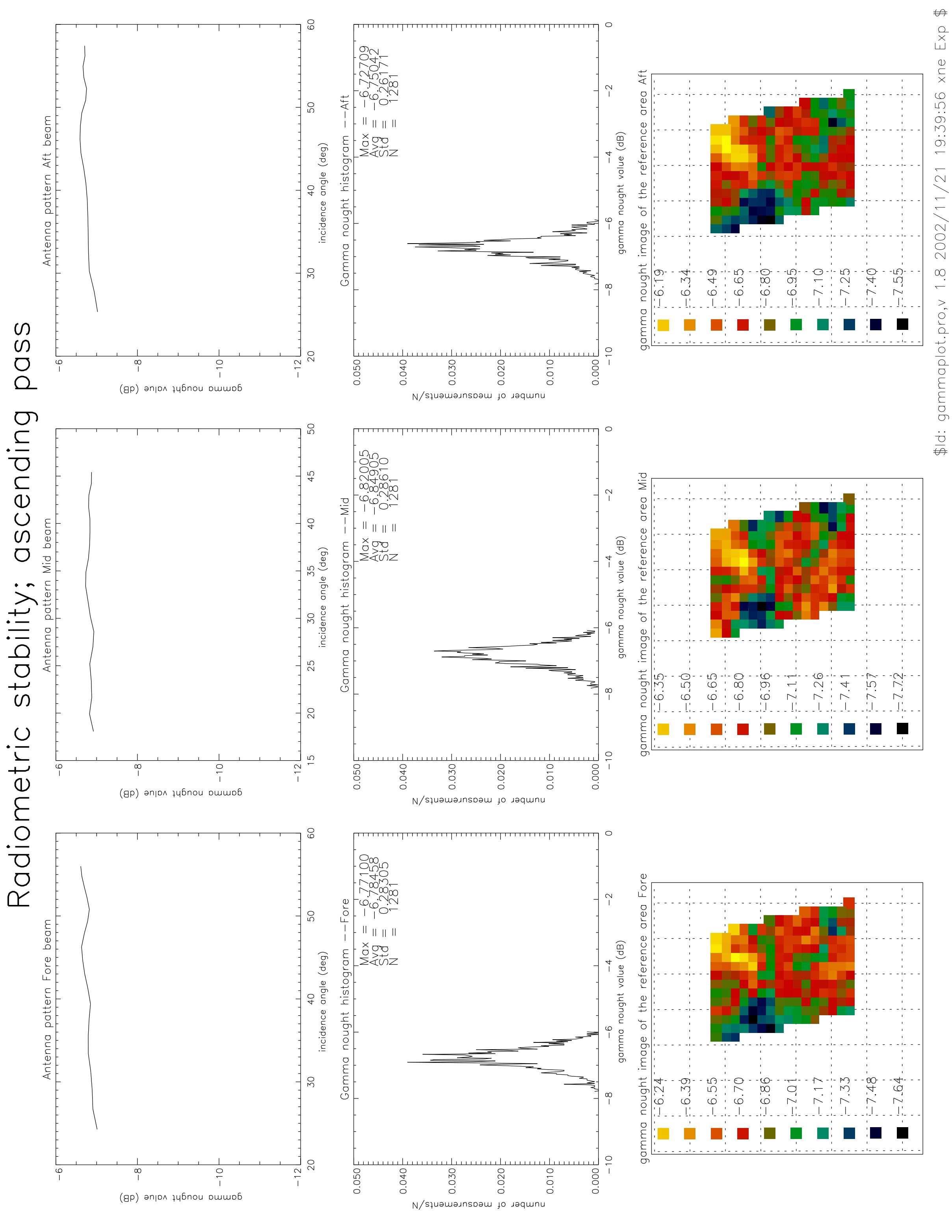

Figure 5.38: $\gamma^0$ histogram and deduced antenna pattern for the ascending passes

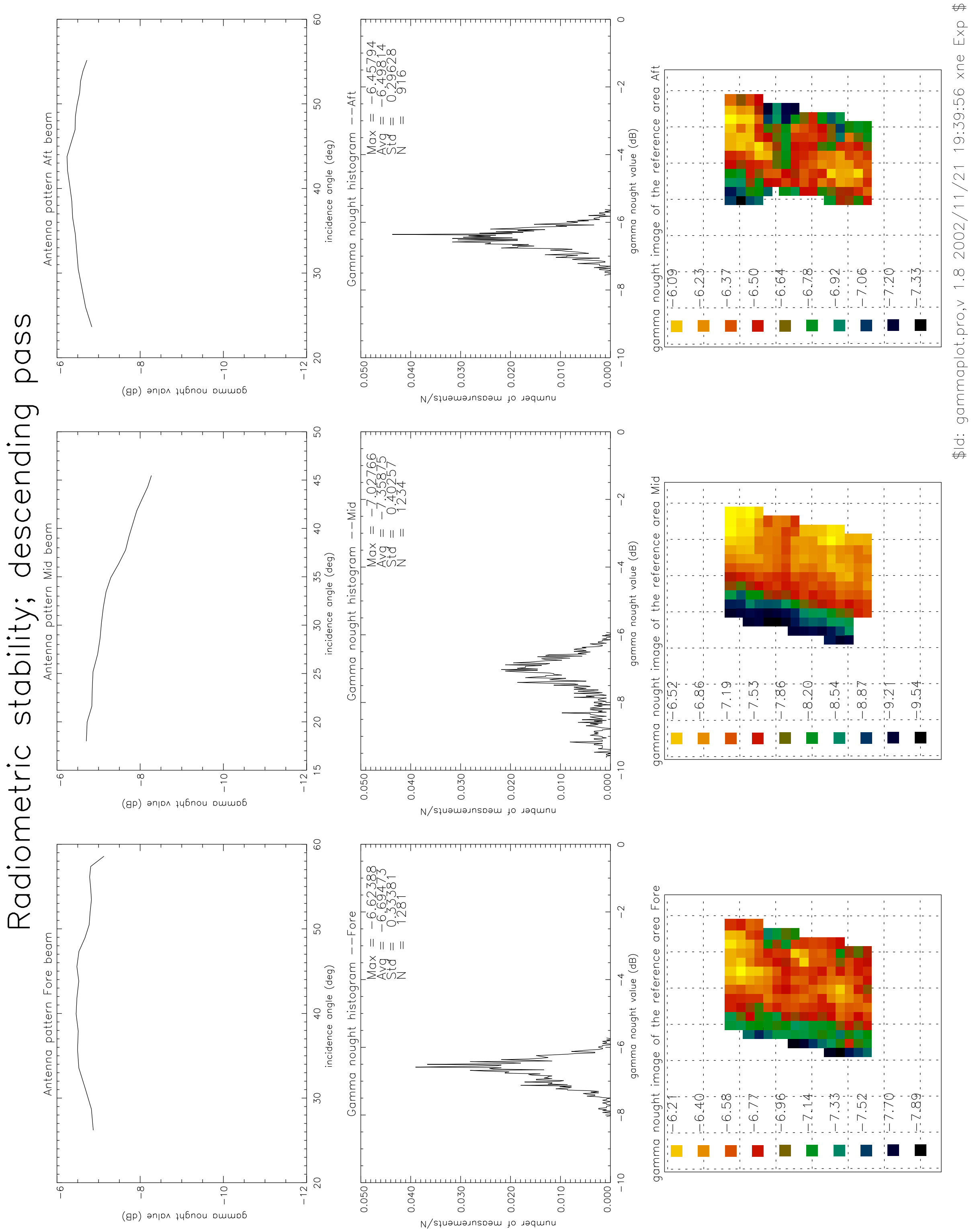


Figure 5.39: $\gamma^0$ histogram and deduced antenna pattern for the descending passes

## 5.16 High resolution product validation

### 5.16.1 Test objective

Assess the correctness of the high resolution product.

### 5.16.2 Test procedure

The values of the $\sigma^0$ and the $K_p$ will be compared between a high-resolution and a nominal resolution product.

The comparison will be performed in areas of constant $\sigma^0$ and in areas where a large variation of $\sigma^0$ can be observed.

### 5.16.3 Success criterions

In areas of constant $\sigma^0$, the values should be the same, up to the statistical variance of the measurements. In areas where there is a discontinuity of the $\sigma^0$ (land-sea interface), the $\sigma^0$ in the high resolution product should exhibit a more pronounced edge.

The $K_p$ should be twice as high for the high resolution product, when compared with the $K_p$ of the nominal resolution product.

### 5.16.4 Test data

The following test data will be considered

- the YSM6 orbit

### 5.16.5 Results

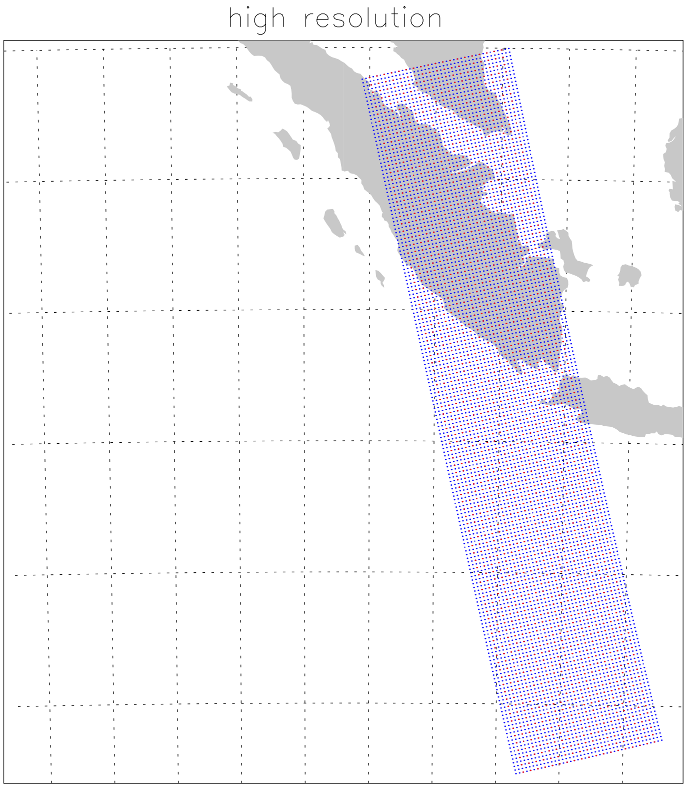


Figure 5.40: Considered area for the comparison

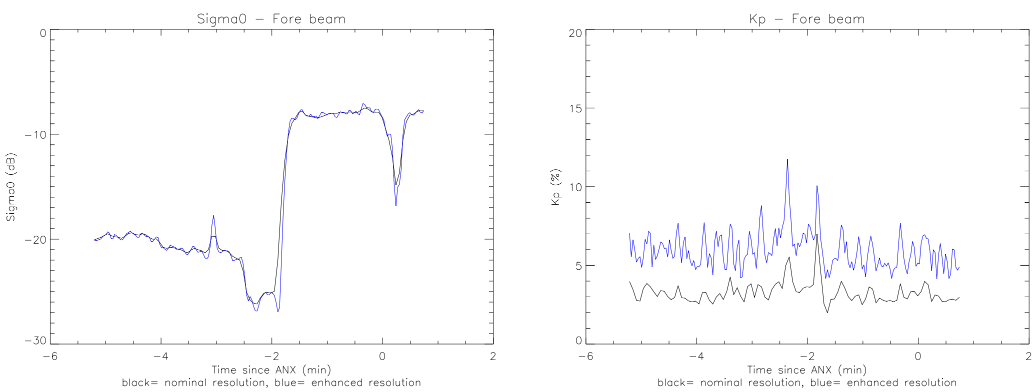


Figure 5.41: Comparison of along-track cuts (node 10) of the $\sigma^0$ (left) and the $K_p$ (right) between the high- and the low-resolution product.

Figure 5.41 (left) shows a comparison of the $\sigma^0$ value between the high and the low resolution product. Where the $\sigma^0$ is nearly constant, i.e. over land or over sea, the $\sigma^0$ values are similar. Where the $\sigma^0$ values exhibit large variations, for instance at land-sea transitions, these variations are indeed less blurred in the high resolution product.

Figure 5.41 (right) shows a comparison of the $K_p$ for the high and the low resolution product. The $K_p$ of the high resolution data is twice as high as the $K_p$ of the low resolution data. This is due to the fact that the high resolution $\sigma^0$ are obtained by averaging 4 times less measurements than the low resolution data, hence an increase of the variance of the $\sigma^0$ by a factor 2.

# Appendix A

# Spectrum monitoring comparison – complete results

## A.1 YSM2

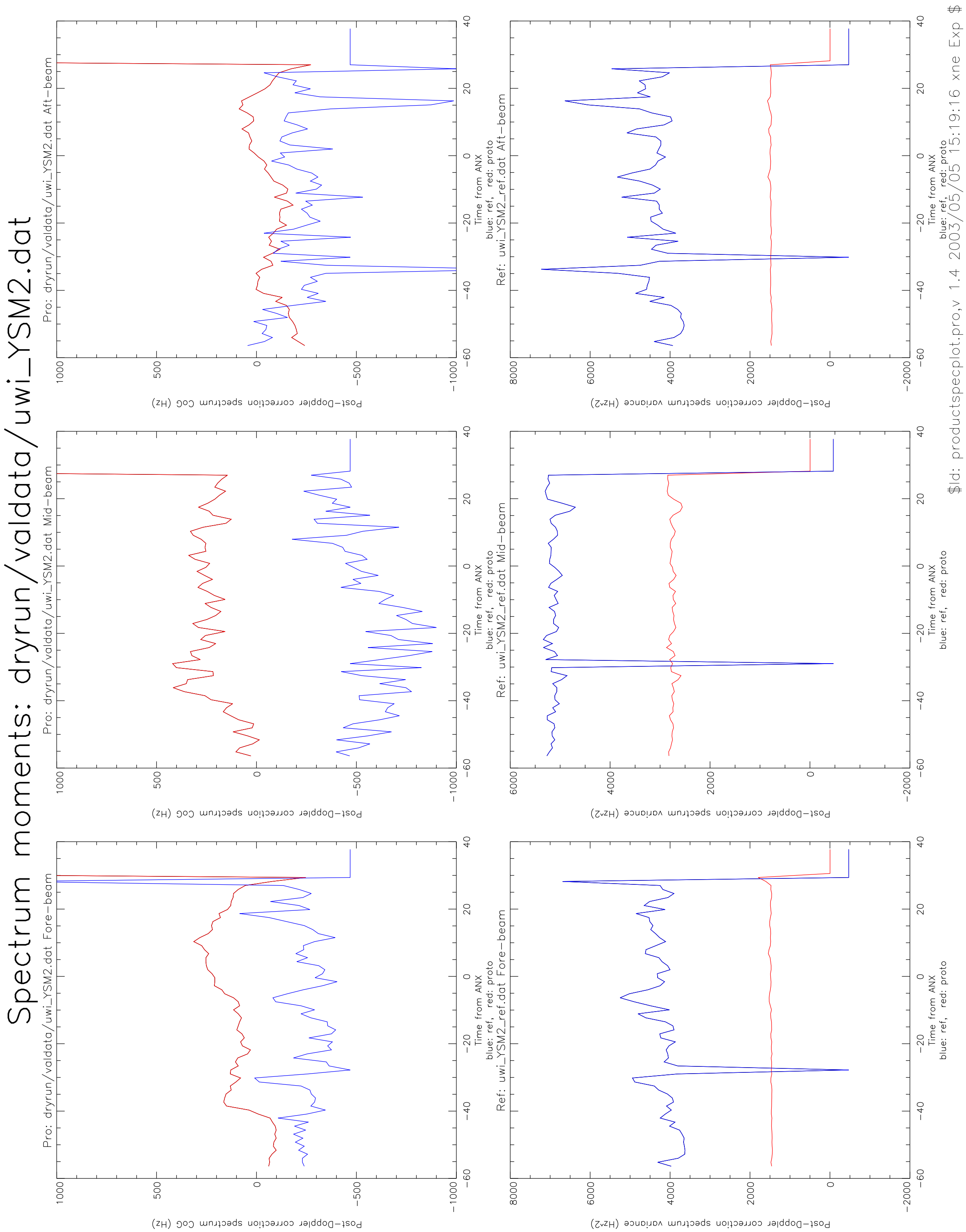


Figure A.1: Report for YSM2

# A.2 YSM3

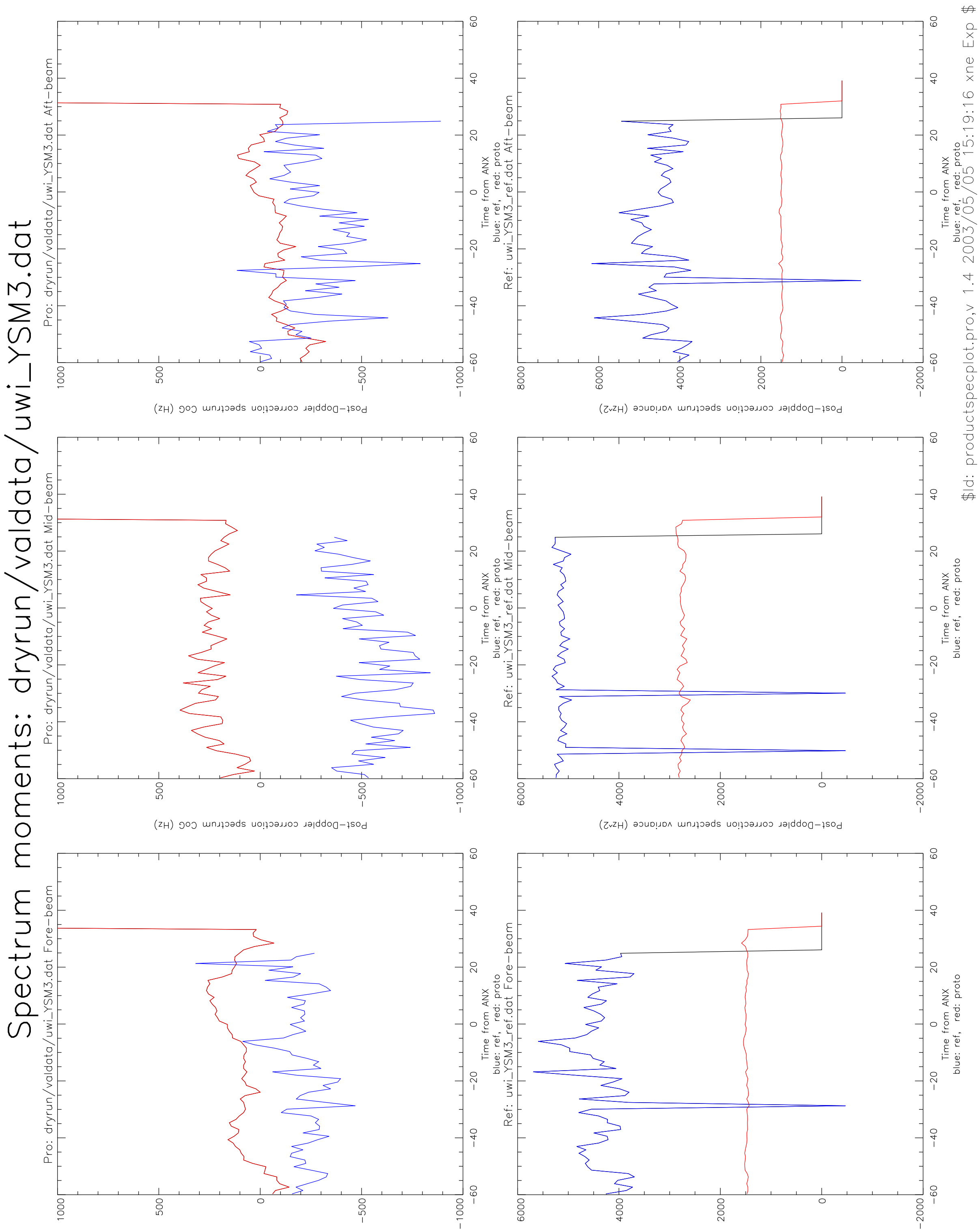


Figure A.2: Report for YSM3

## A.3 YSM4

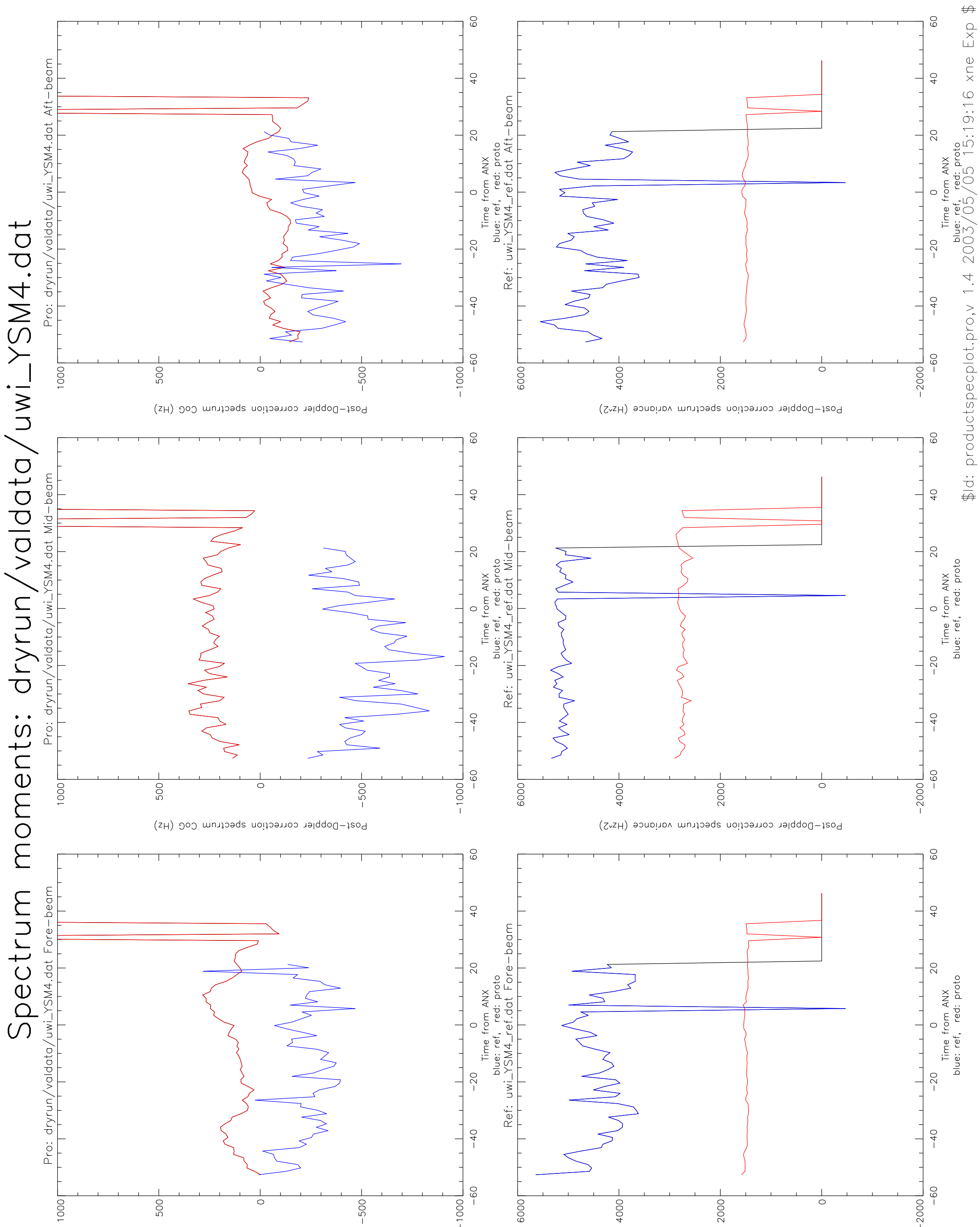

Figure A.3: Report for YSM4

## A.4 YSM5

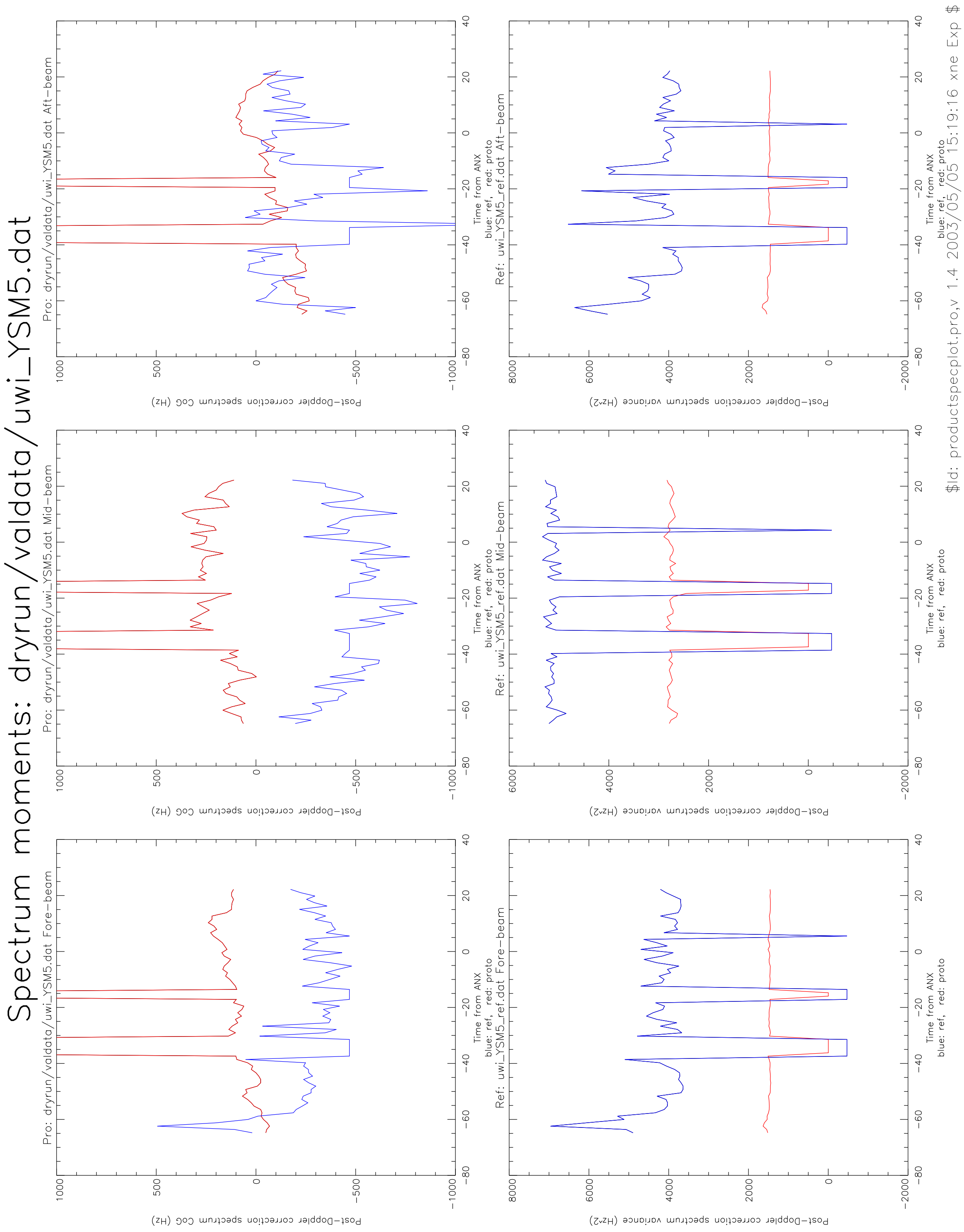


Figure A.4: Report for YSM5

## A.5 YSM6

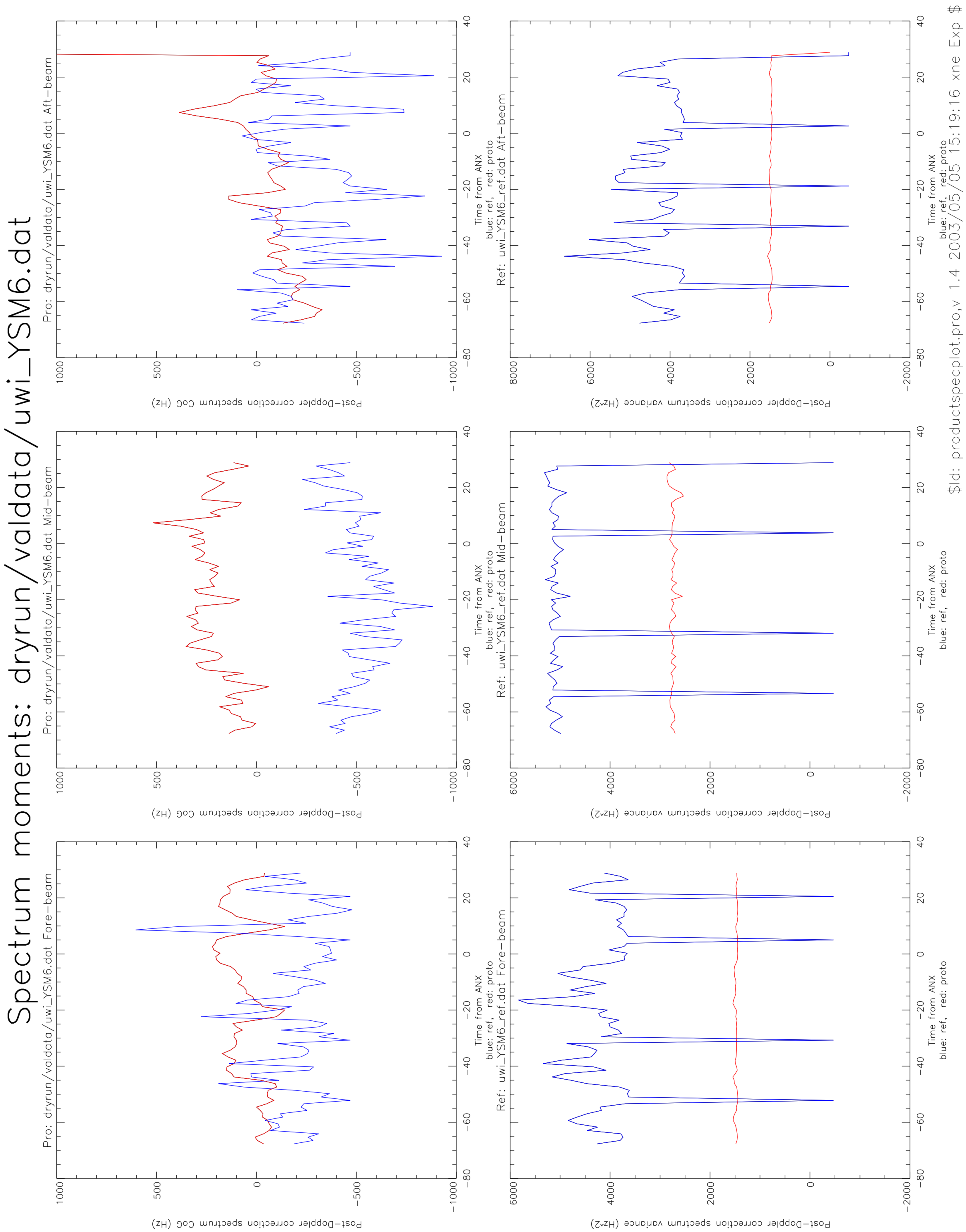


Figure A.5: Report for YSM6

## A.6 YSM7

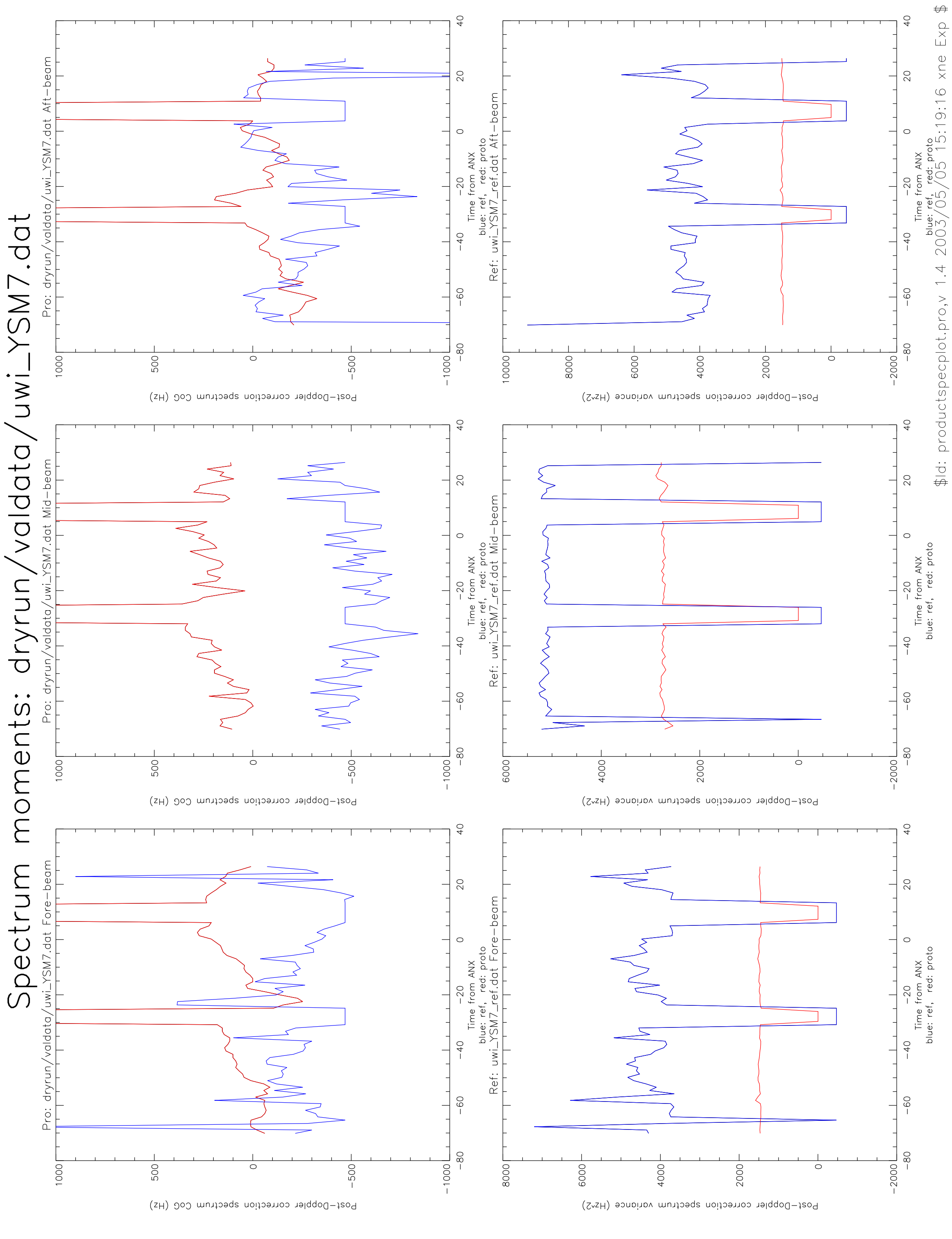


Figure A.6: Report for YSM7

## A.7 YSM8

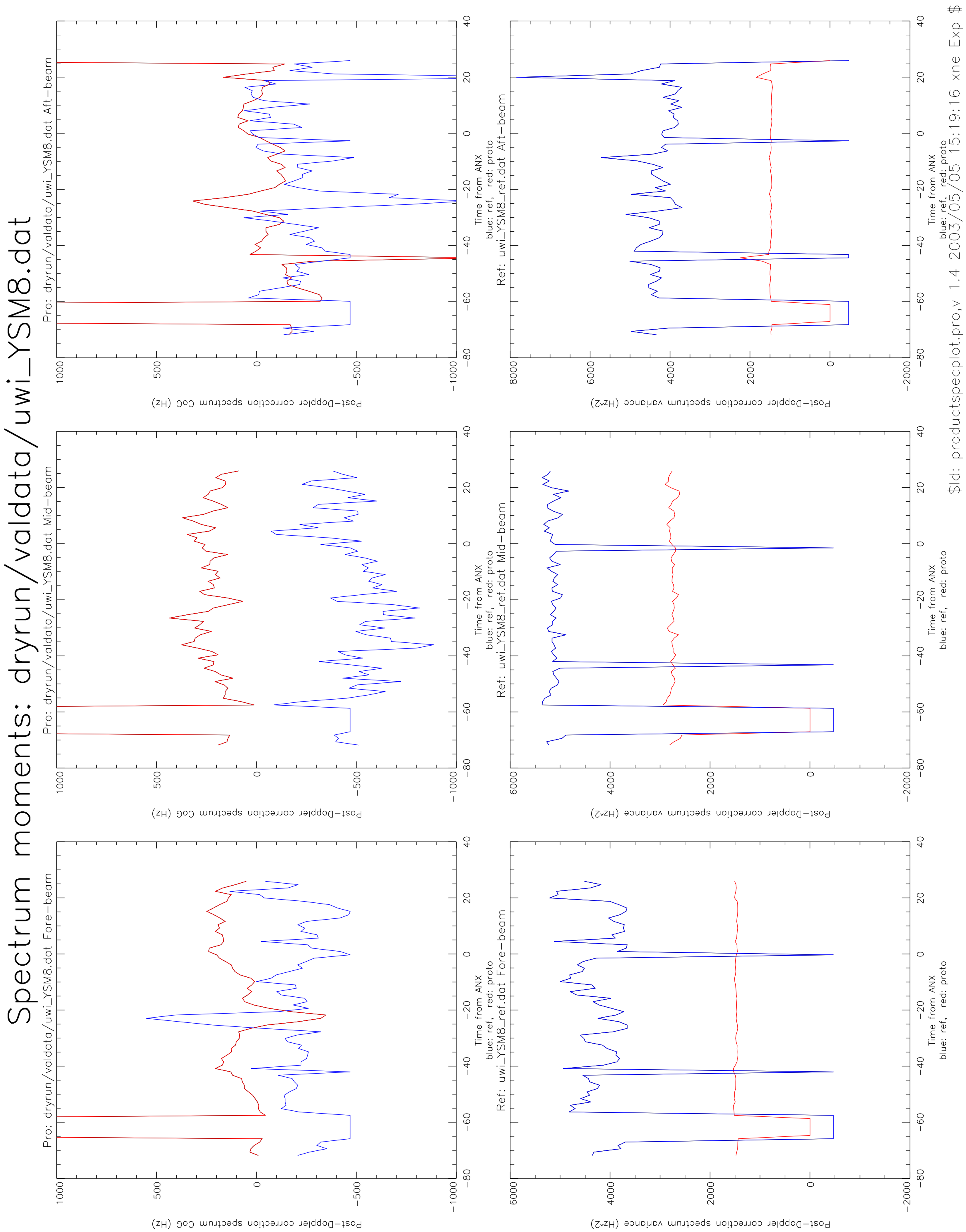


Figure A.7: Report for YSM8

## A.8 YSM9

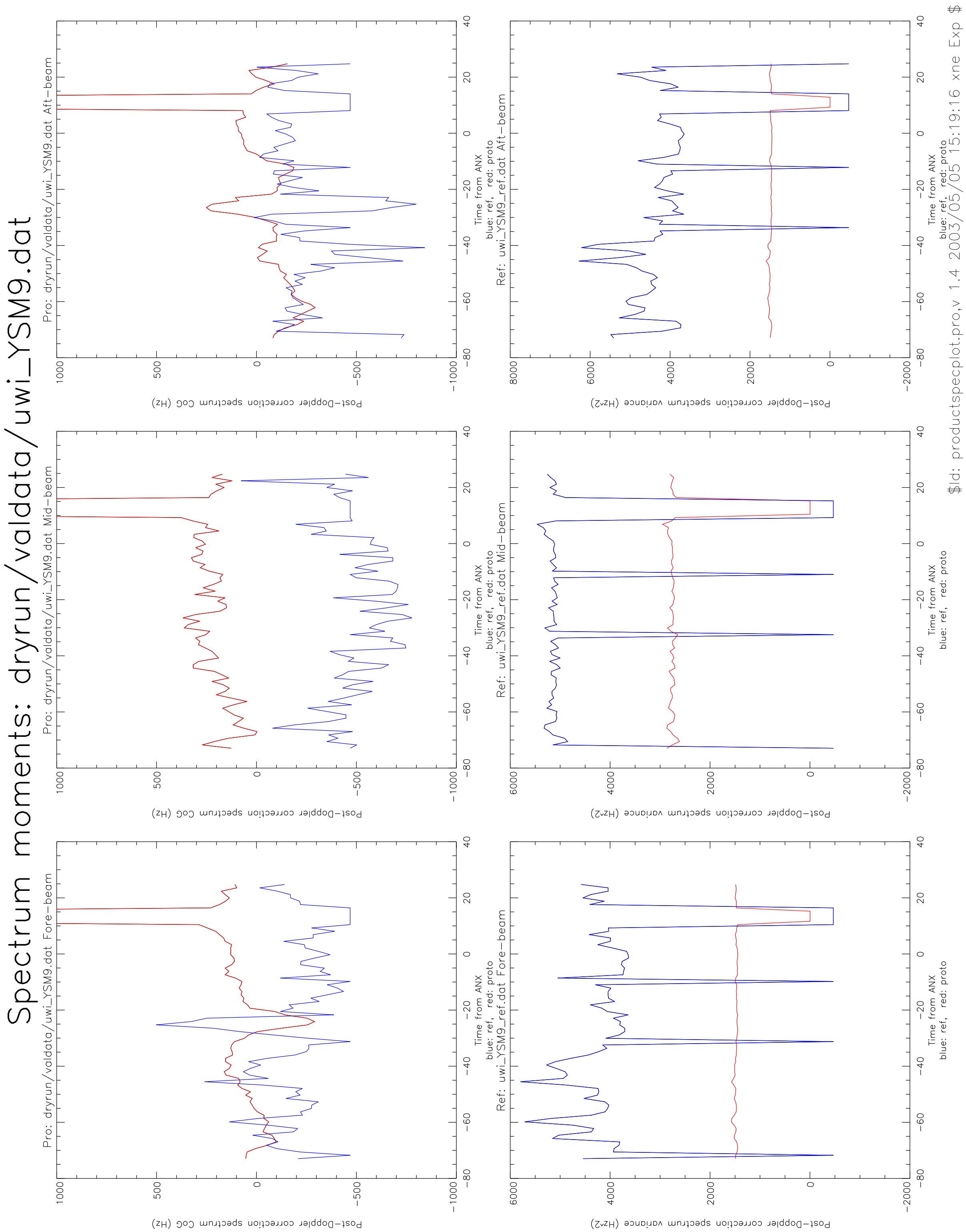


Figure A.8: Report for YSM9

# Appendix B

# Node location comparison – complete results

## B.1 YSM orbits

### B.1.1 YSM2

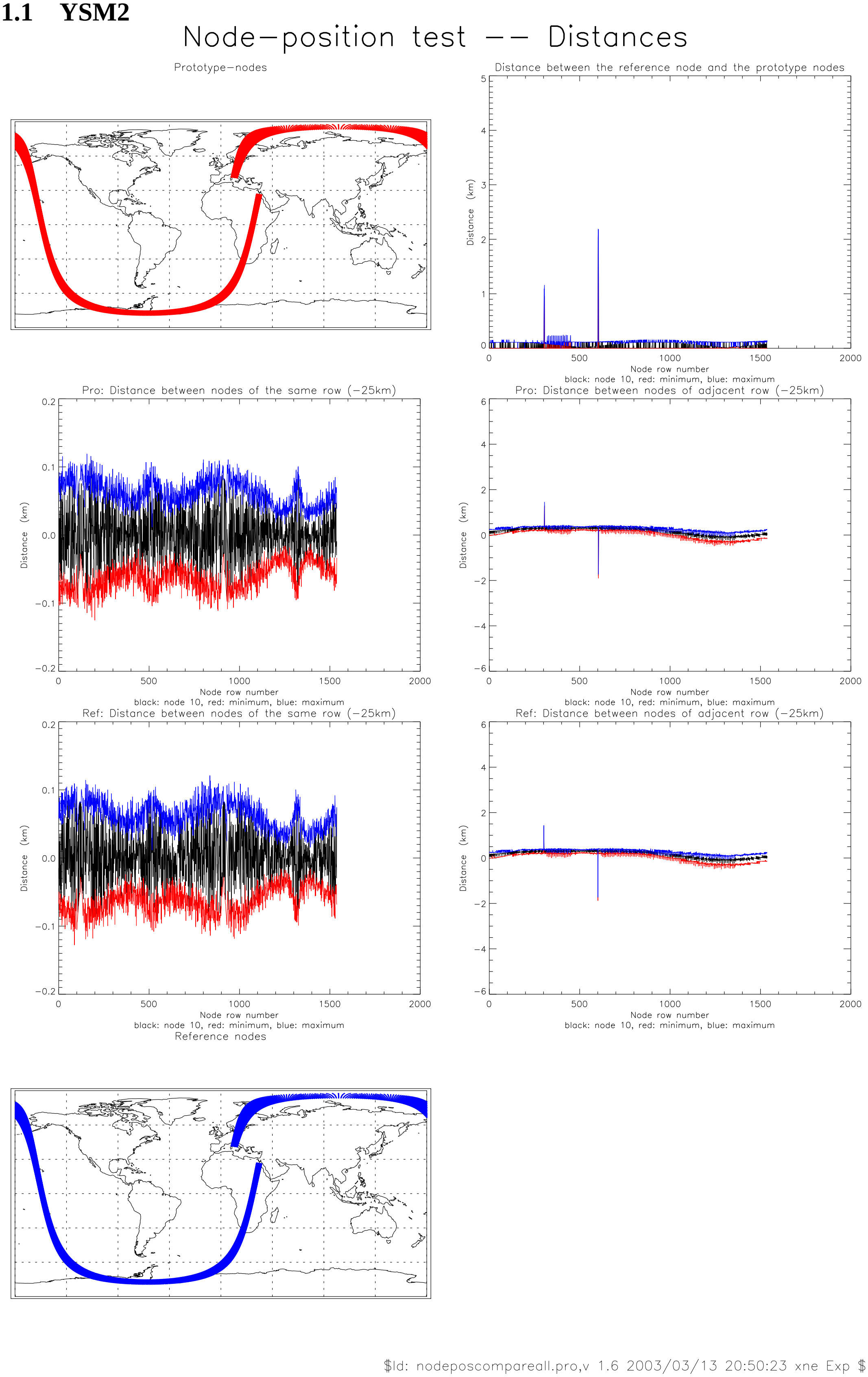


Figure B.1: Report for YSM2

### B.1.2 YSM3

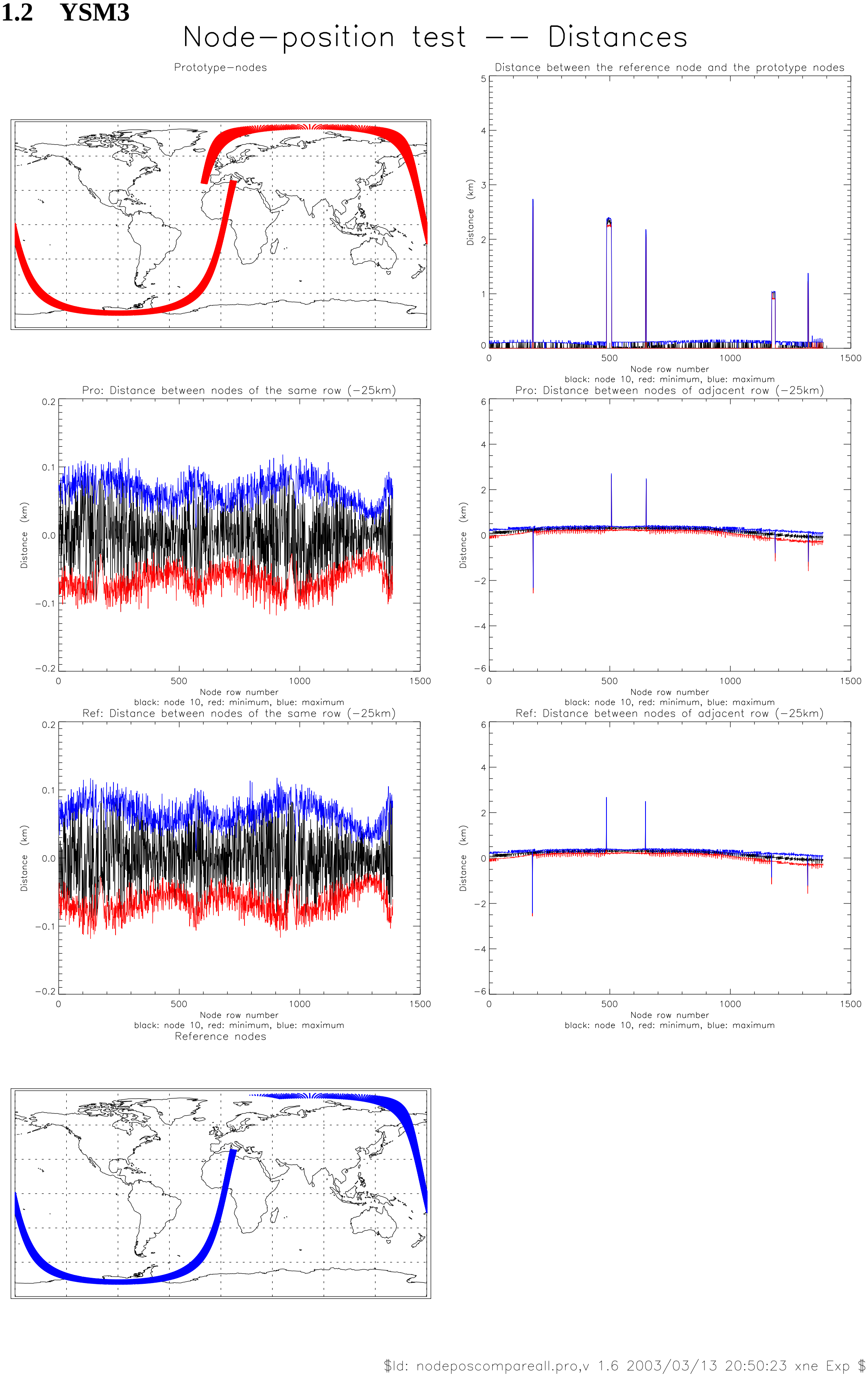


Figure B.2: Report for YSM3

### B.1.3 YSM4

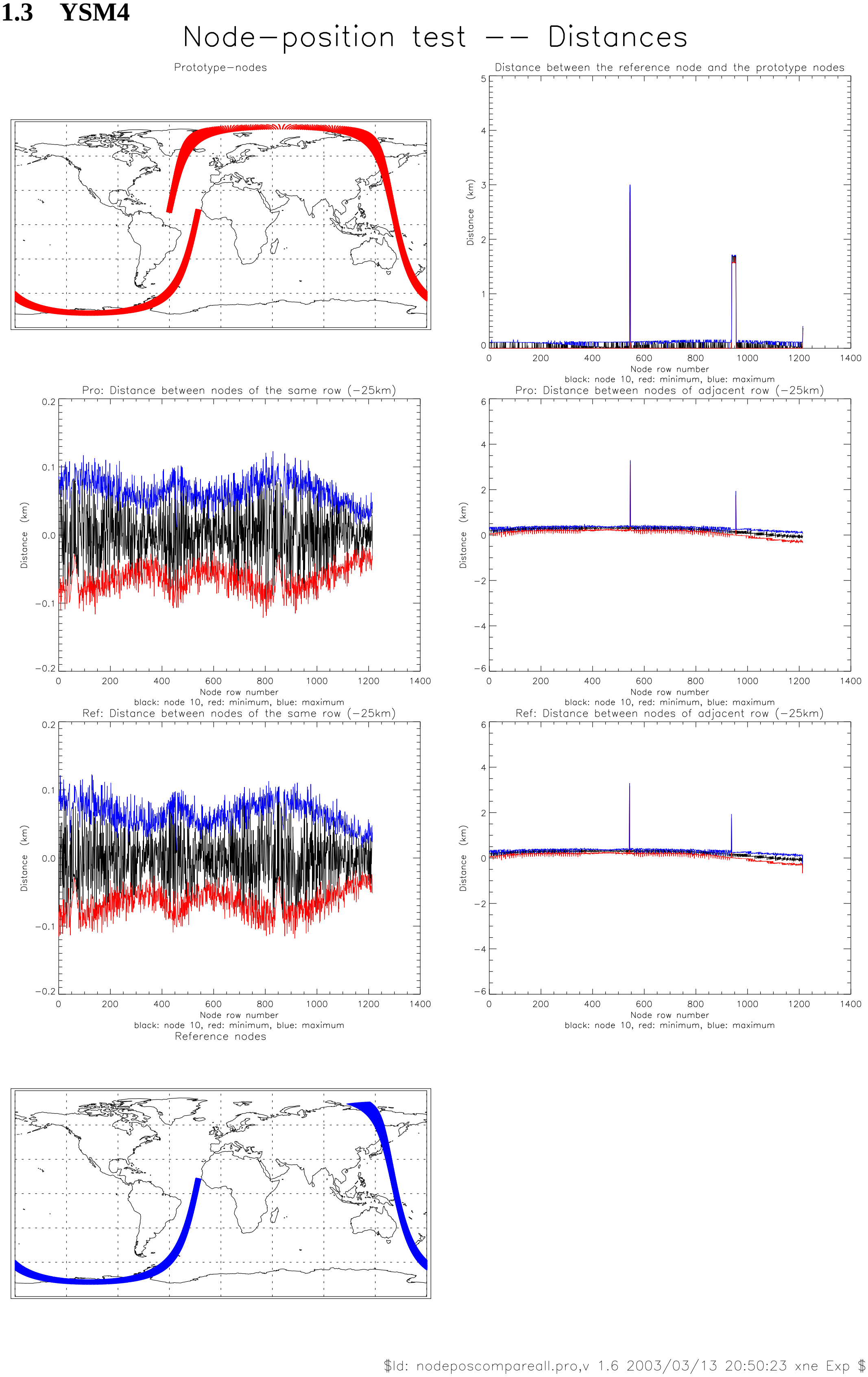


Figure B.3: Report for YSM4

### B.1.4 YSM5

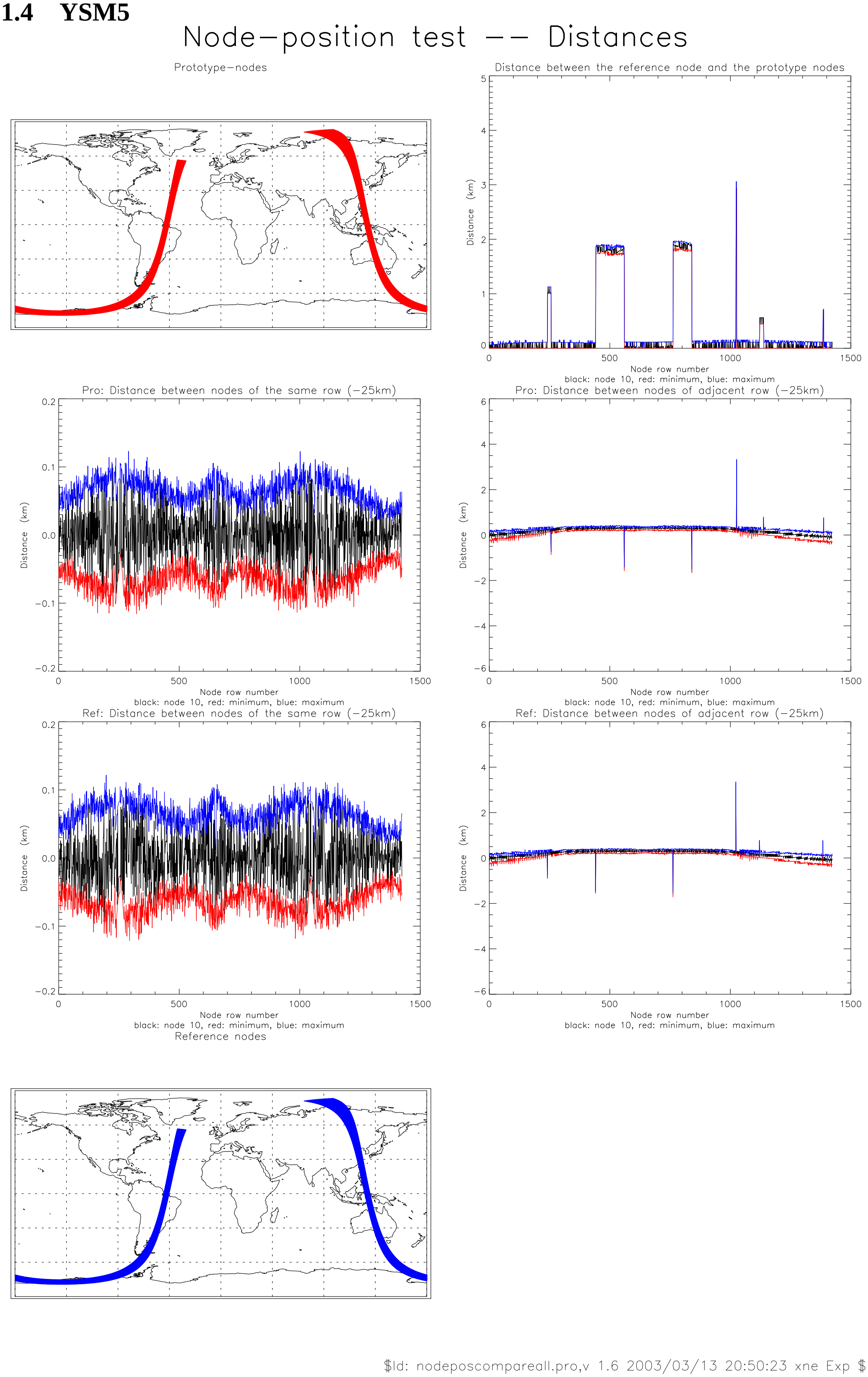


Figure B.4: Report for YSM5

### B.1.5 YSM6

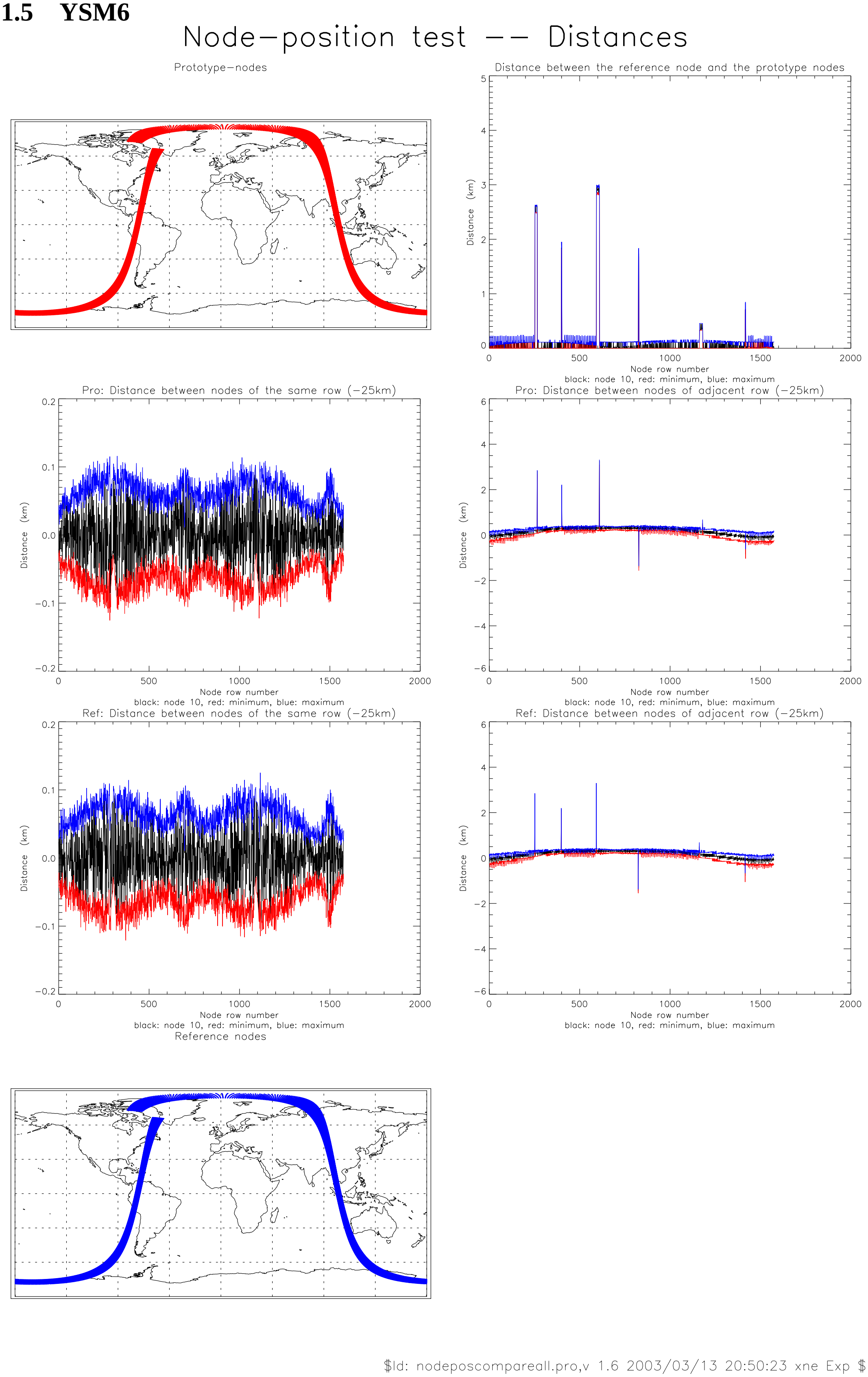


Figure B.5: Report for YSM6

### B.1.6 YSM7

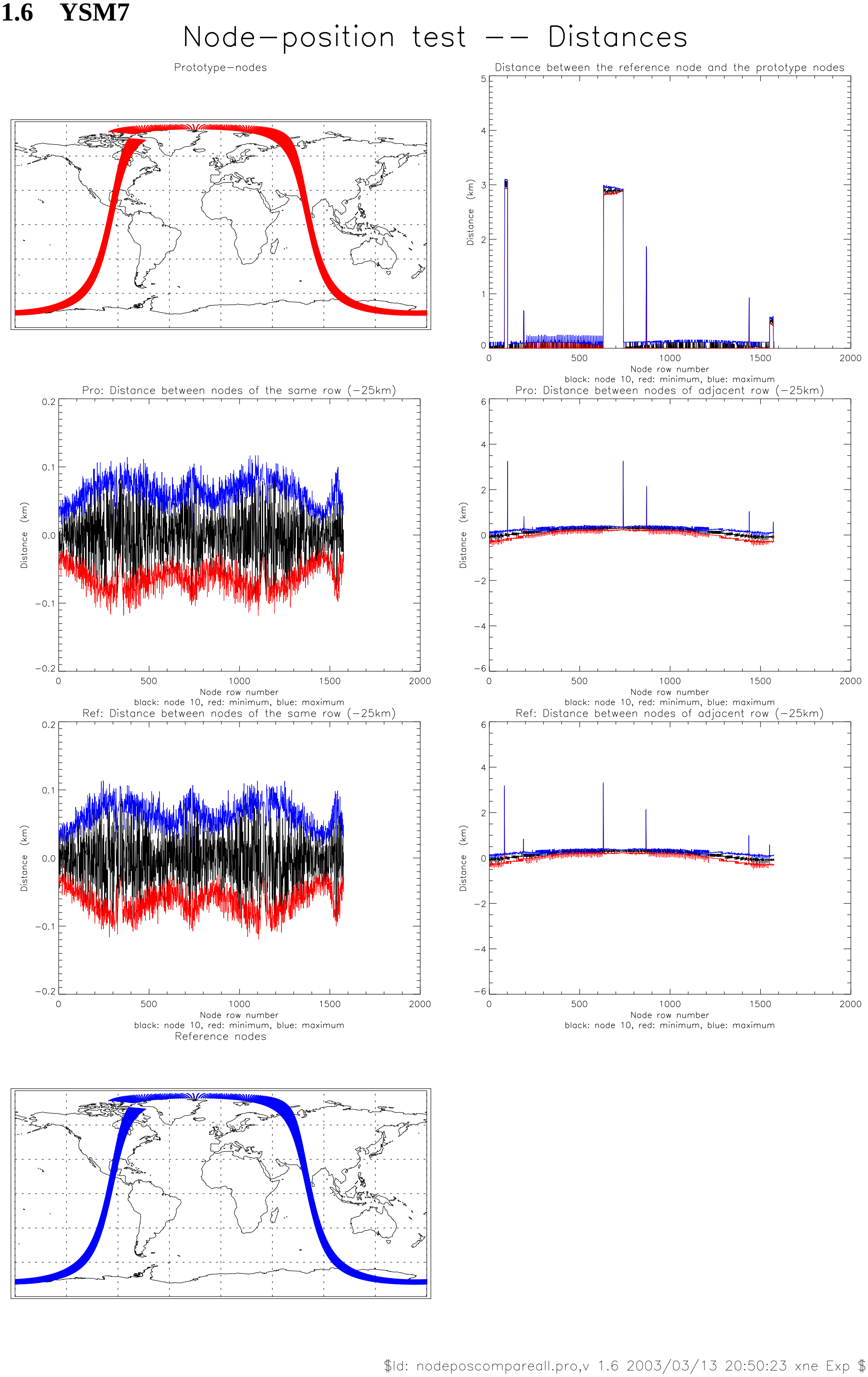


Figure B.6: Report for YSM7

### B.1.7 YSM8

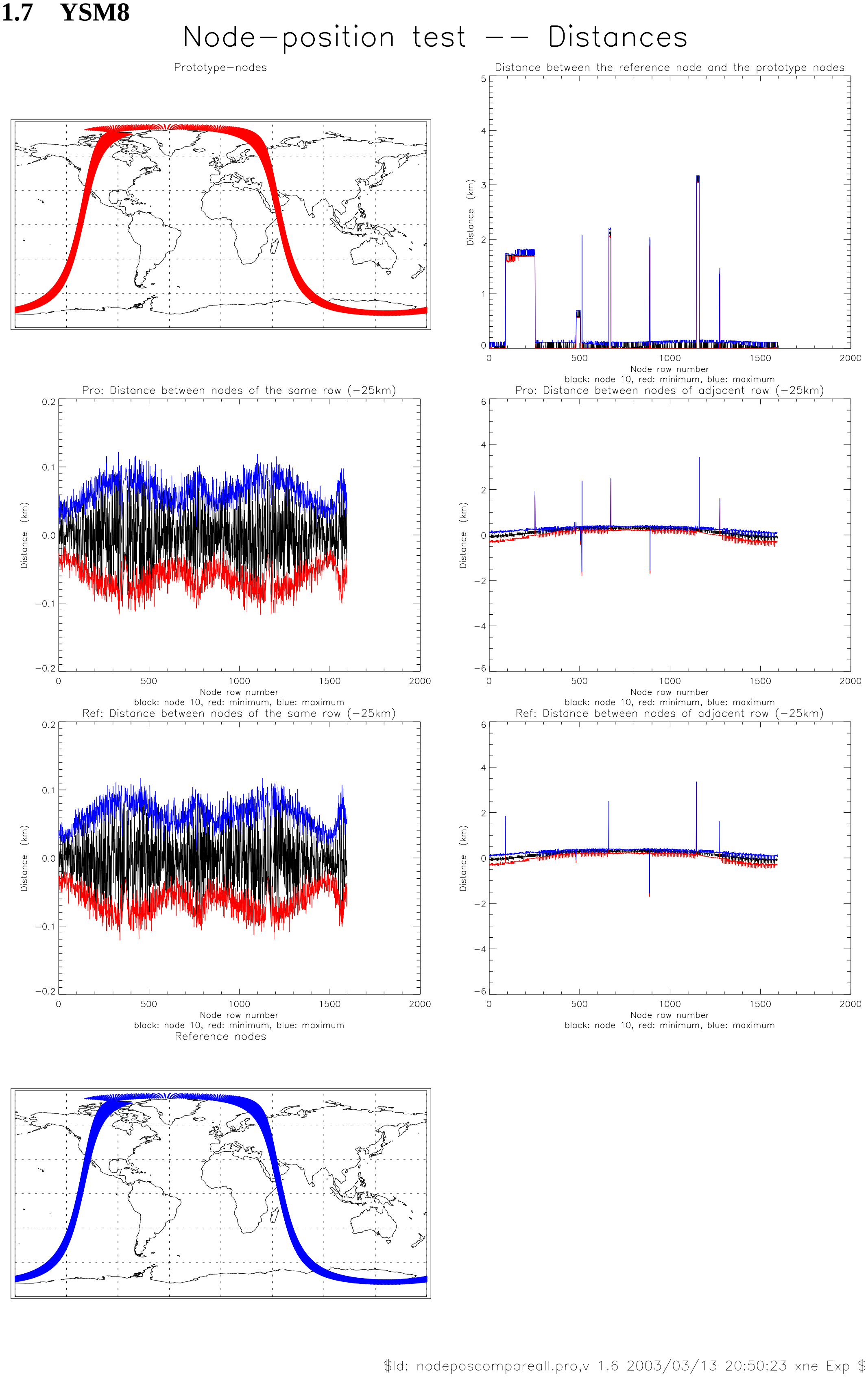


Figure B.7: Report for YSM8

### B.1.8 YSM9

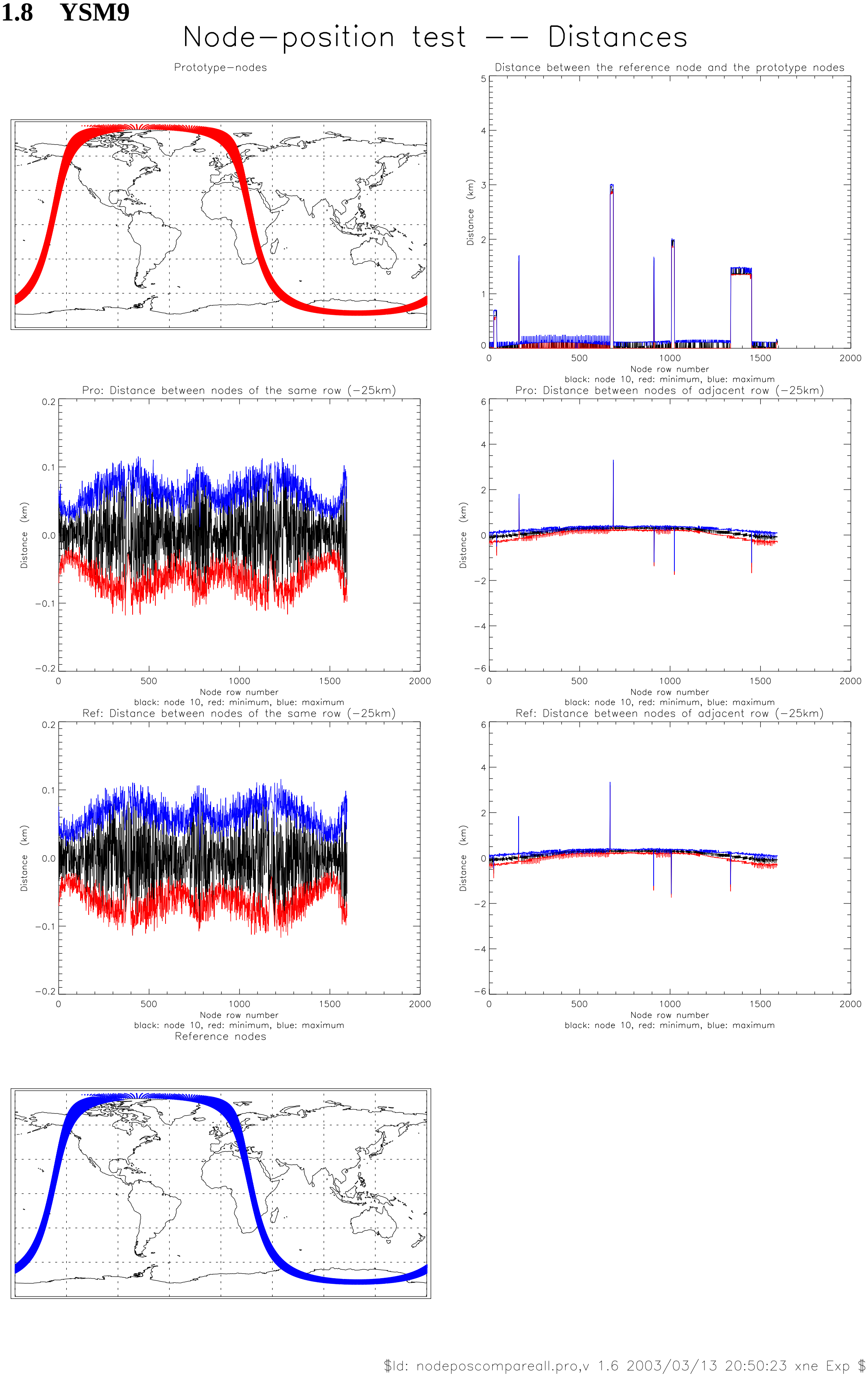


Figure B.8: Report for YSM9

## B.2 ZGM orbits

### B.2.1 ZGM1

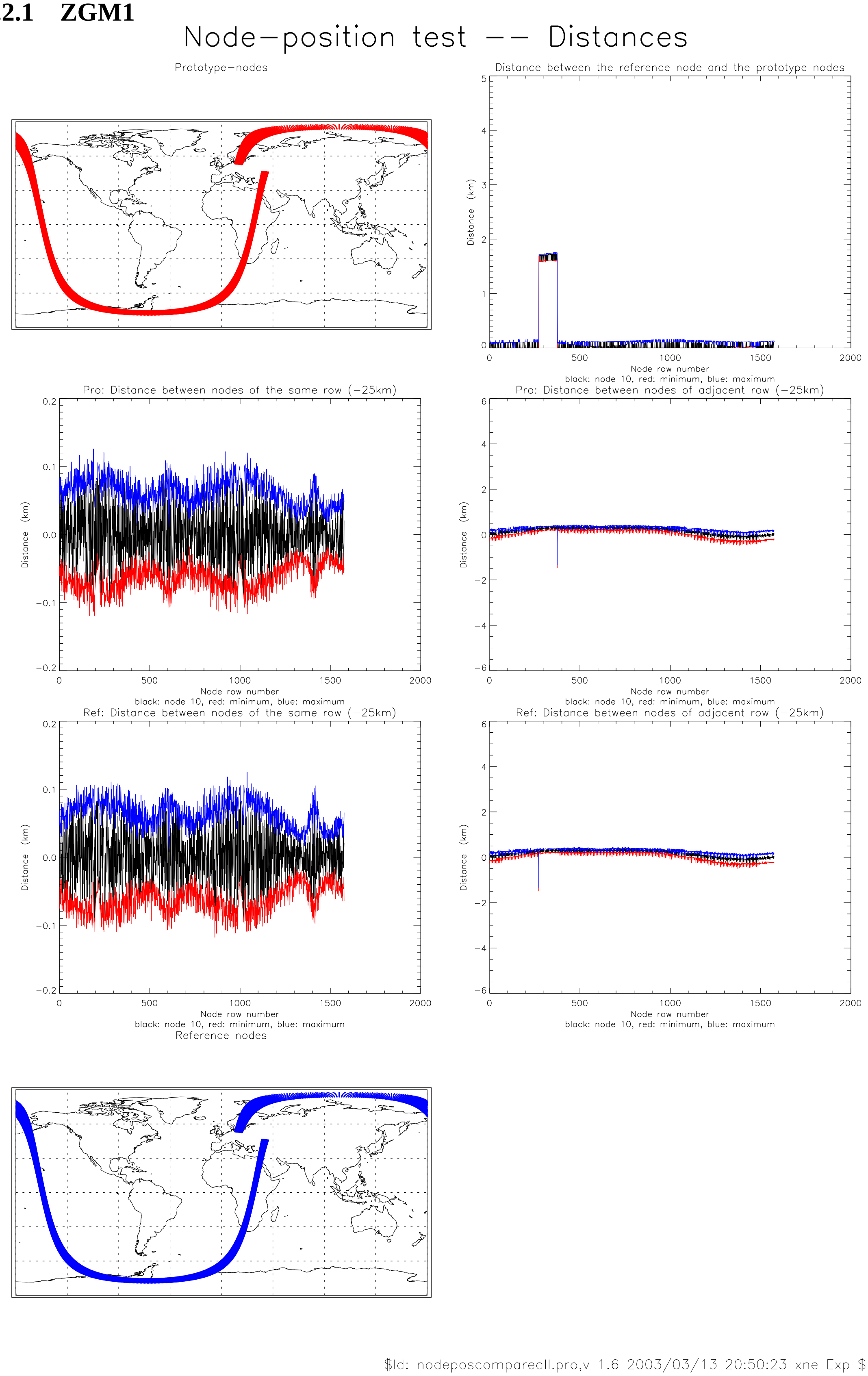


Figure B.9: Report for ZGM1

### B.2.2 ZGM2

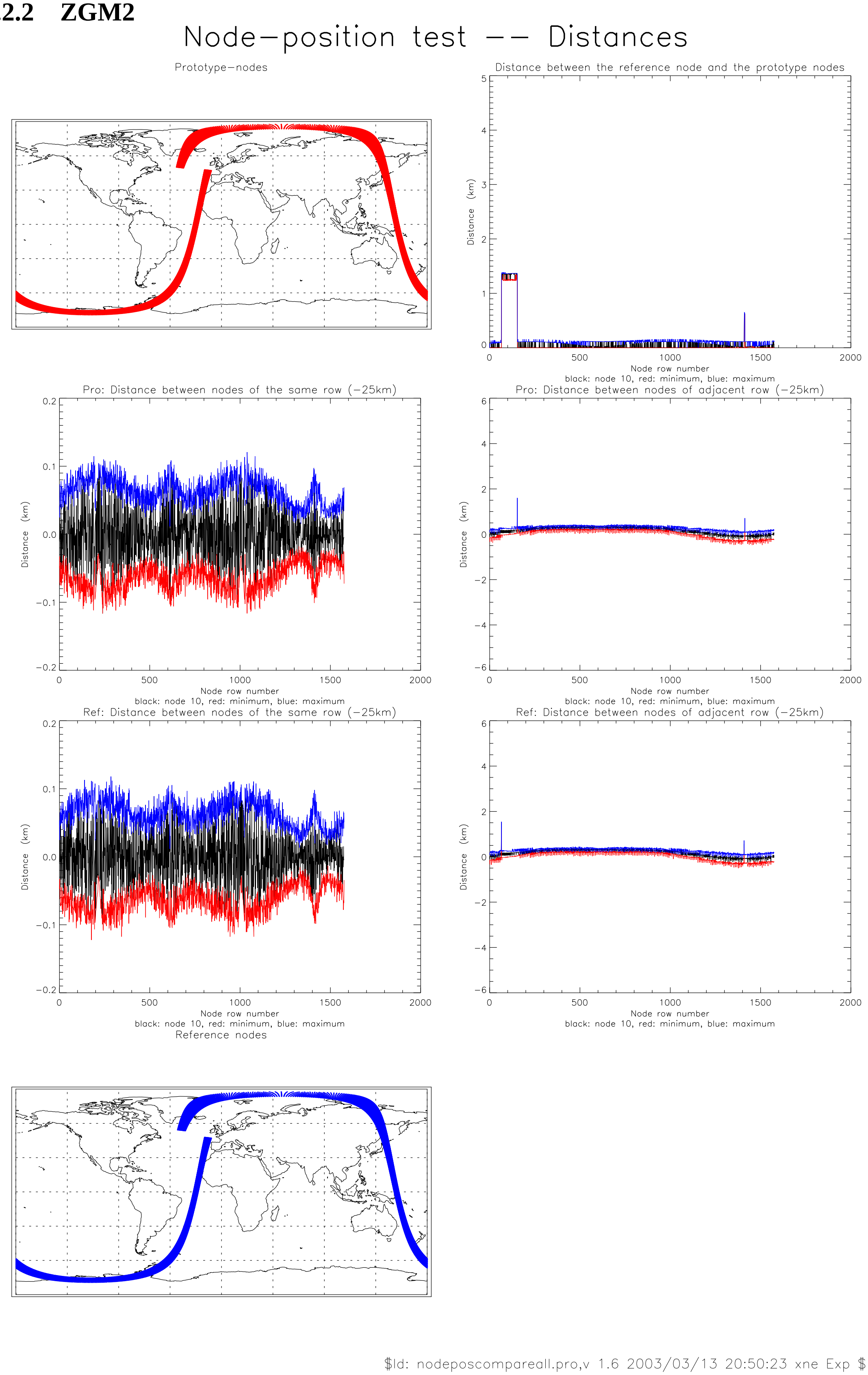


Figure B.10: Report for ZGM2

### B.2.3 ZGM3

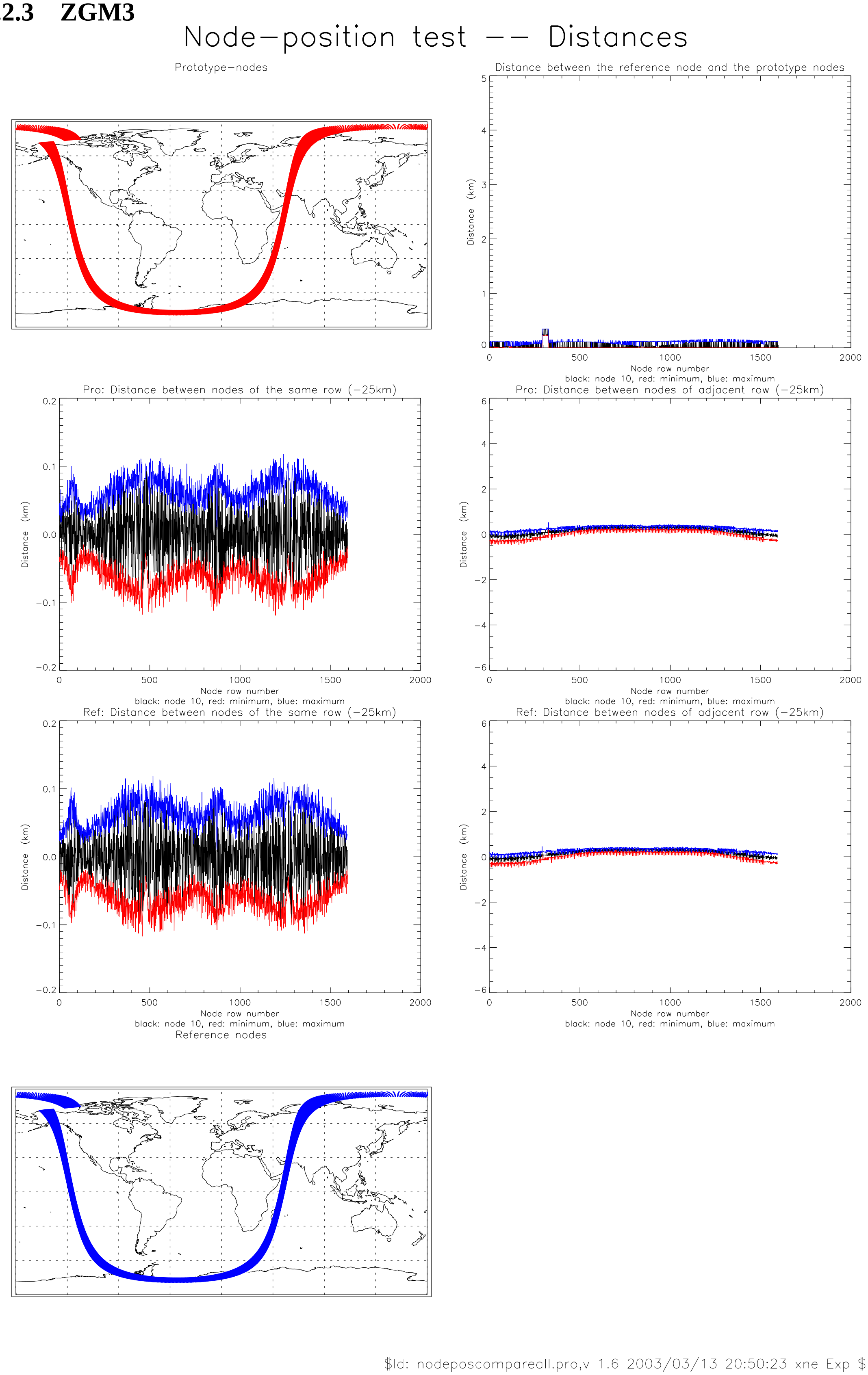


Figure B.11: Report for ZGM3

### B.2.4 ZGM4

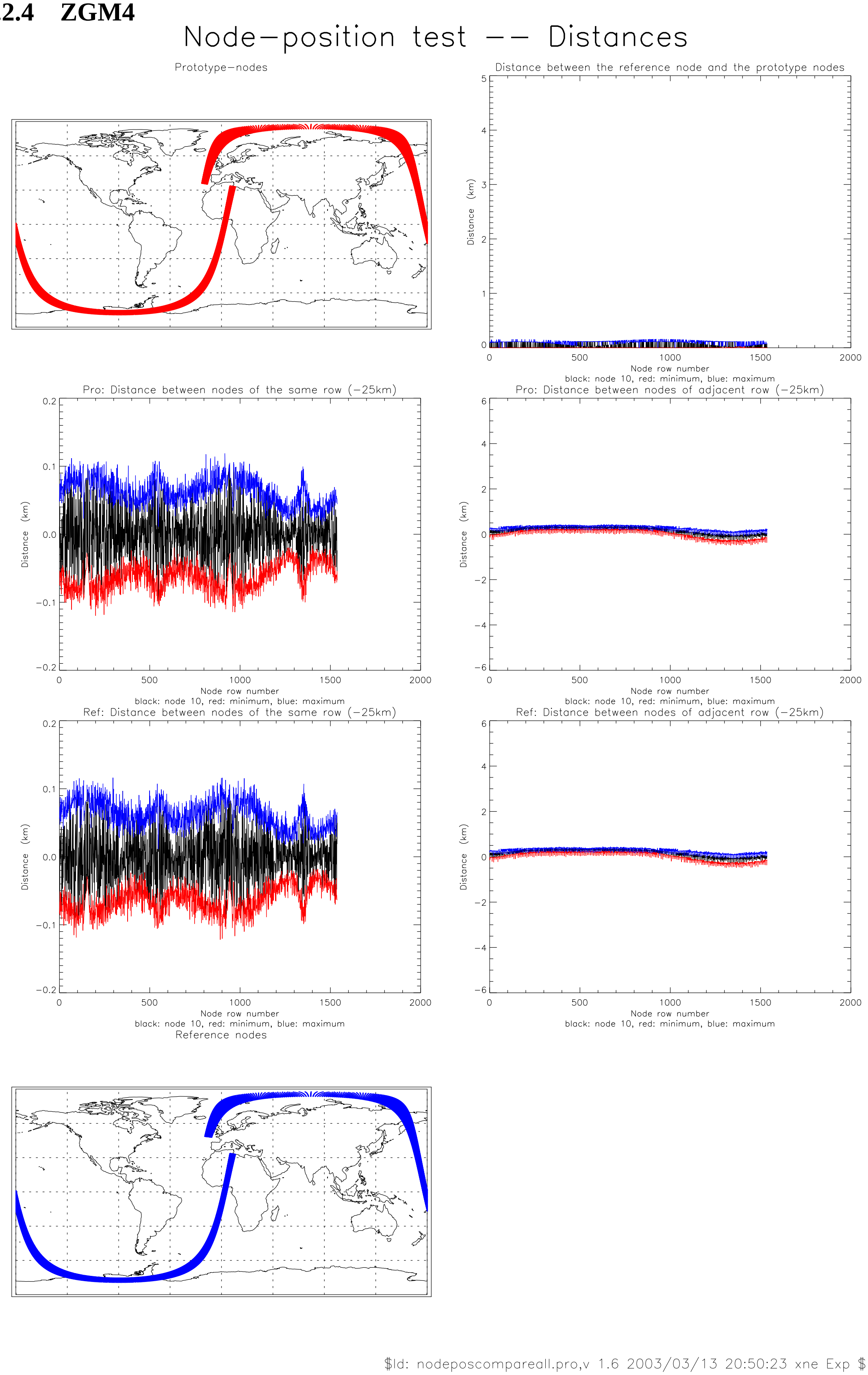


Figure B.12: Report for ZGM4

### B.2.5 ZGM5

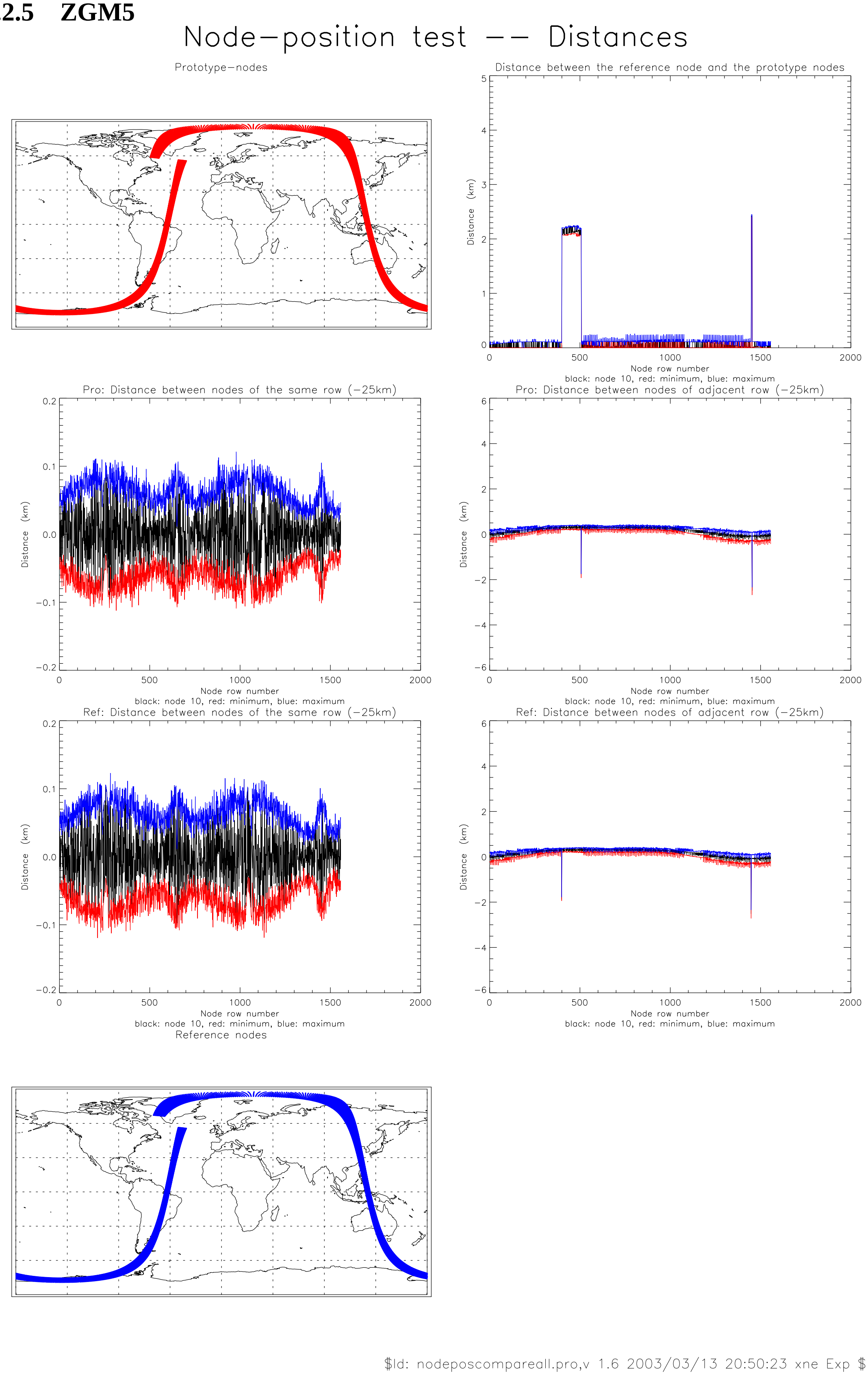


Figure B.13: Report for ZGM5

### B.2.6 ZGM6

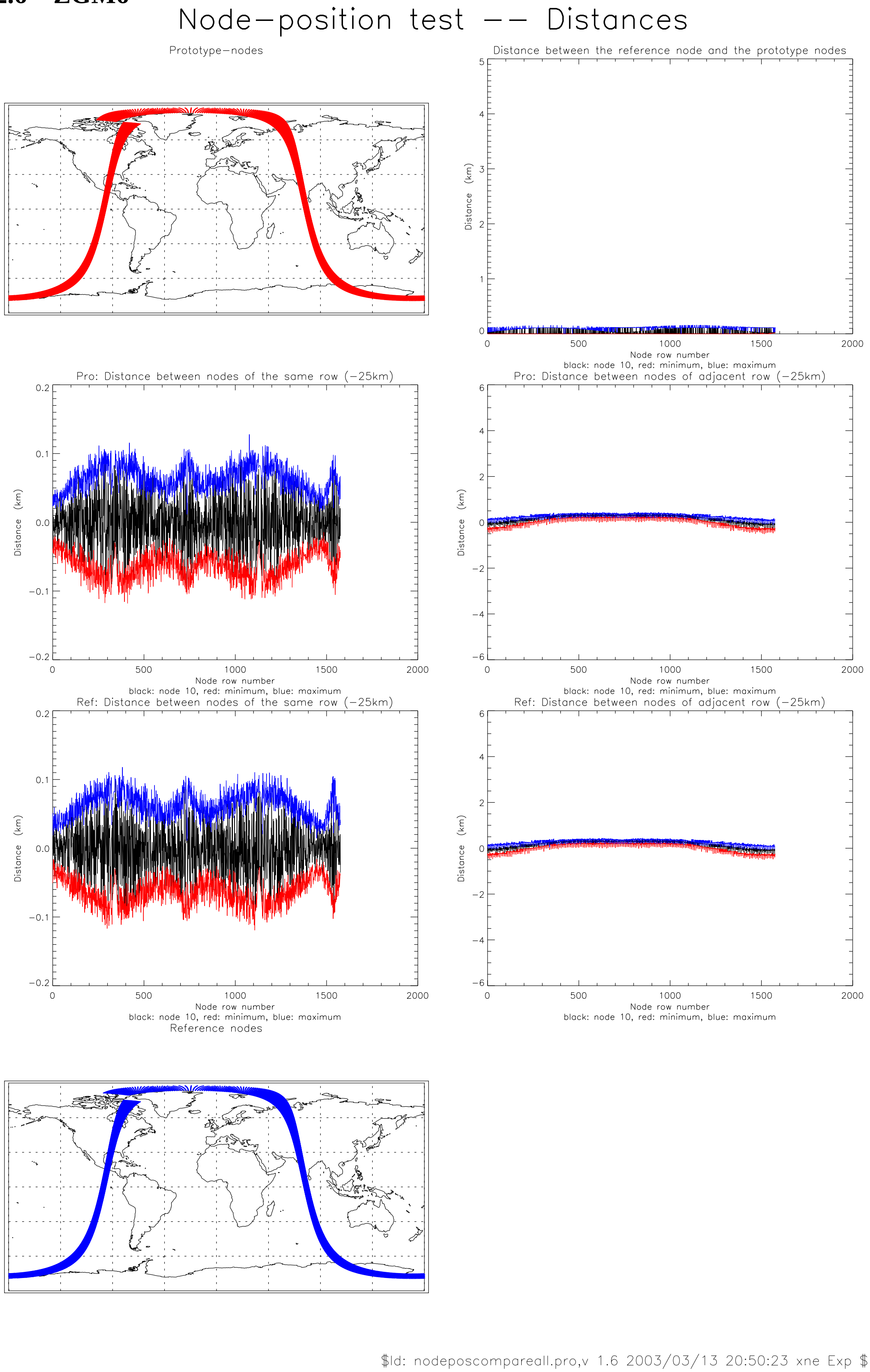


Figure B.14: Report for ZGM6

### B.2.7 ZGM7

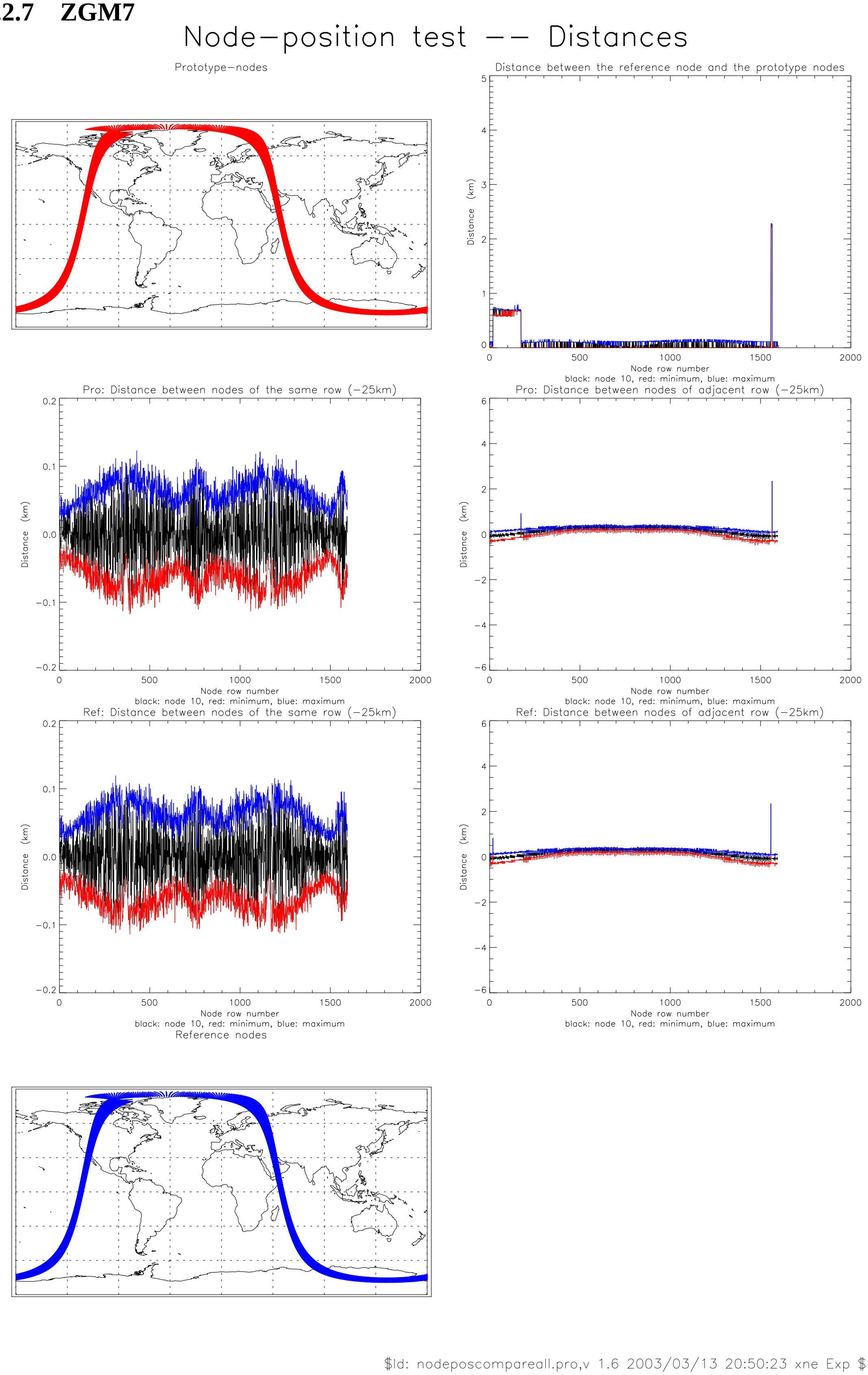


Figure B.15: Report for ZGM7

### B.2.8 ZGM8

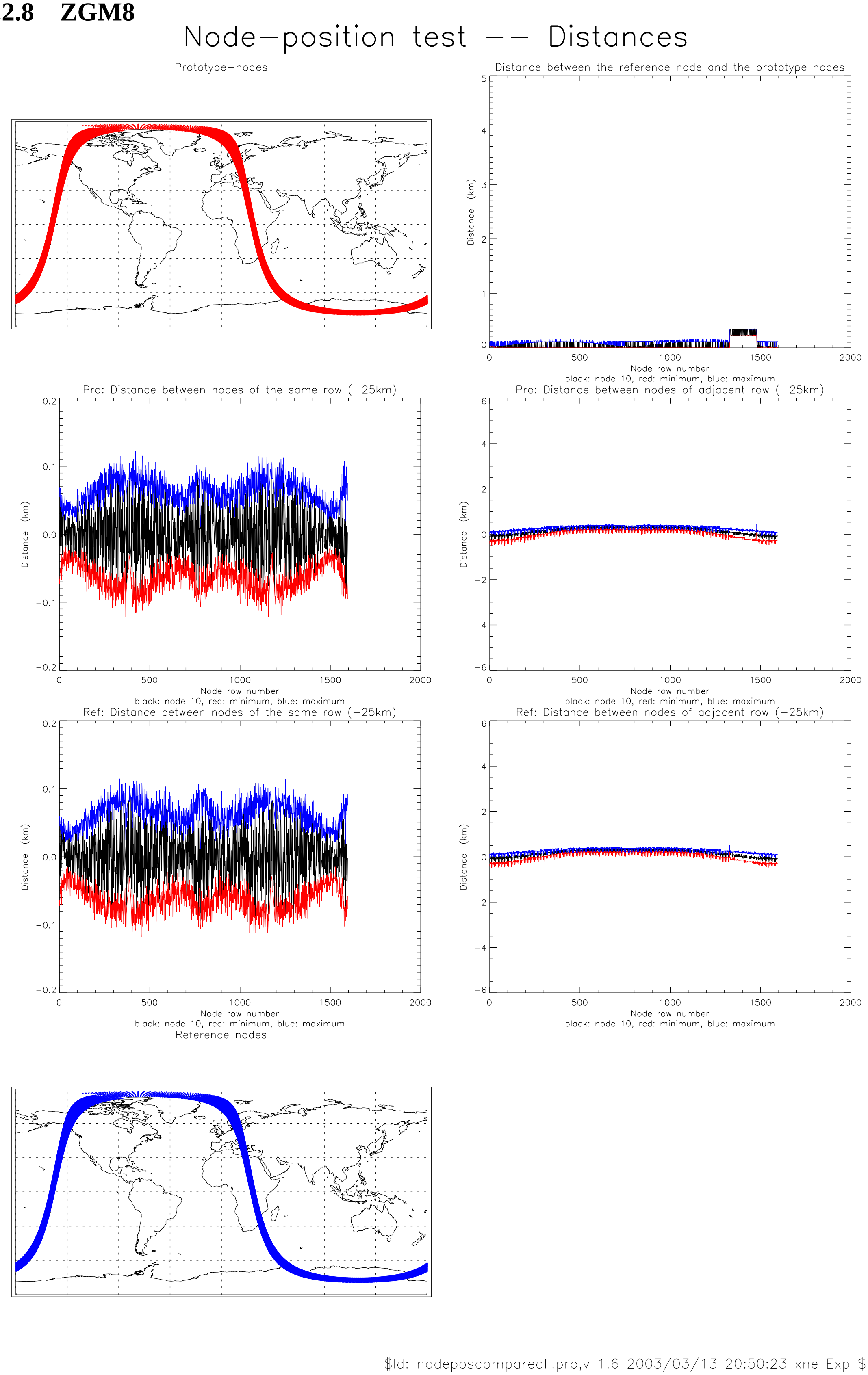


Figure B.16: Report for ZGM8

## Appendix C

# Angle comparison – complete results

## C.1 YSM2

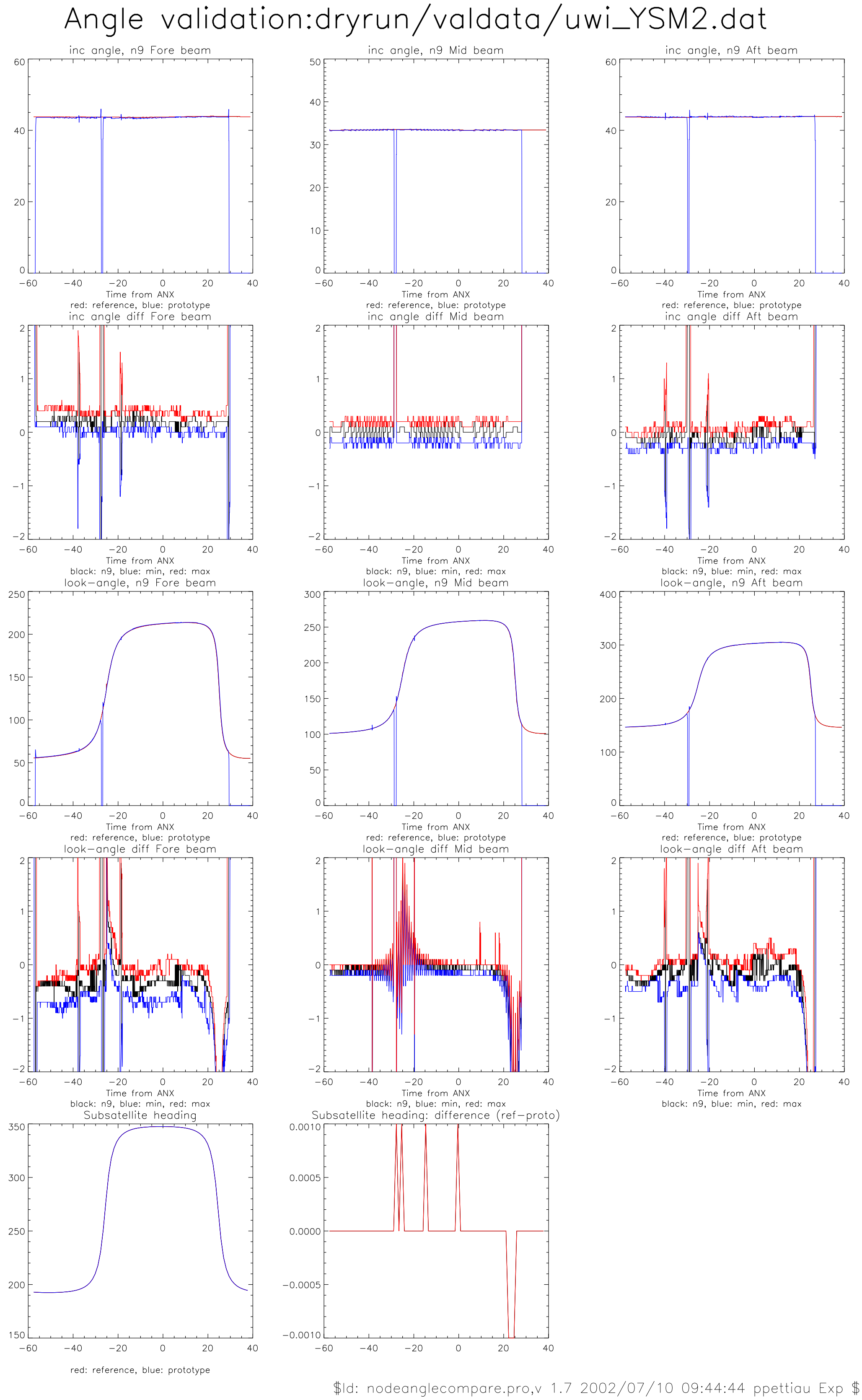


Figure C.1: Report for YSM2

## C.2 YSM3

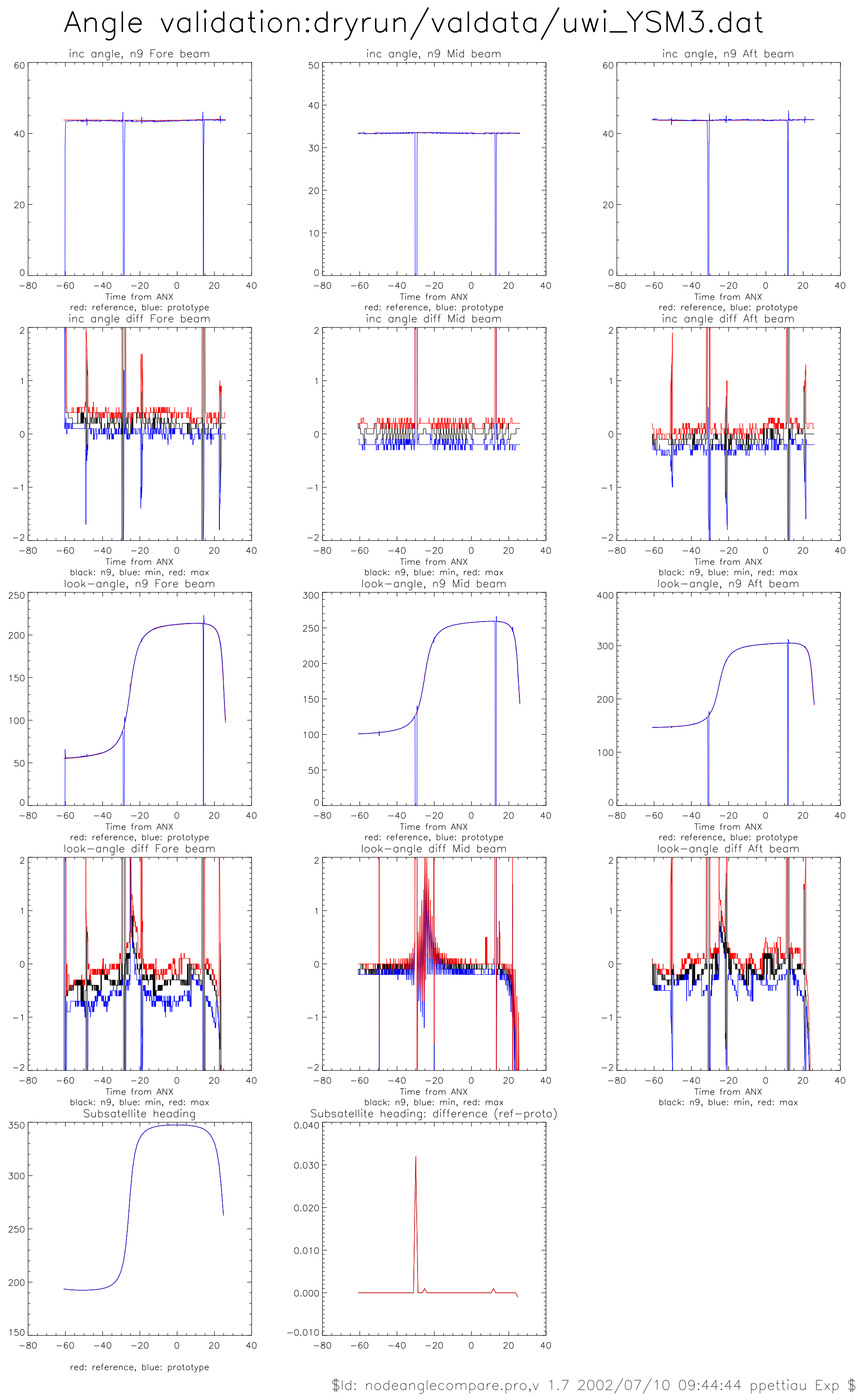


Figure C.2: Report for YSM3

## C.3 YSM4

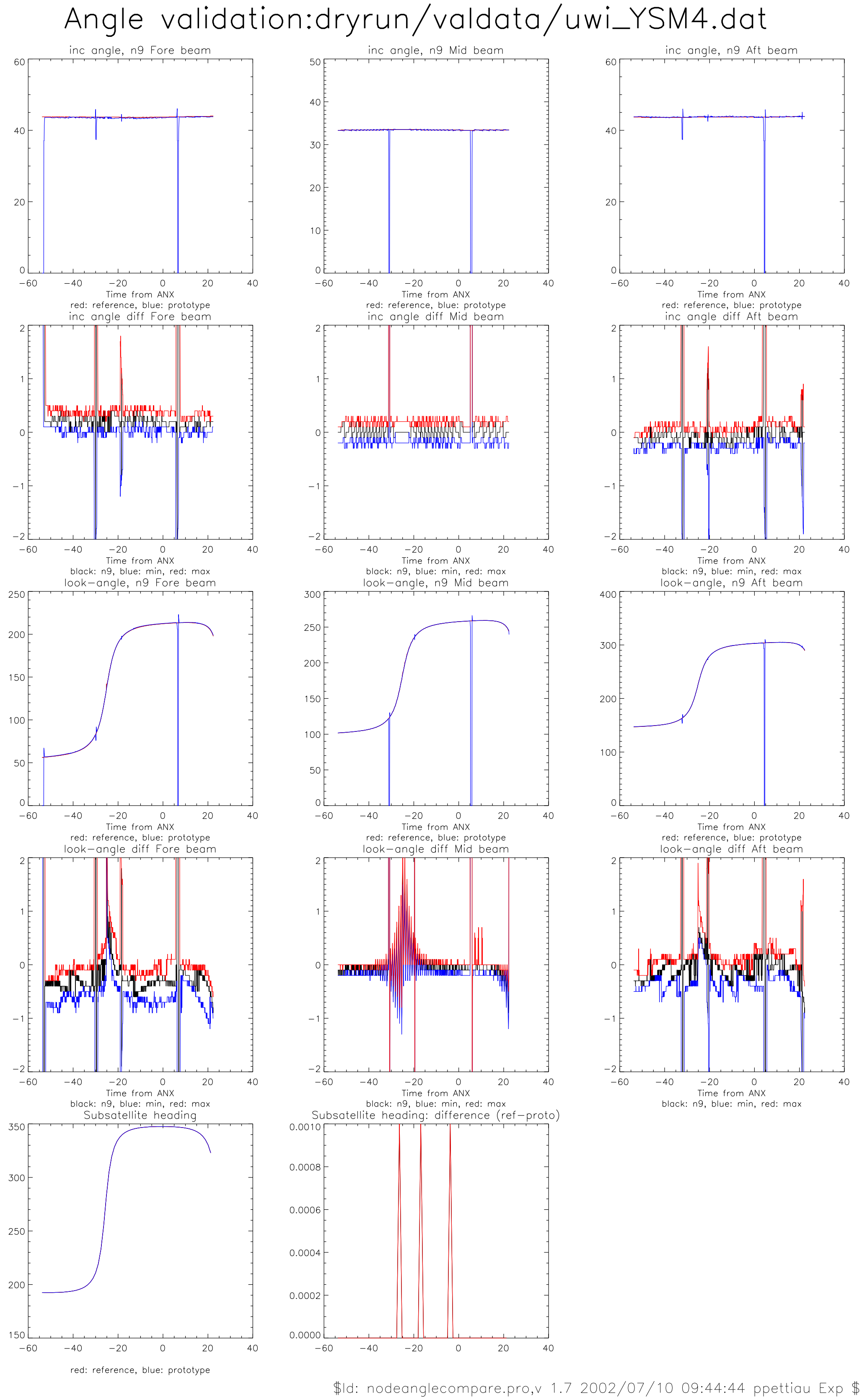


Figure C.3: Report for YSM4

## C.4 YSM5

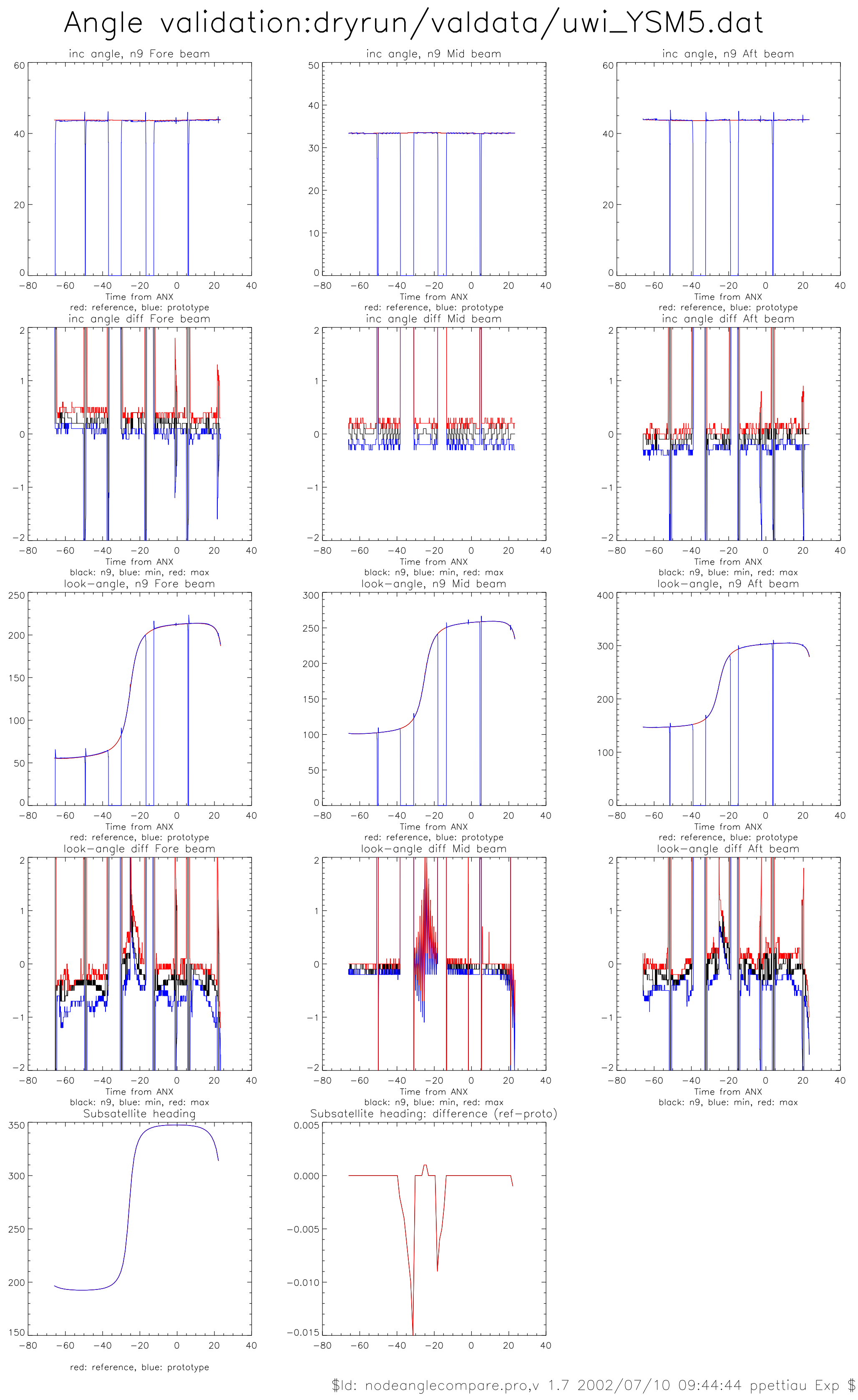


Figure C.4: Report for YSM5

## C.5 YSM6

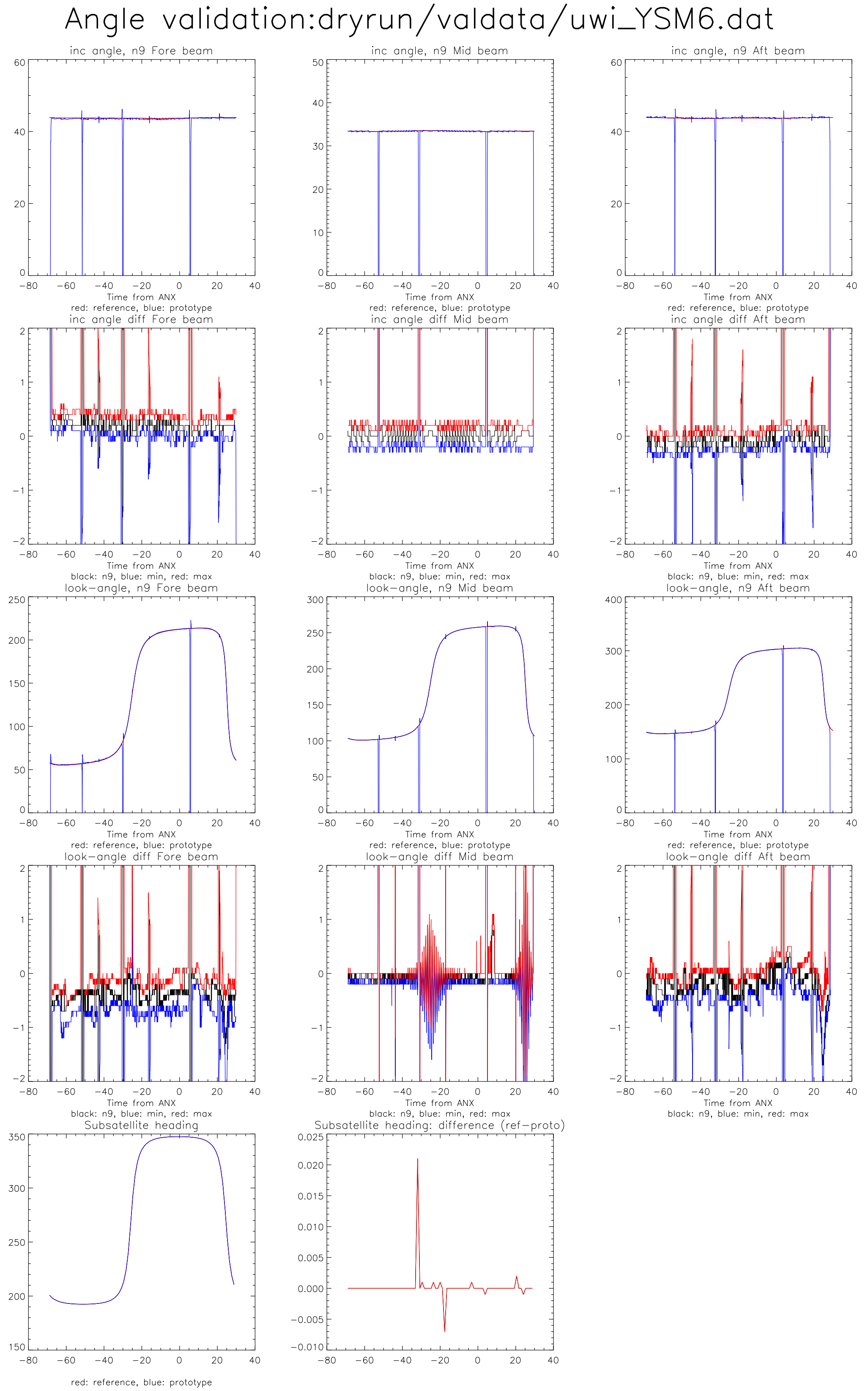


Figure C.5: Report for YSM6

## C.6 YSM7

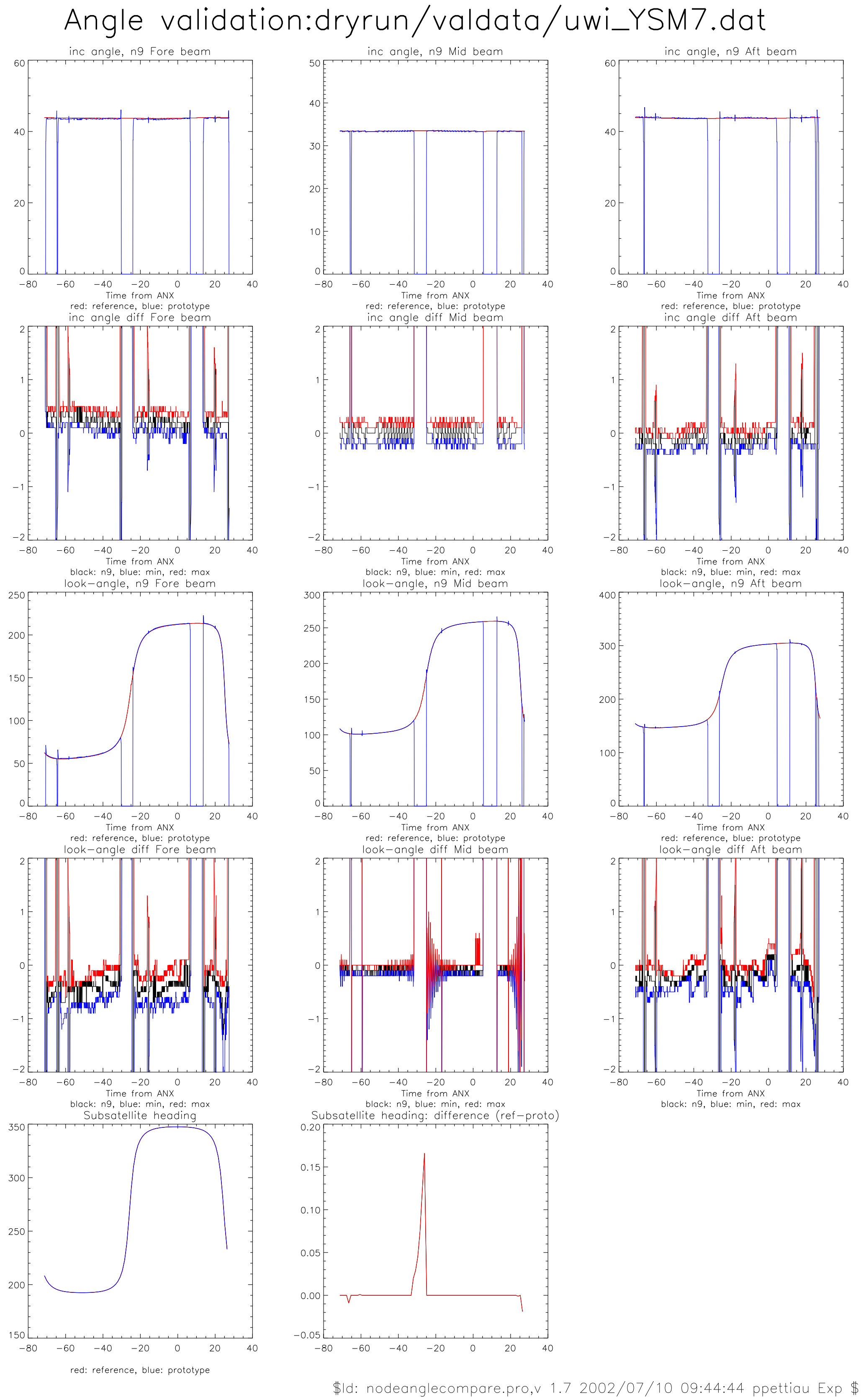


Figure C.6: Report for YSM7

## C.7 YSM8

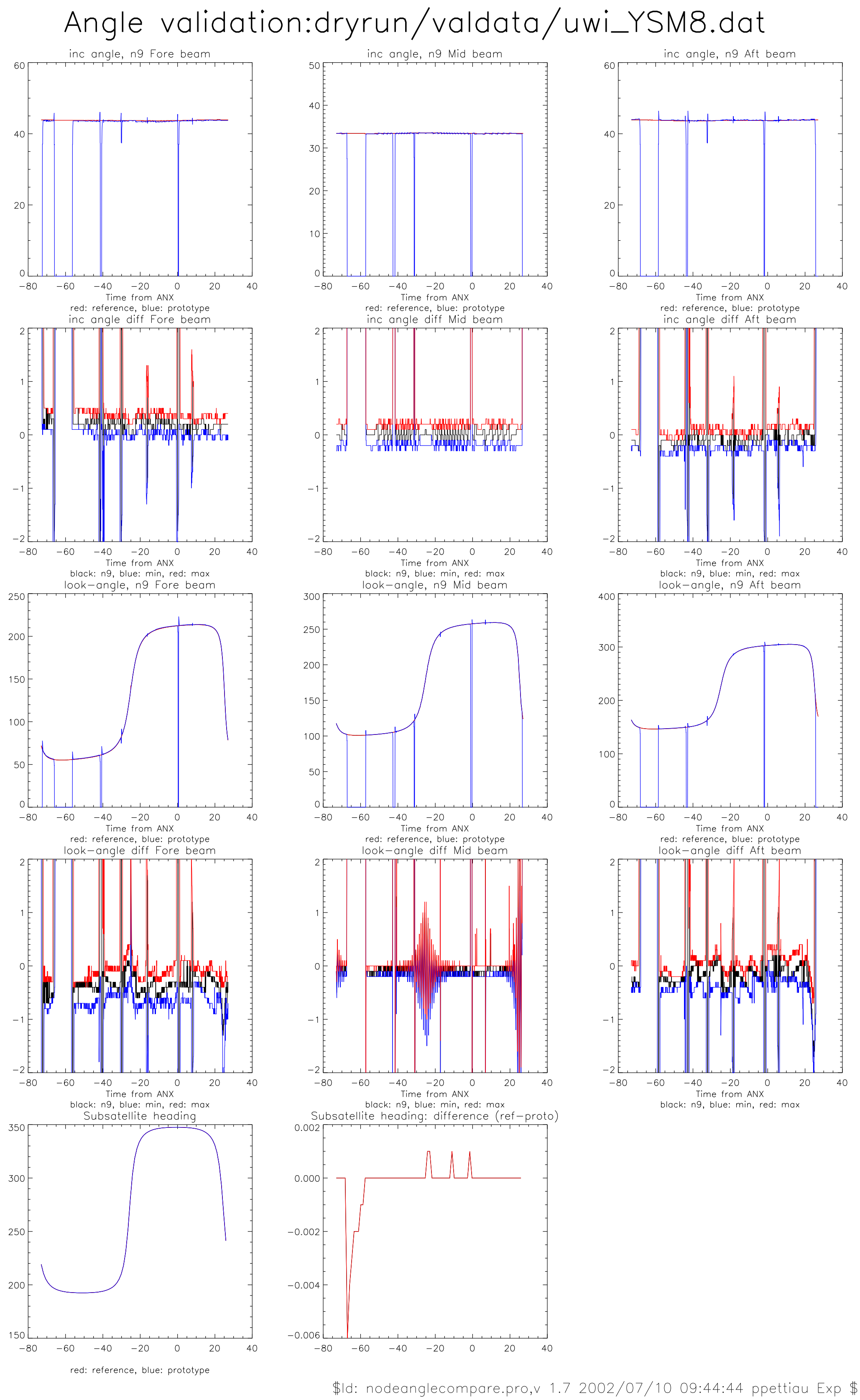


Figure C.7: Report for YSM8

## C.8 YSM9

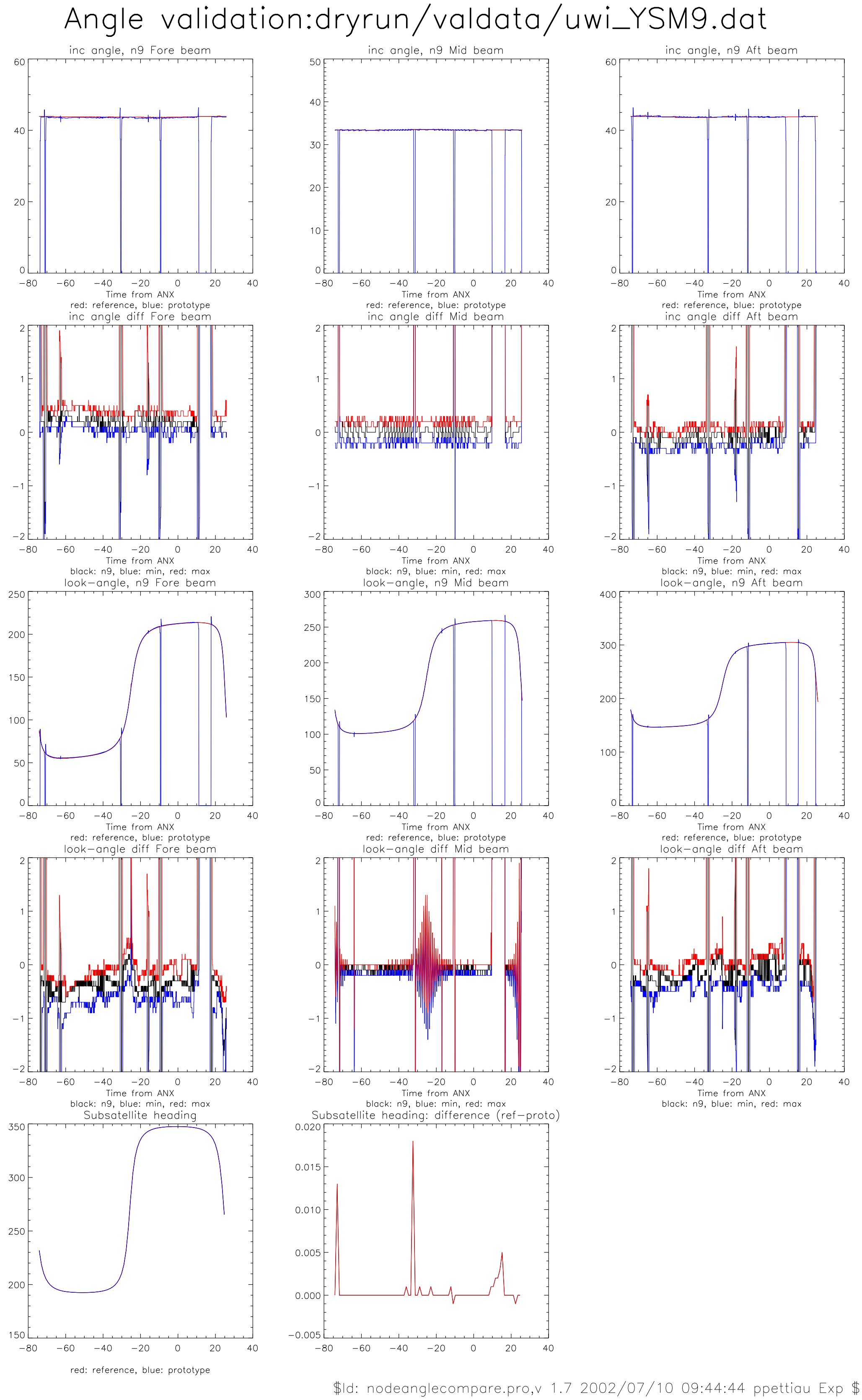


Figure C.8: Report for YSM9

## Appendix D

# Sigma 0 comparison – nominal cases – complete results

## D.1 YSM2

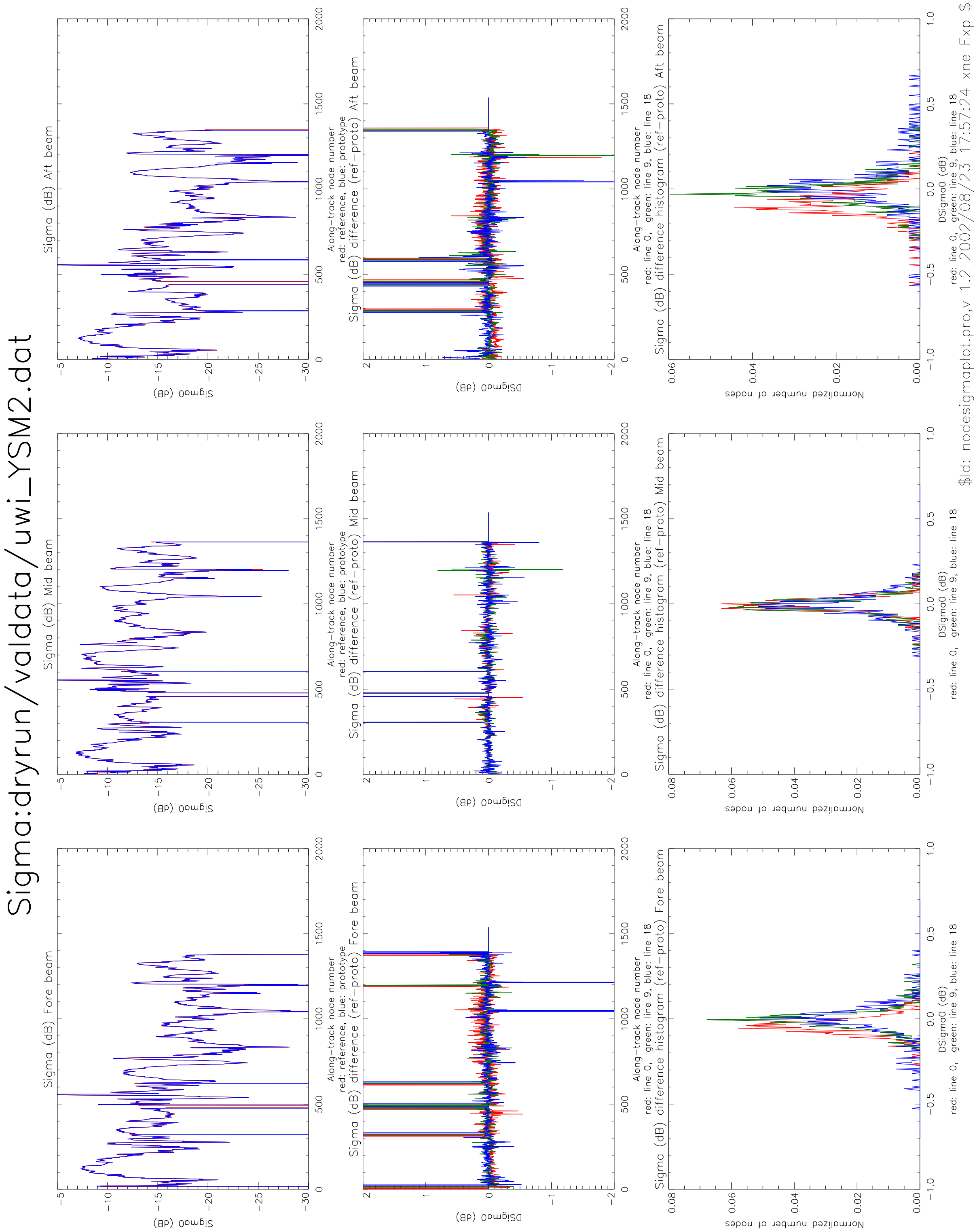


Figure D.1: Report for YSM2

## D.2 YSM3

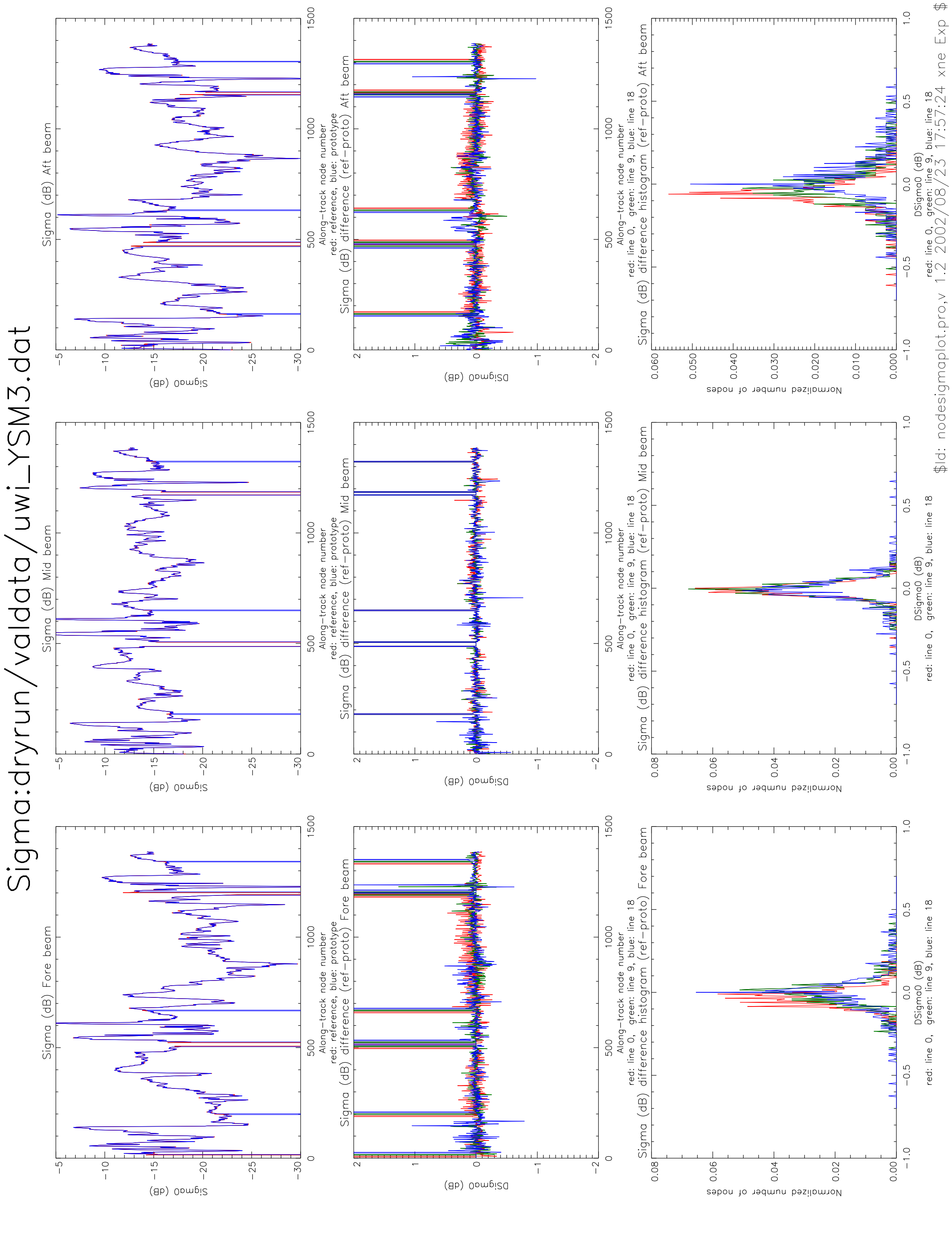


Figure D.2: Report for YSM3

## D.3 YSM4

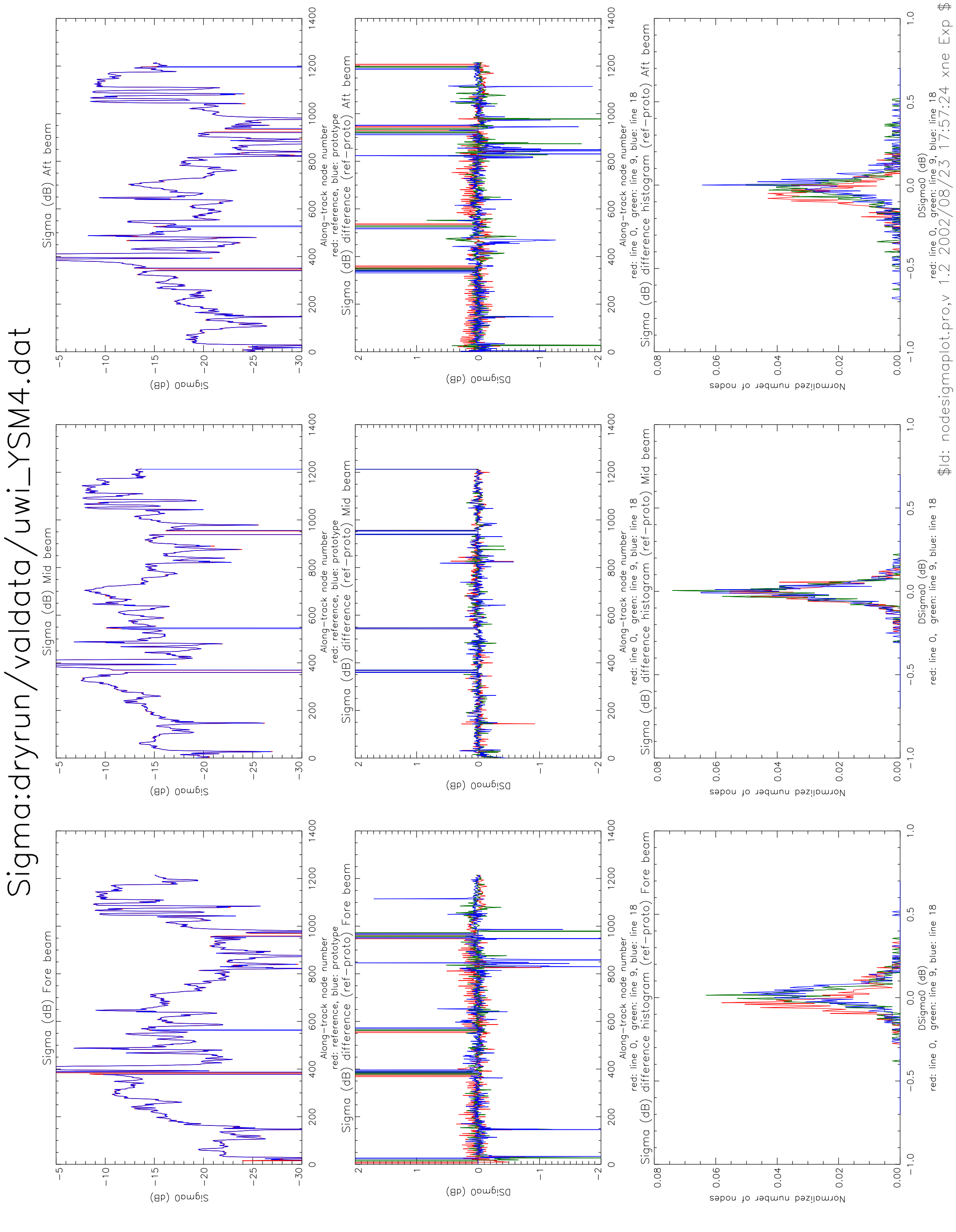


Figure D.3: Report for YSM4

## D.4 YSM5

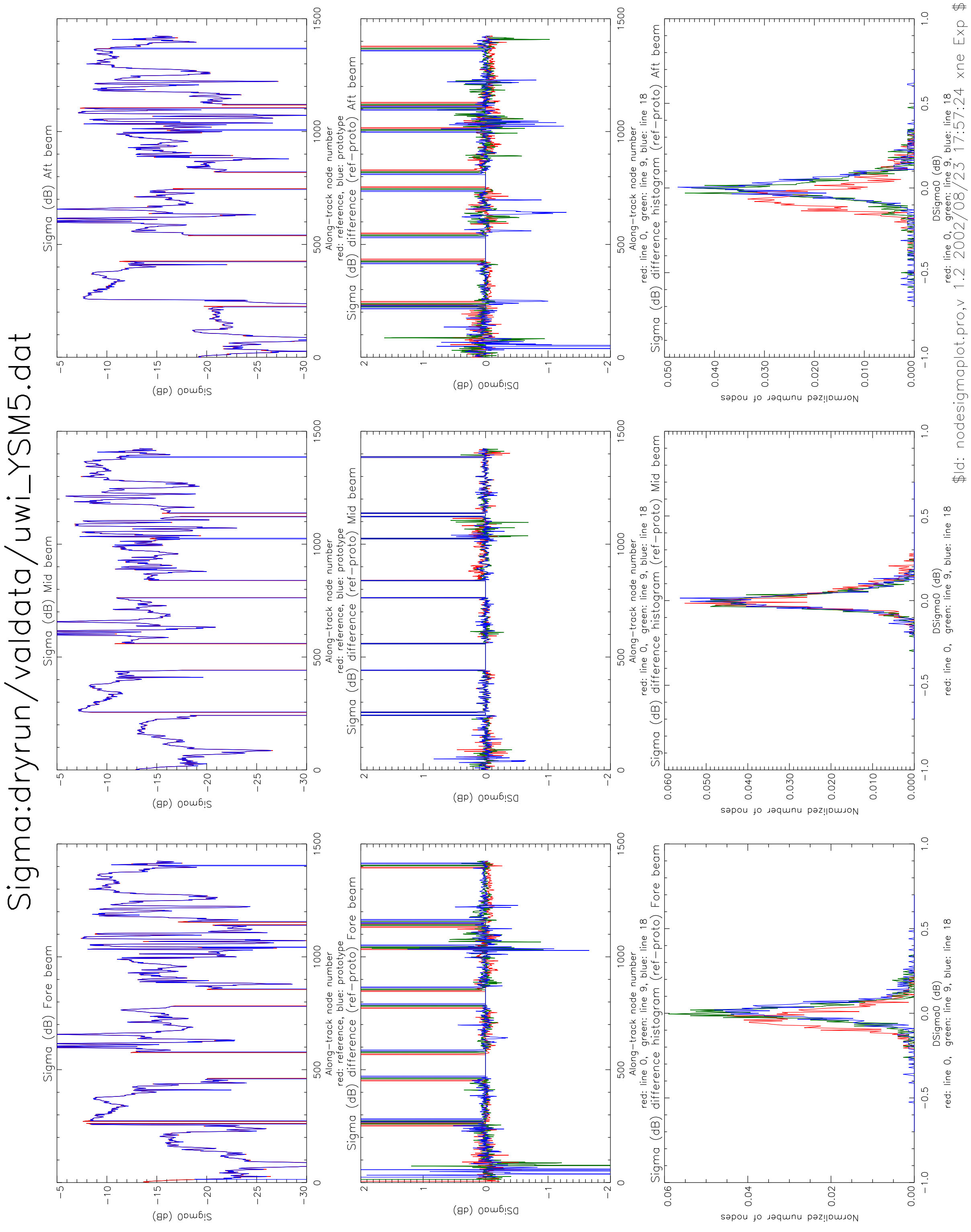

Figure D.4: Report for YSM5

## D.5 YSM6

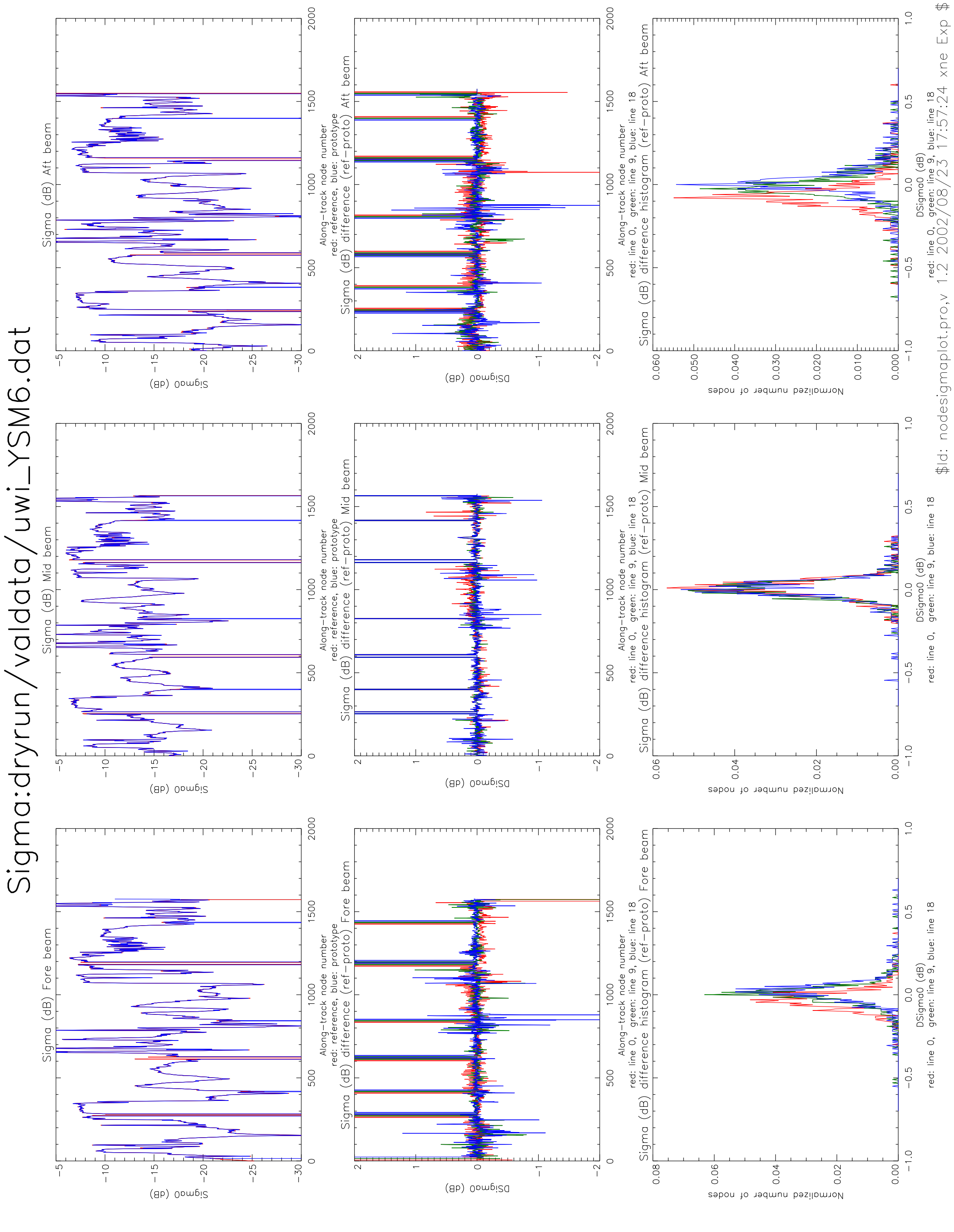


Figure D.5: Report for YSM6

## D.6 YSM7

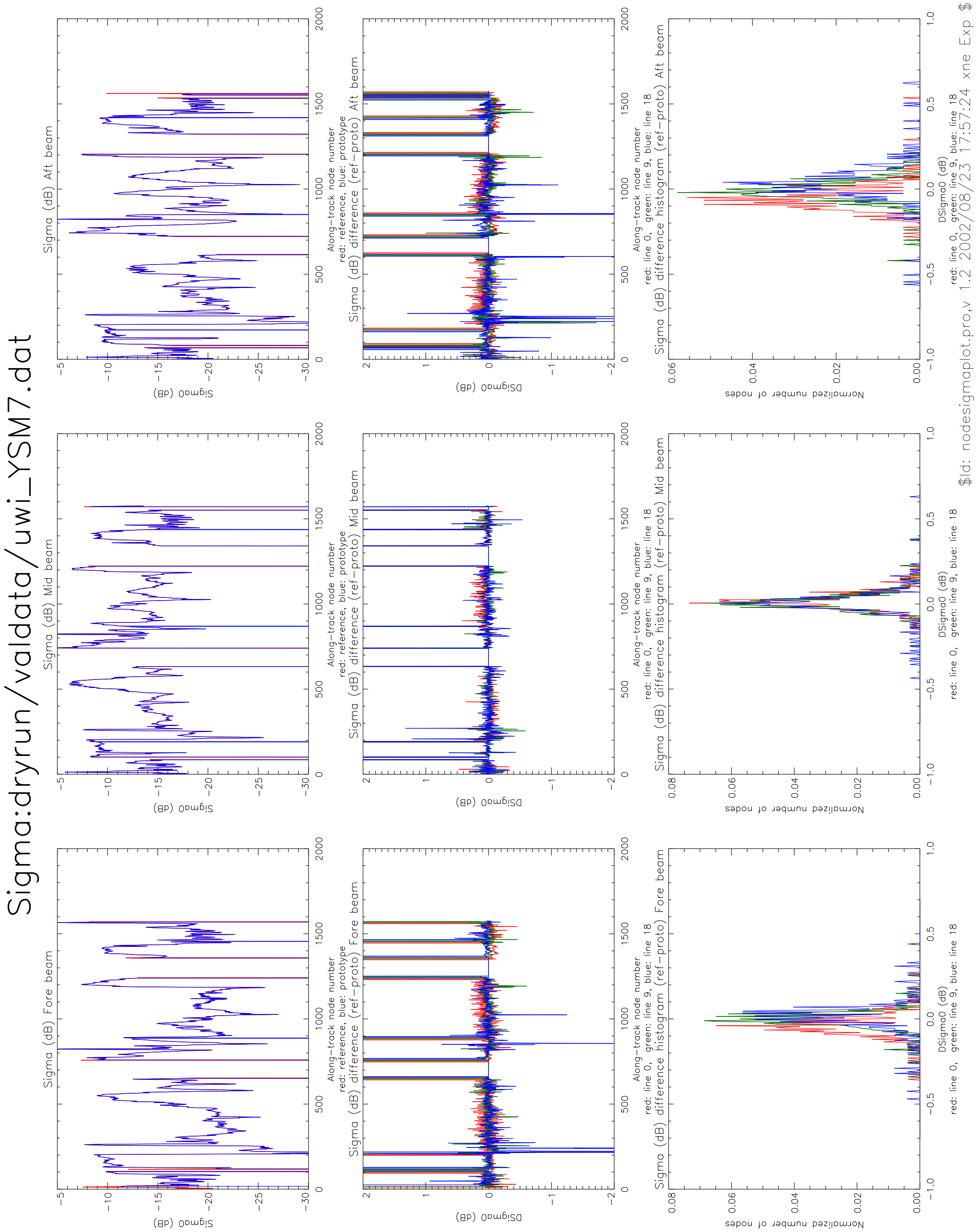


Figure D.6: Report for YSM7

## D.7 YSM8

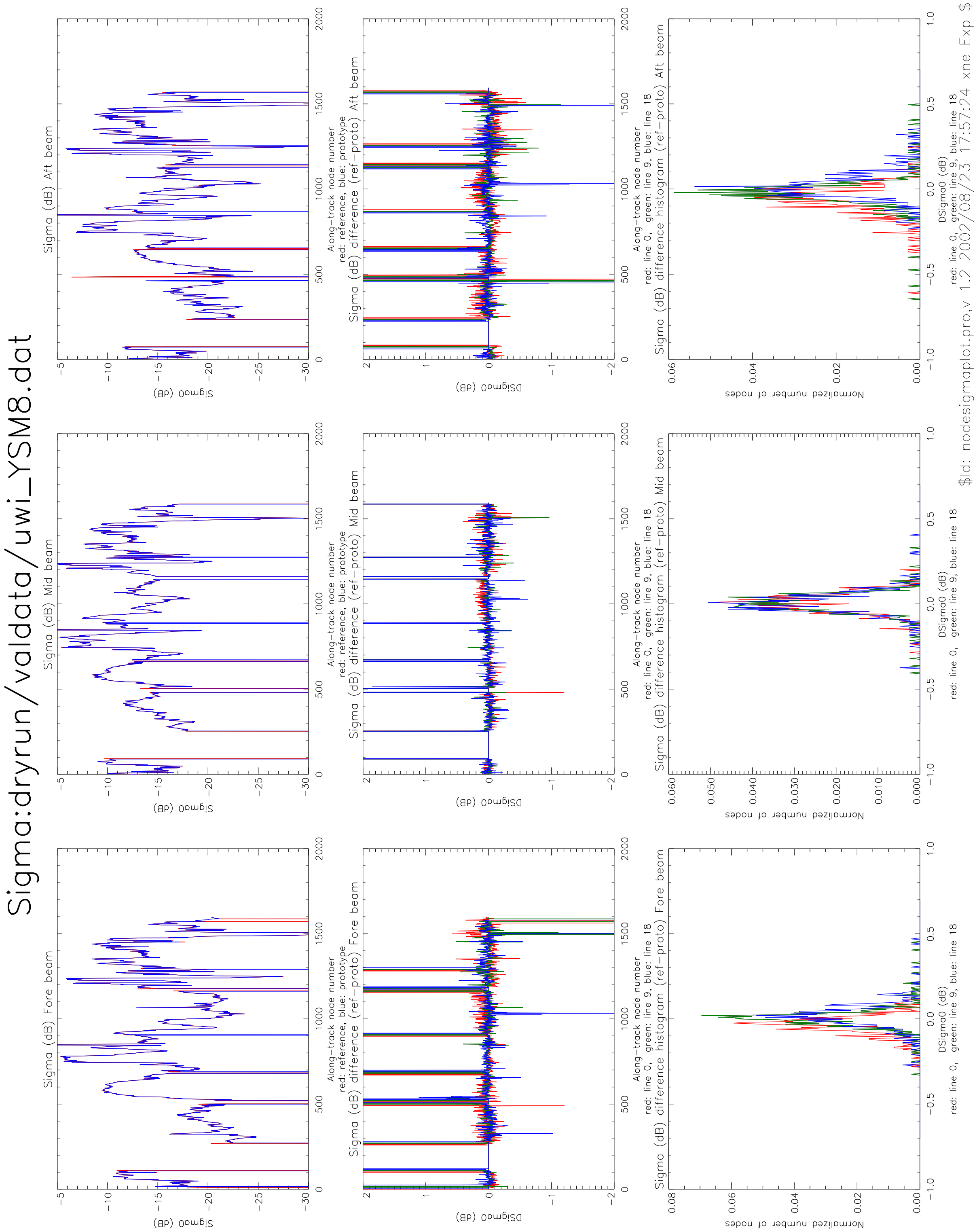


Figure D.7: Report for YSM8

## D.8 YSM9

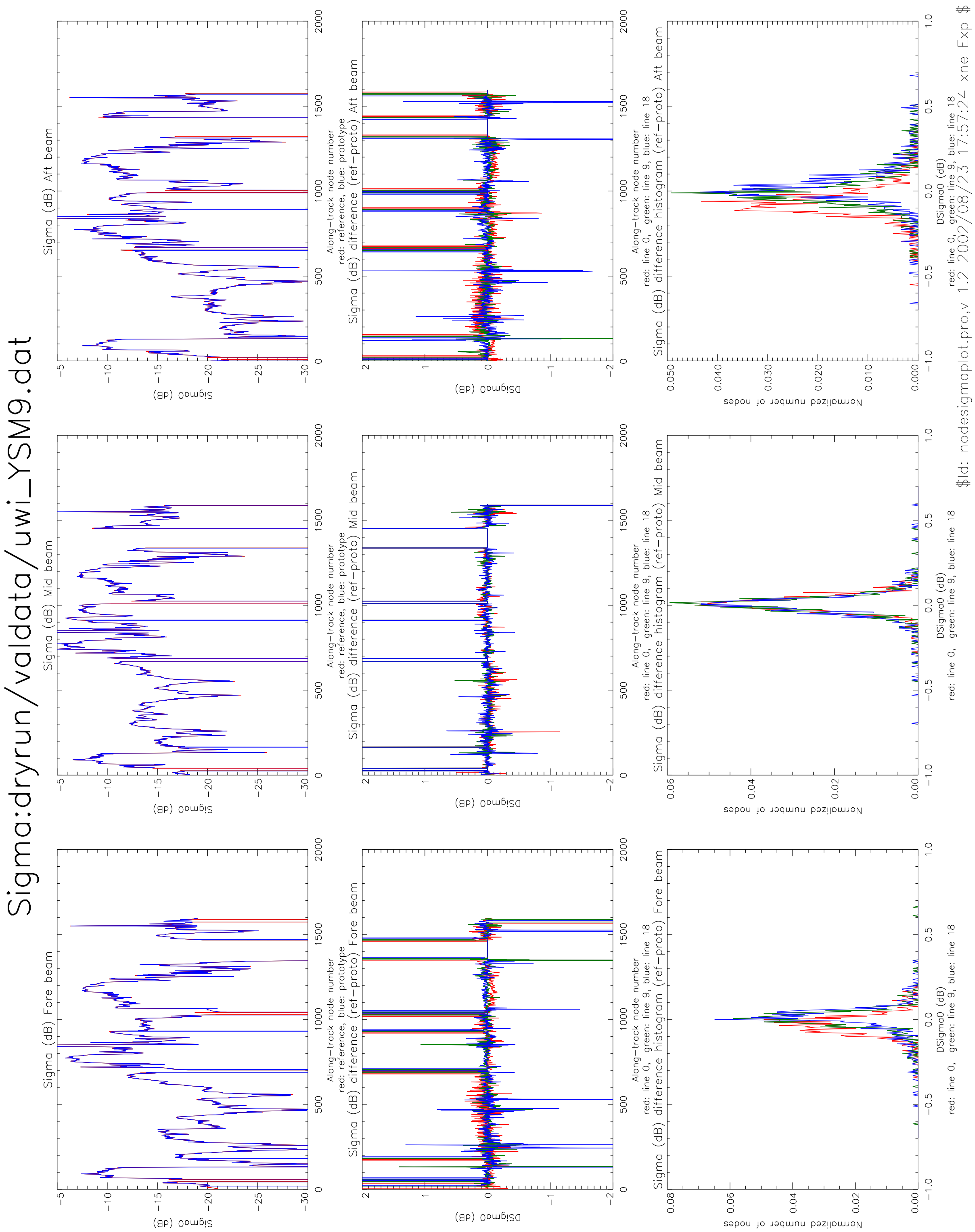


Figure D.8: Report for YSM9

## D.9 Biases

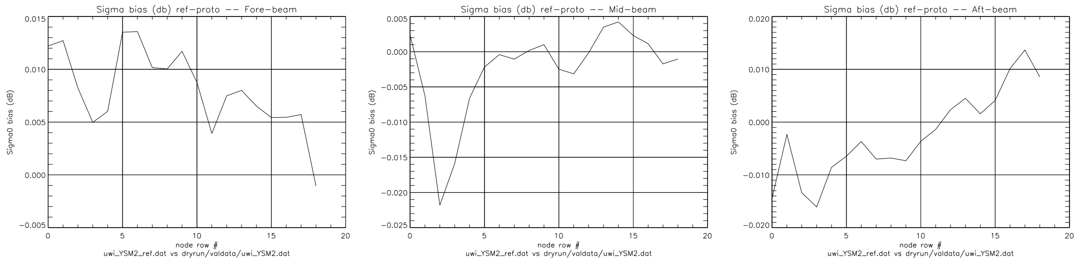


Figure D.9: Bias for YSM2

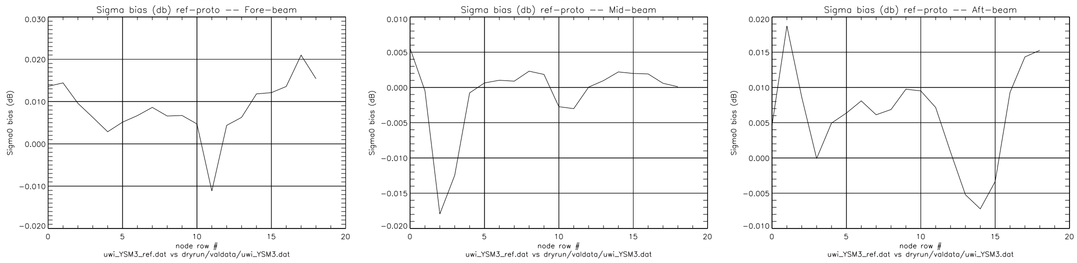


Figure D.10: Bias for YSM3

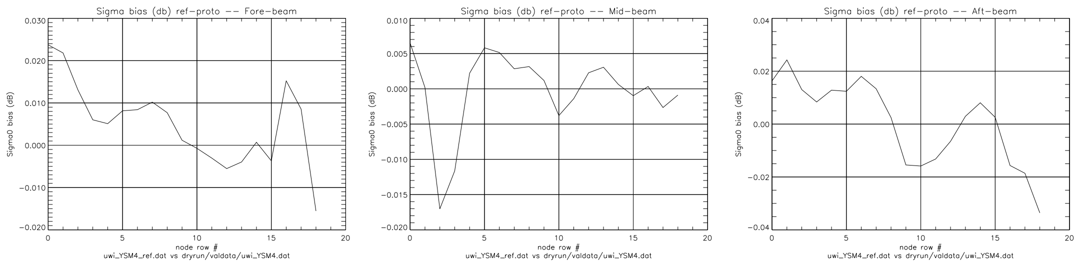


Figure D.11: Bias for YSM4

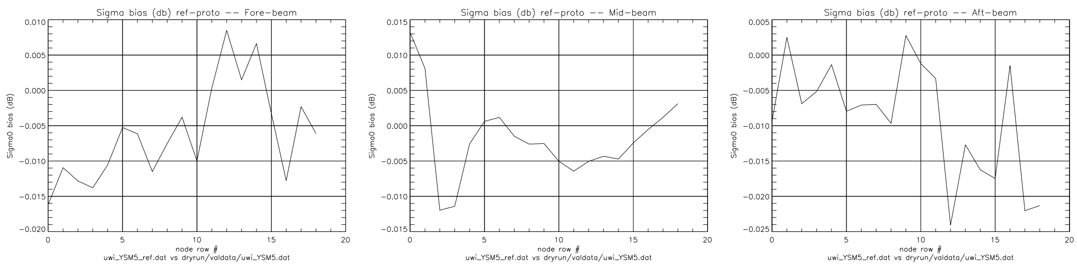


Figure D.12: Bias for YSM5

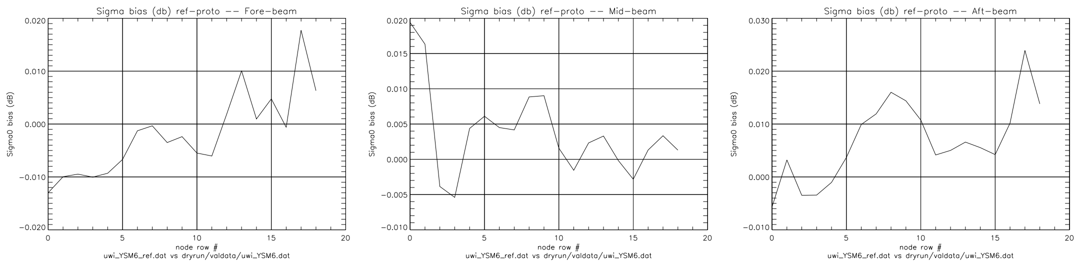


Figure D.13: Bias for YSM6

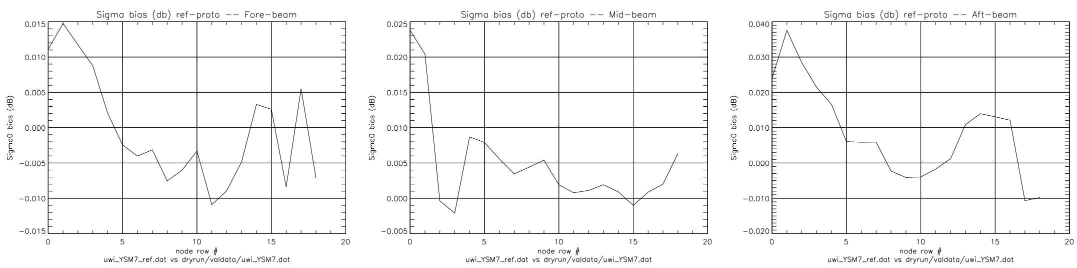


Figure D.14: Bias for YSM7

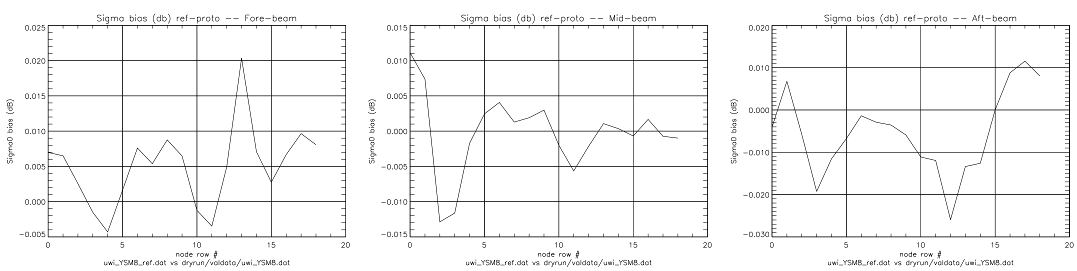


Figure D.15: Bias for YSM8

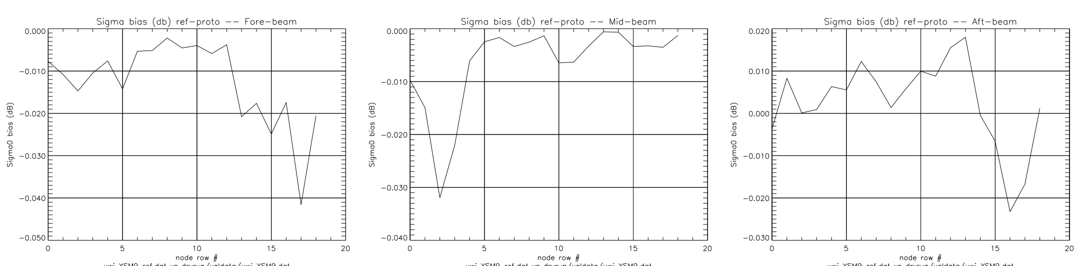


Figure D.16: Bias for YSM9

## Appendix E

# Sigma 0 comparison – non-nominal cases – complete results

## E.1 FPM orbits

### E.1.1 FPM1

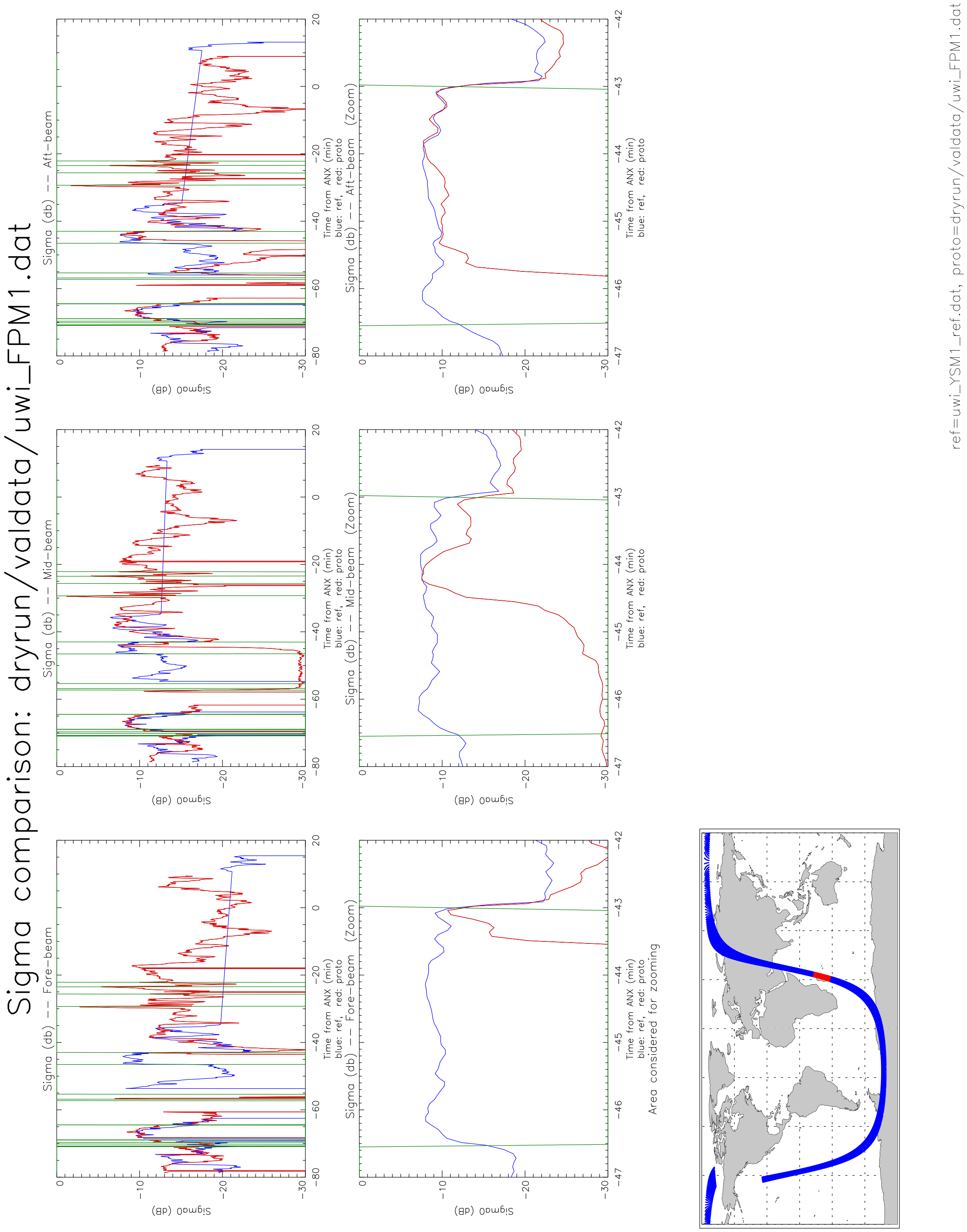


Figure E.1: Report for YSM1/FPM1

### E.1.2 FPM2

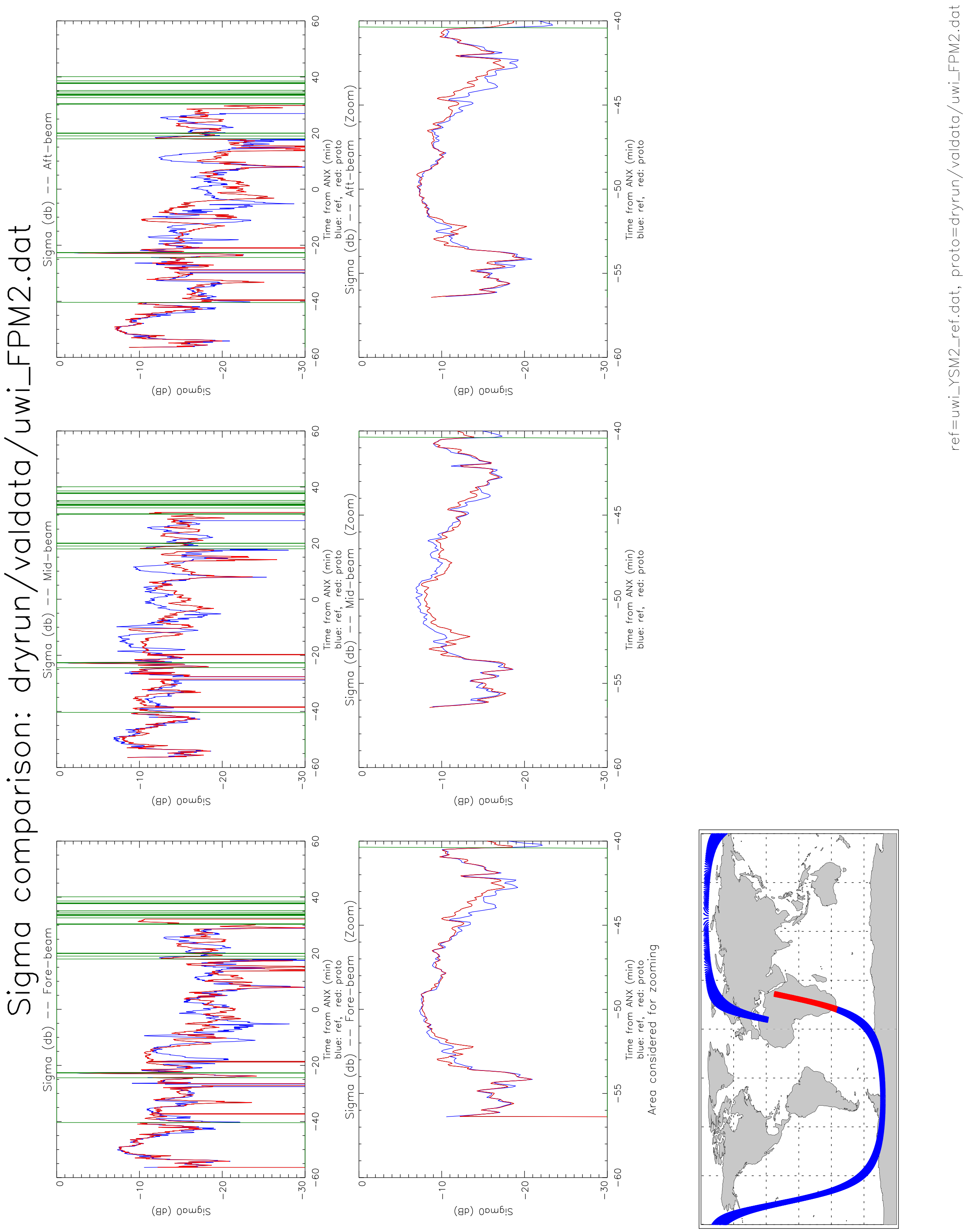


Figure E.2: Report for YSM2/FPM2

### E.1.3 FPM3

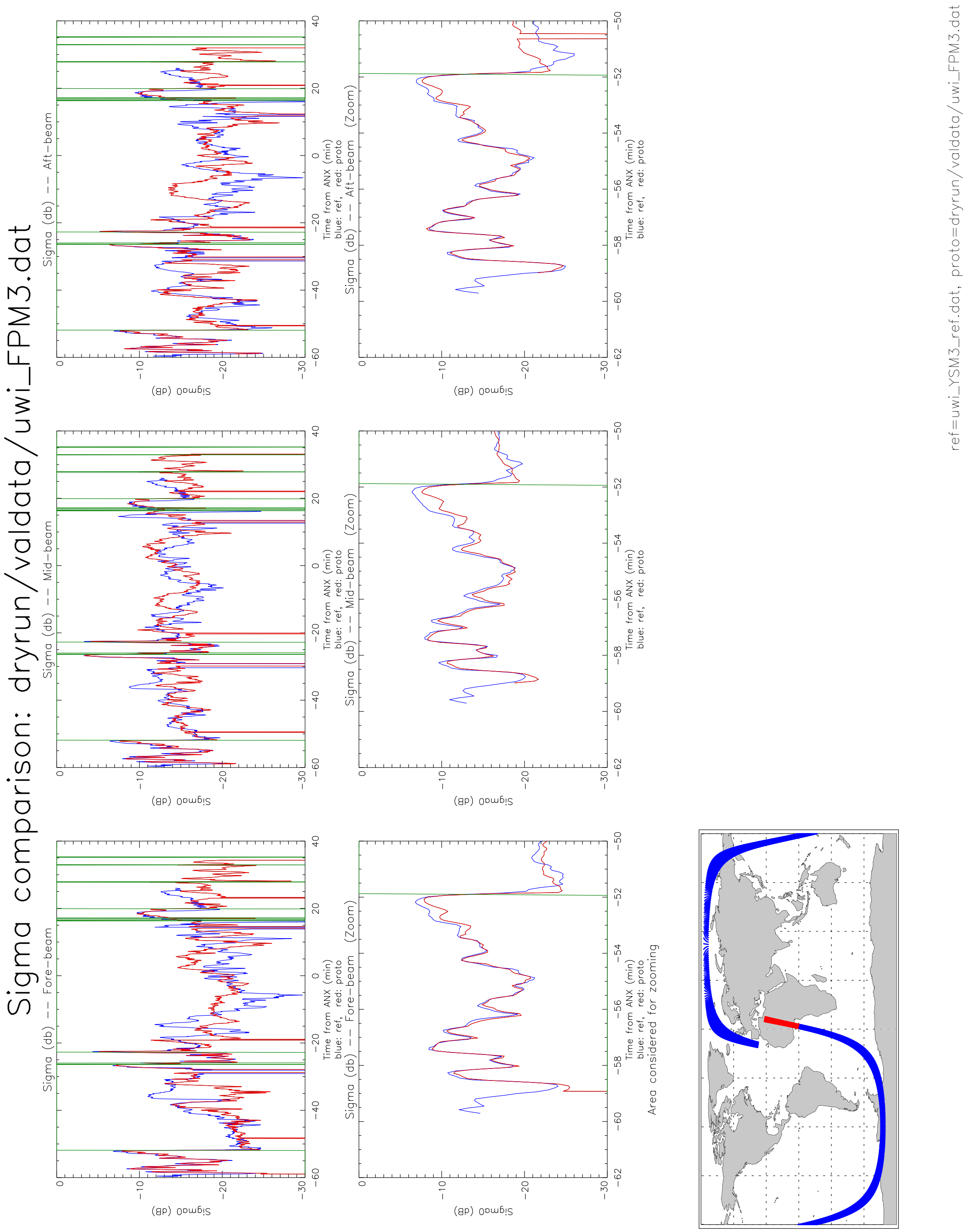


Figure E.3: Report for YSM3/FPM3

## E.1.4 FPM4

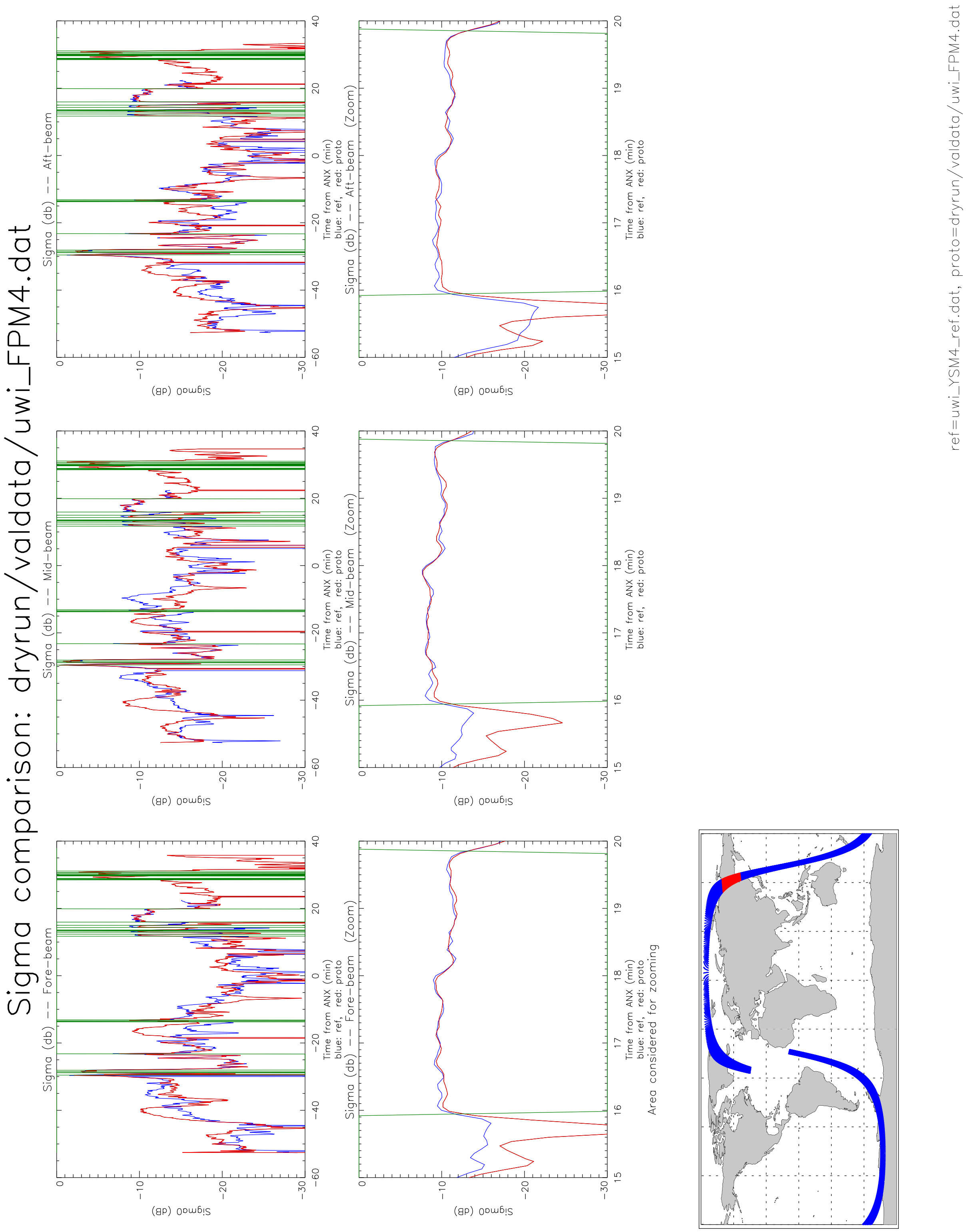


Figure E.4: Report for YSM4/FPM4

### E.1.5 FPM5

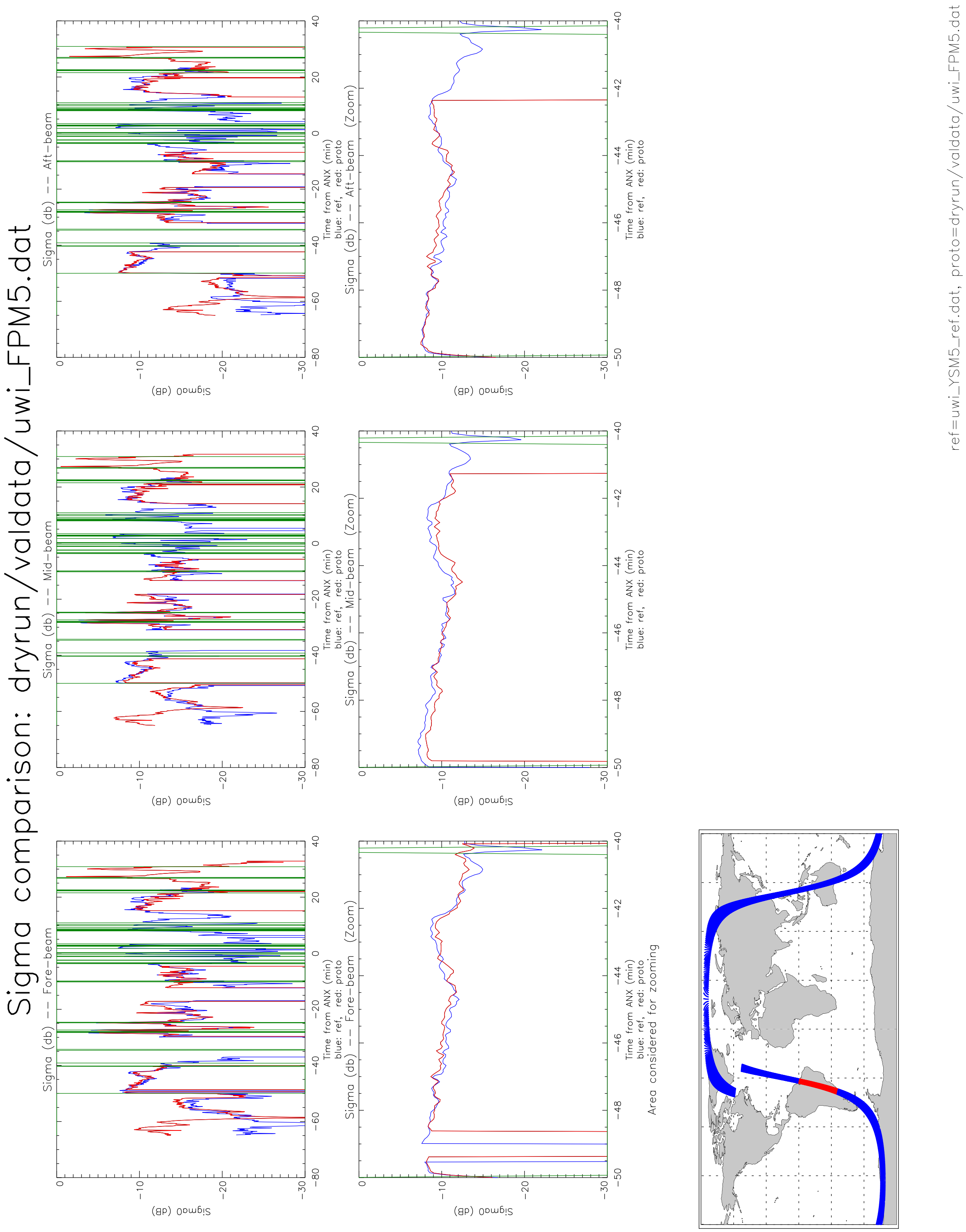


Figure E.5: Report for YSM5/FPM5

### E.1.6 FPM6

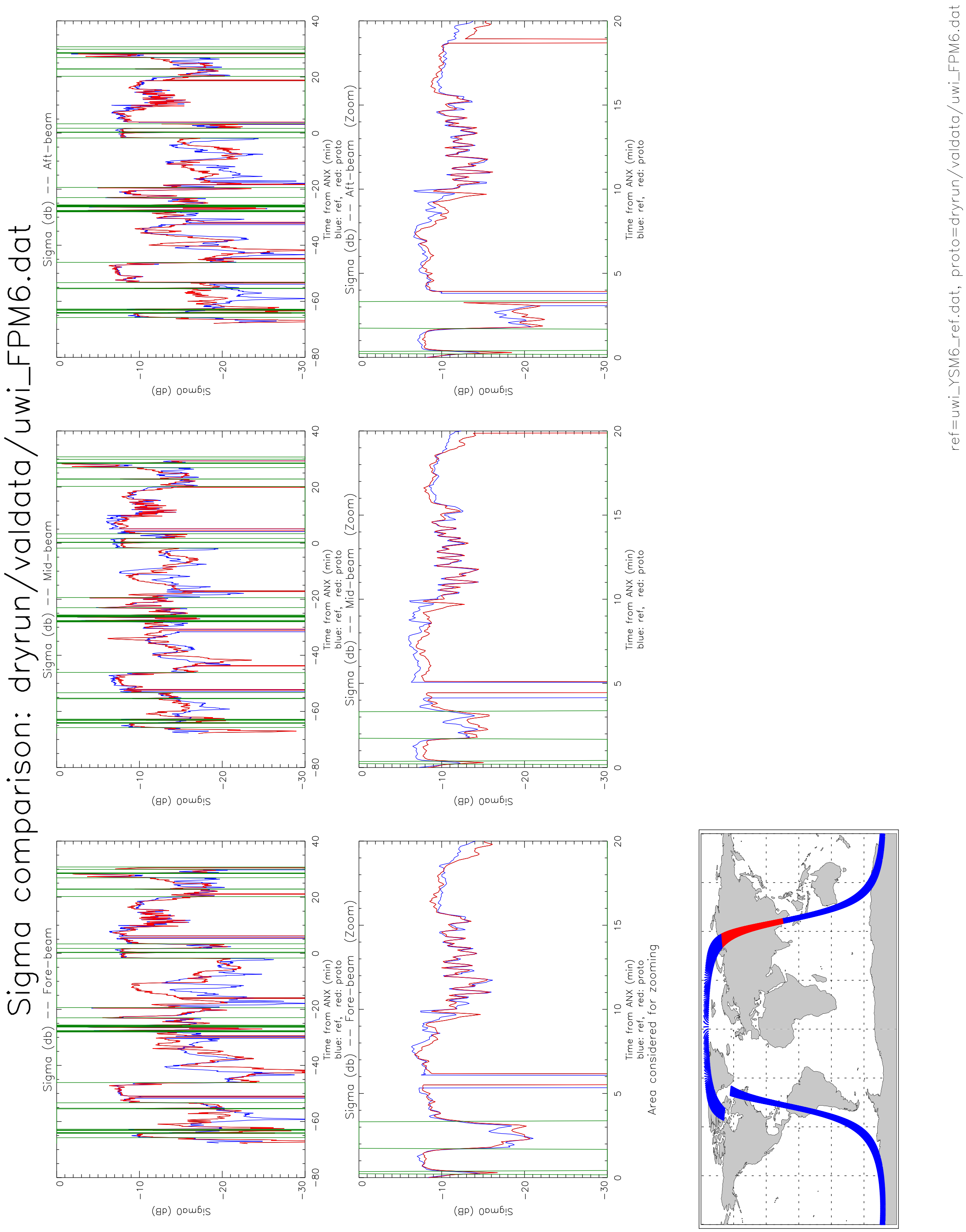


Figure E.6: Report for YSM6/FPM6

### E.1.7 FPM7

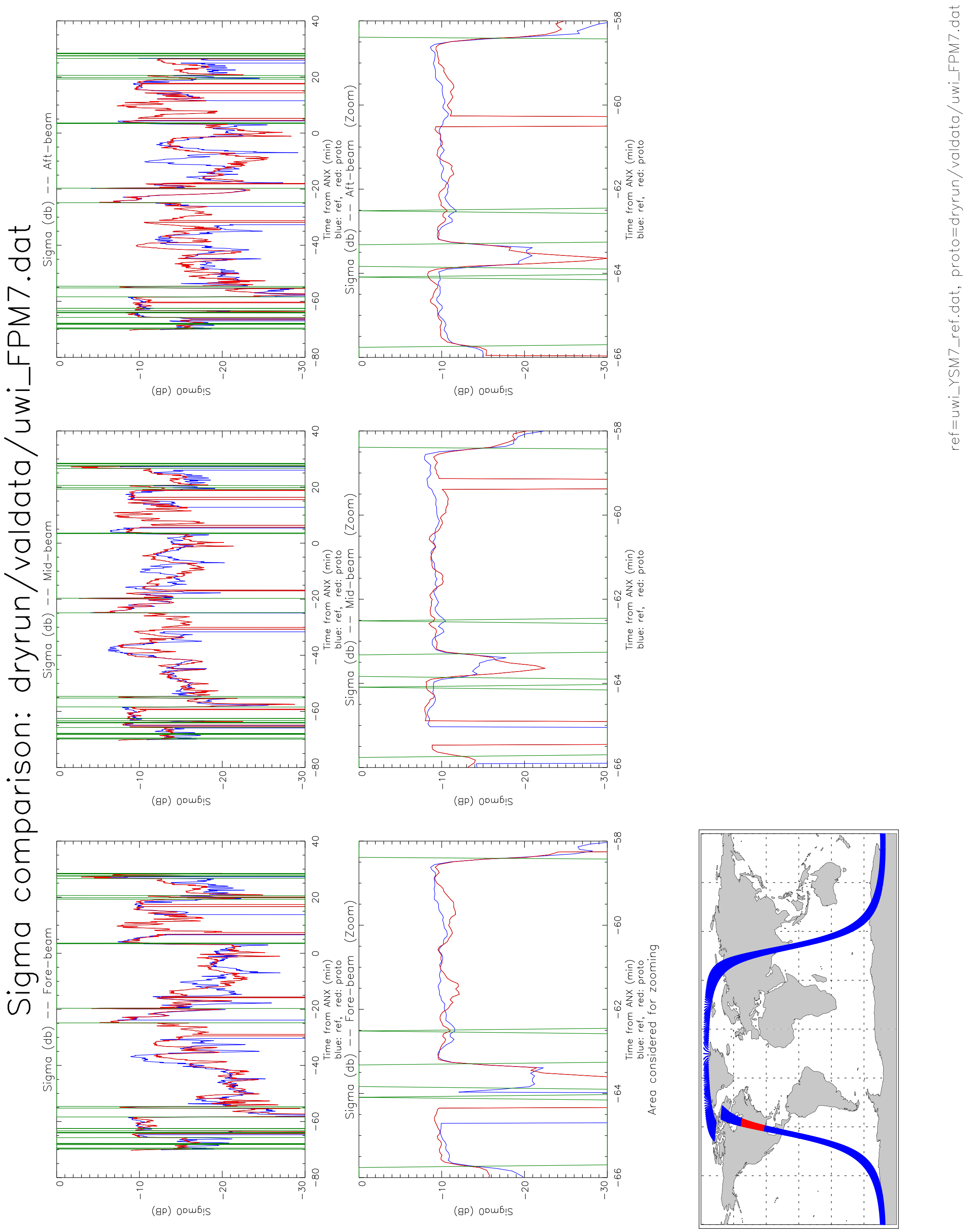


Figure E.7: Report for YSM7/FPM7

### E.1.8 FPM8

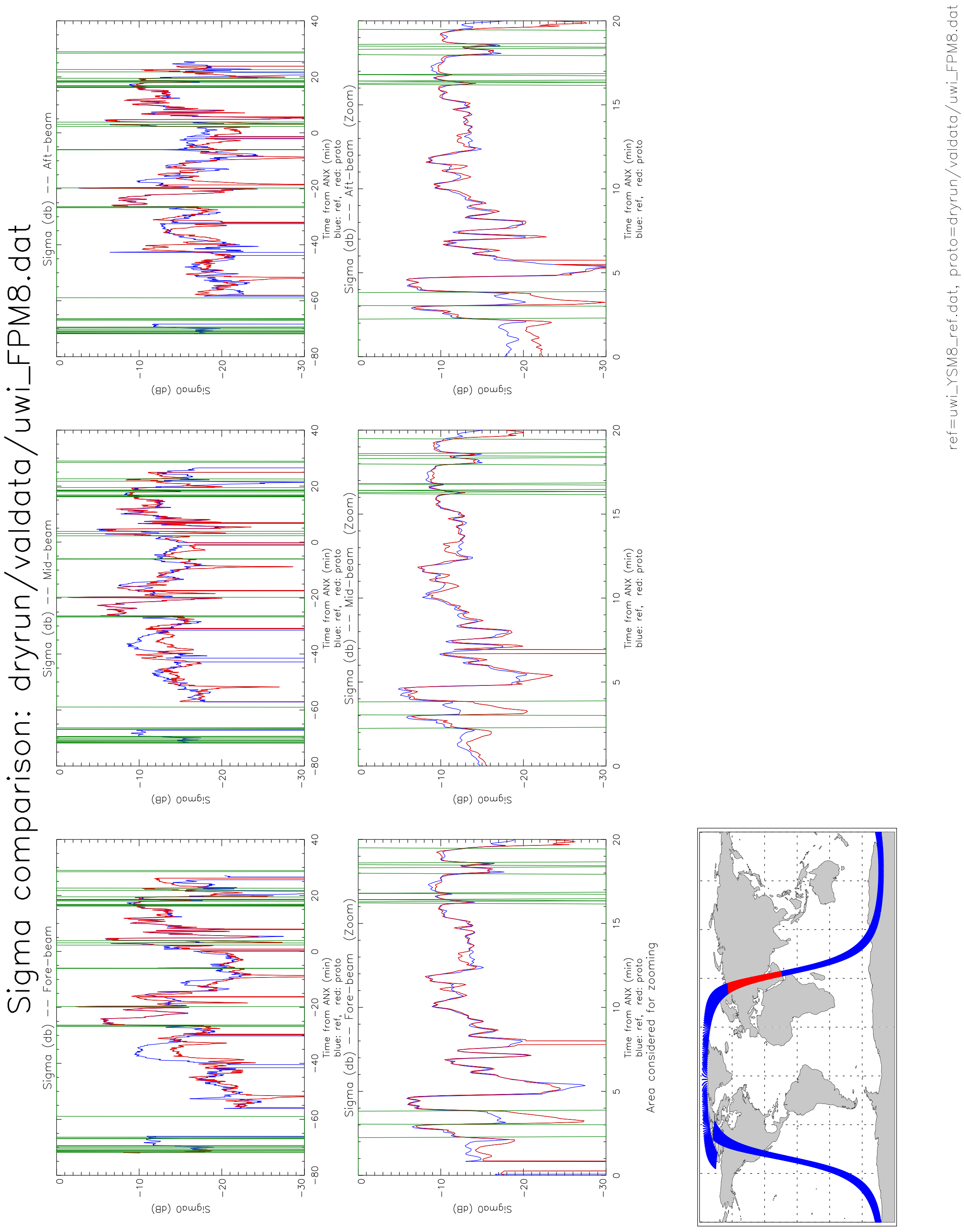


Figure E.8: Report for YSM8/FPM8

### E.1.9 FPM9

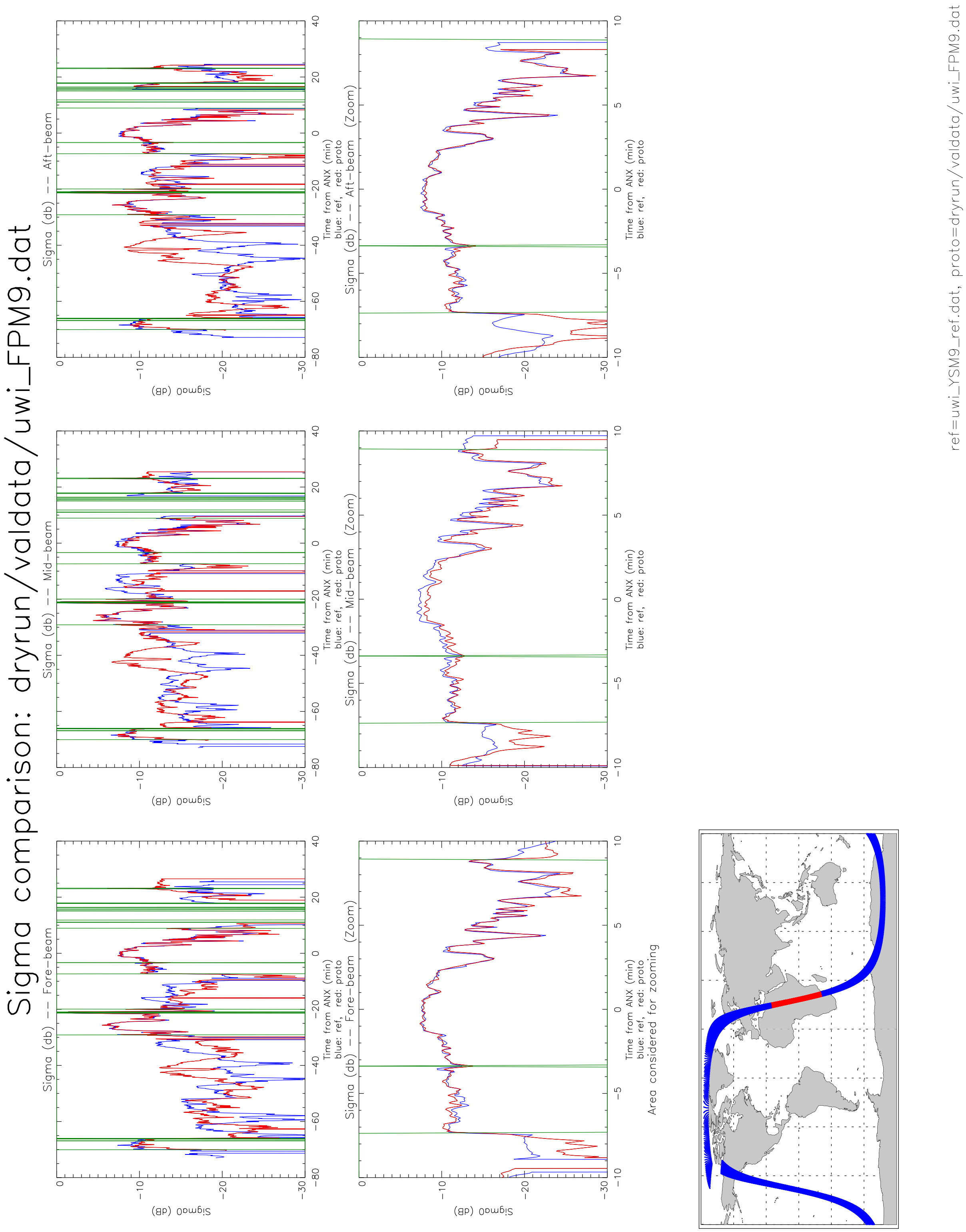


Figure E.9: Report for YSM9/FPM9

## E.2 ZGM orbits

### E.2.1 ZGM1

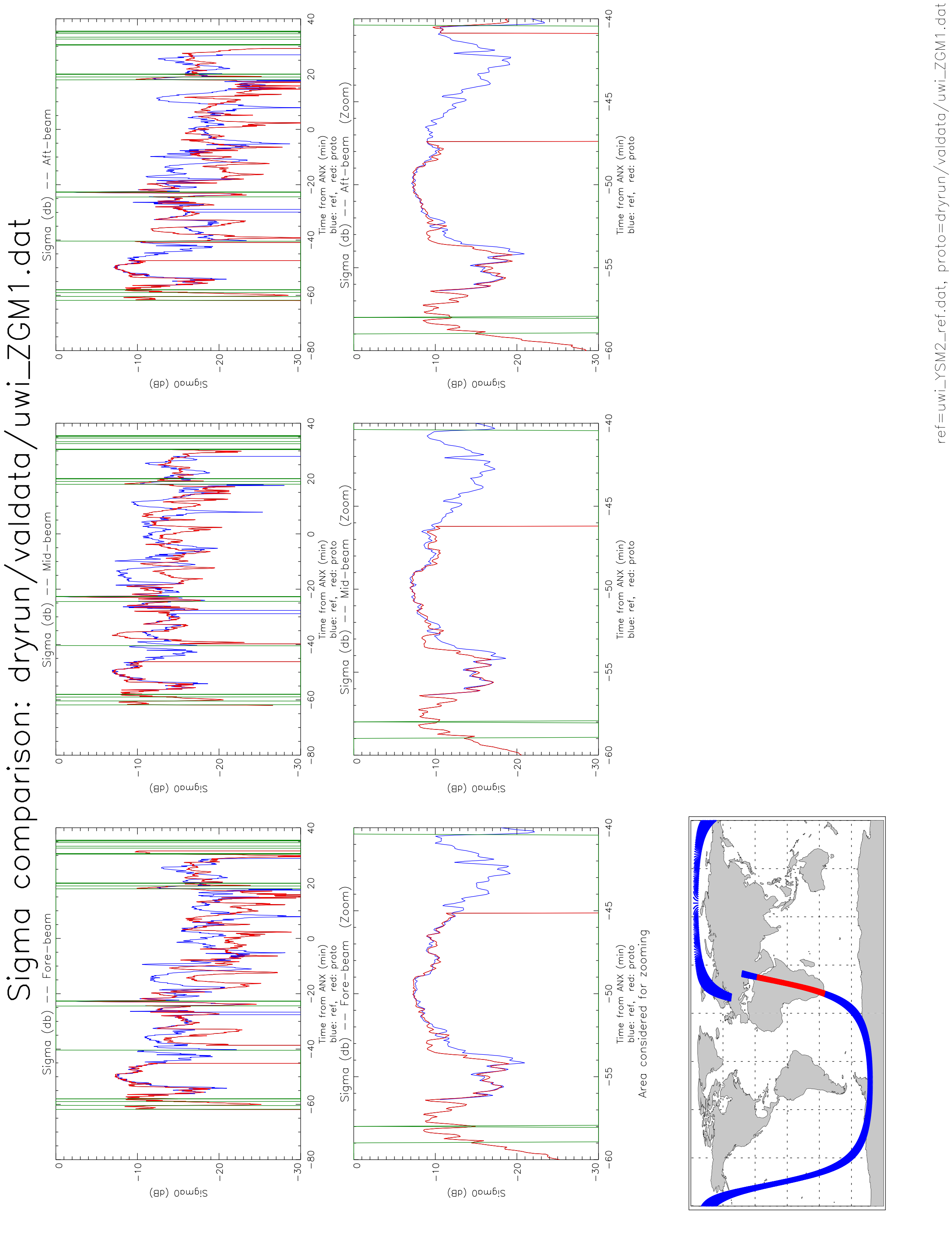


Figure E.10: Report for YSM2/ZGM1

### E.2.2 ZGM2

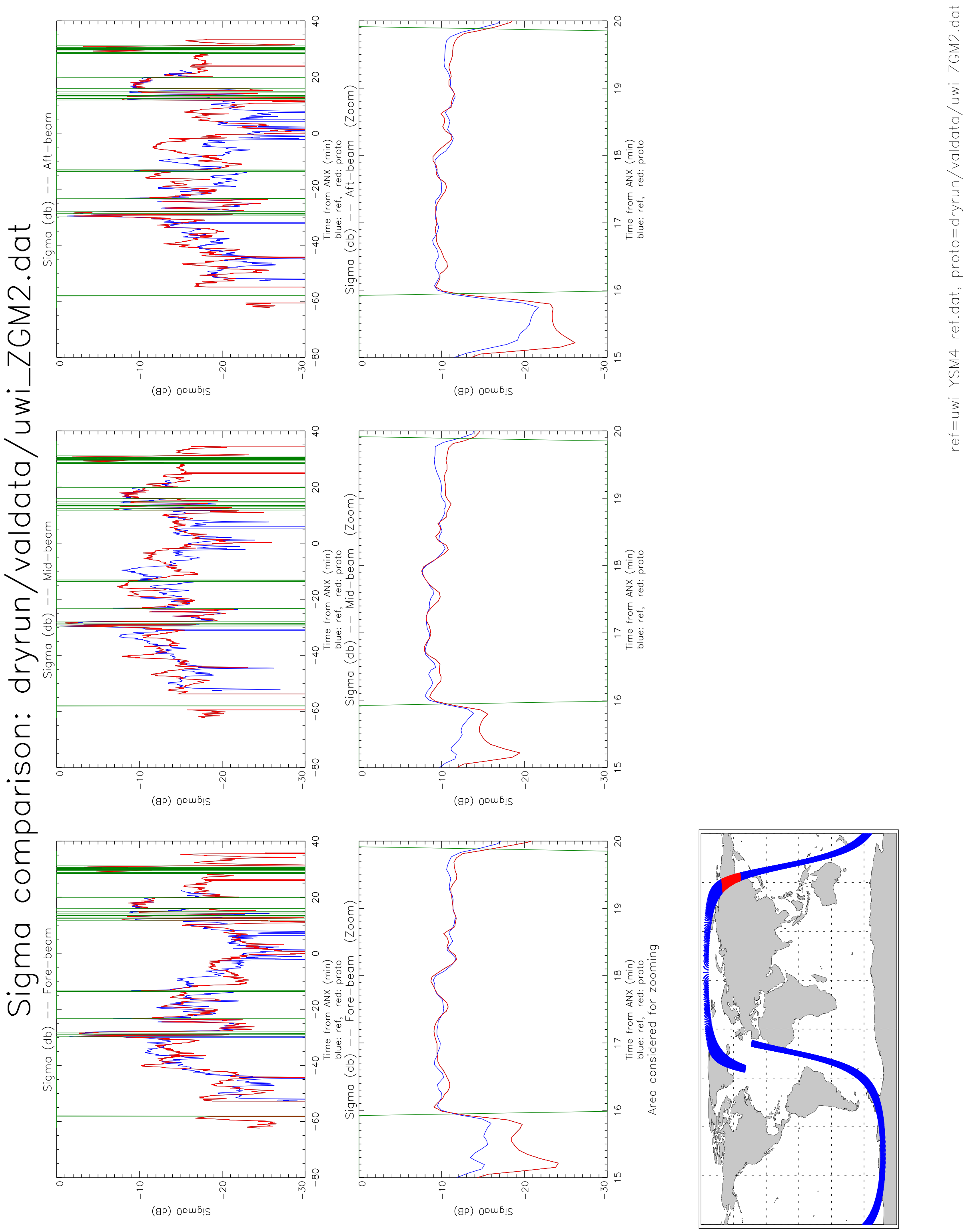


Figure E.11: Report for YSM4/ZGM2

### E.2.3 ZGM3

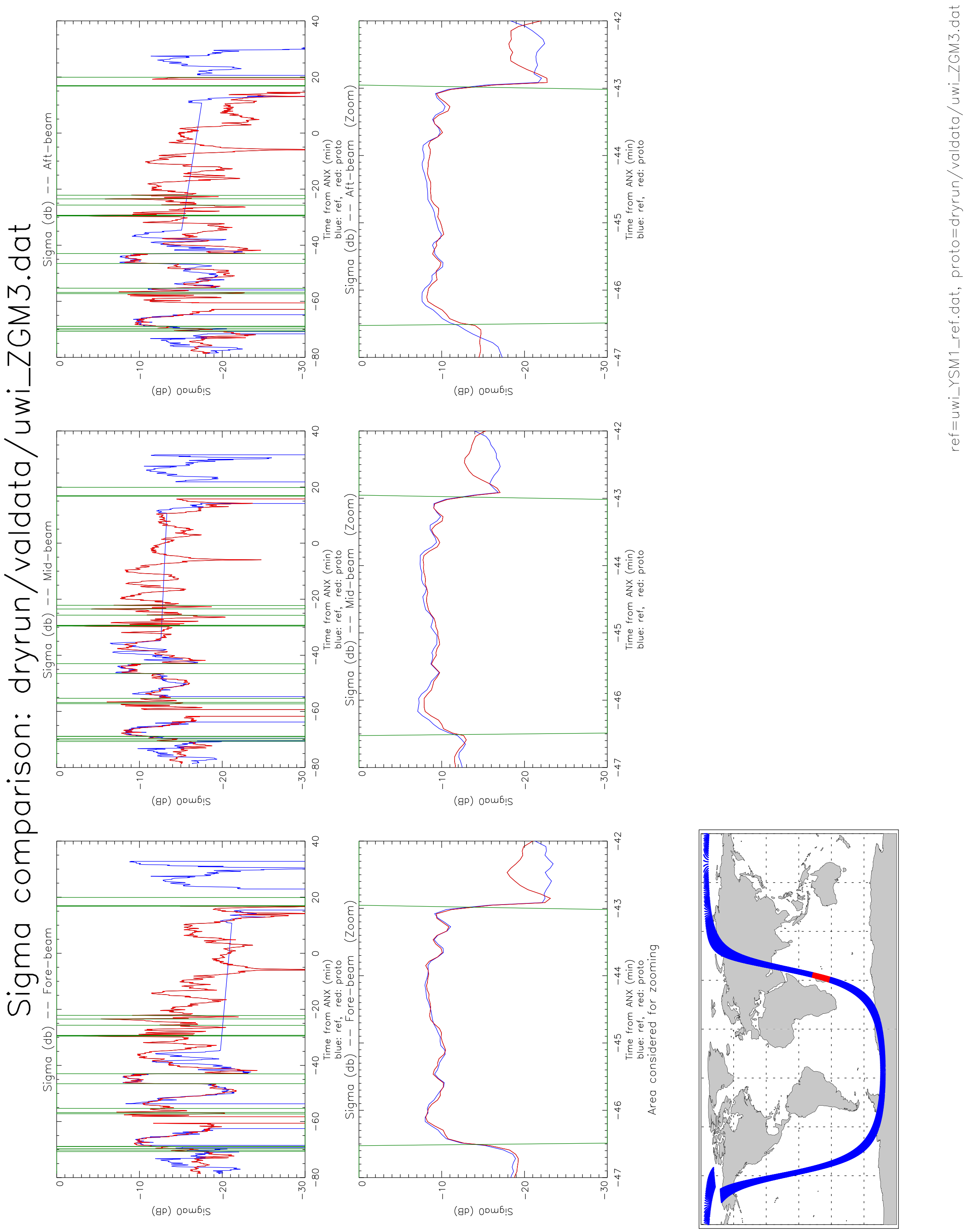


Figure E.12: Report for YSM1/ZGM3

### E.2.4 ZGM4

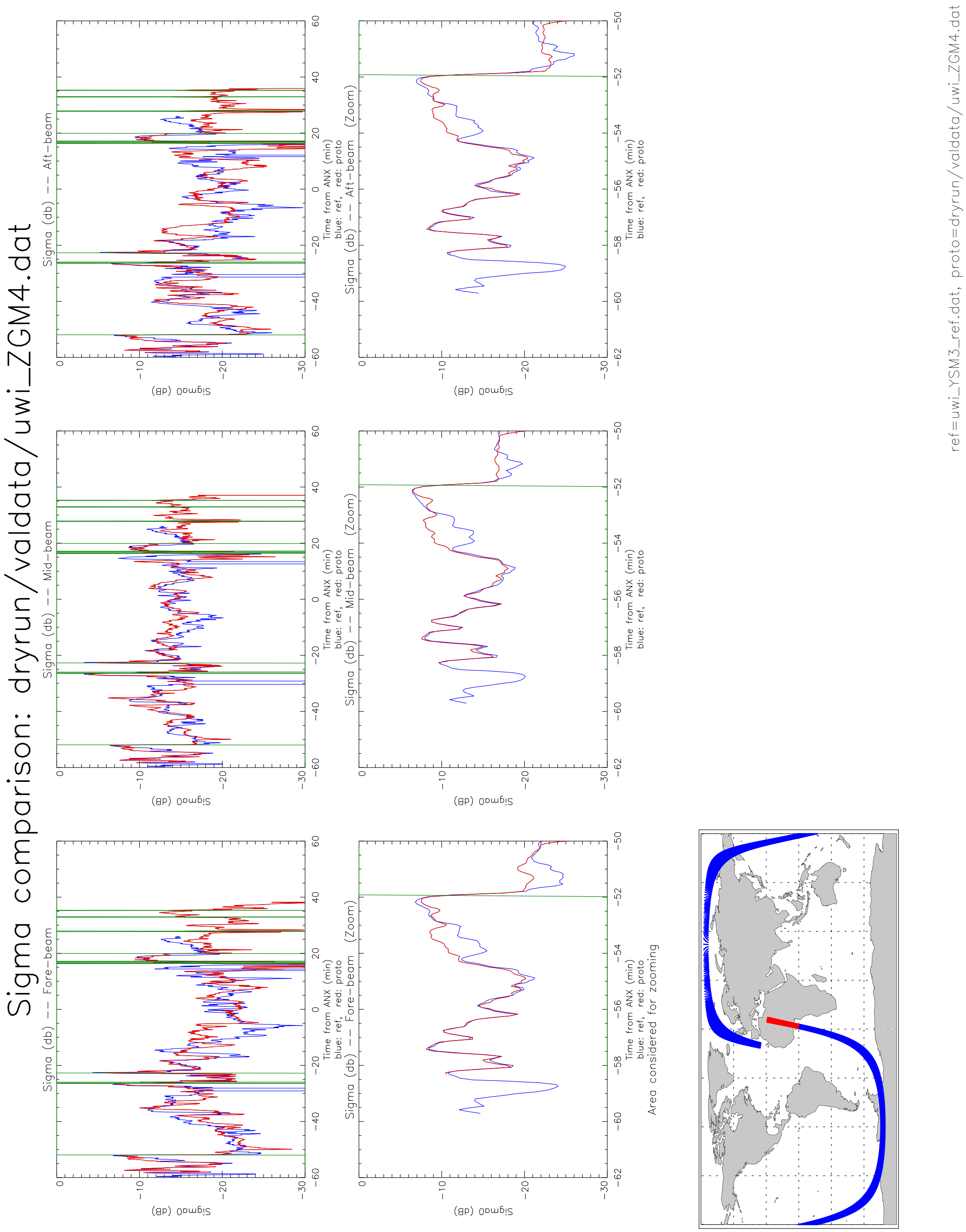


Figure E.13: Report for YSM3/ZGM4

### E.2.5 ZGM5

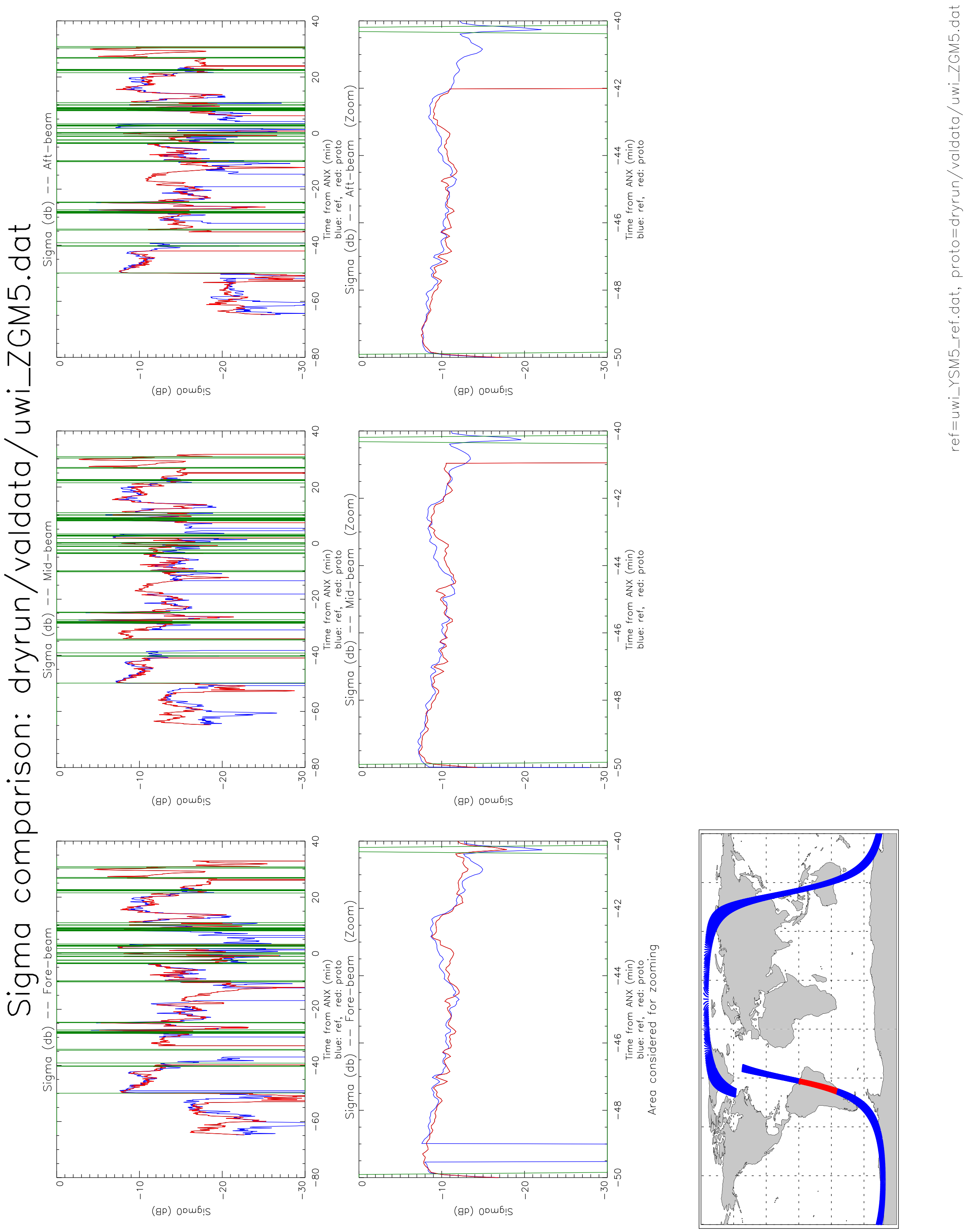


Figure E.14: Report for YSM5/ZGM5

### E.2.6 ZGM6

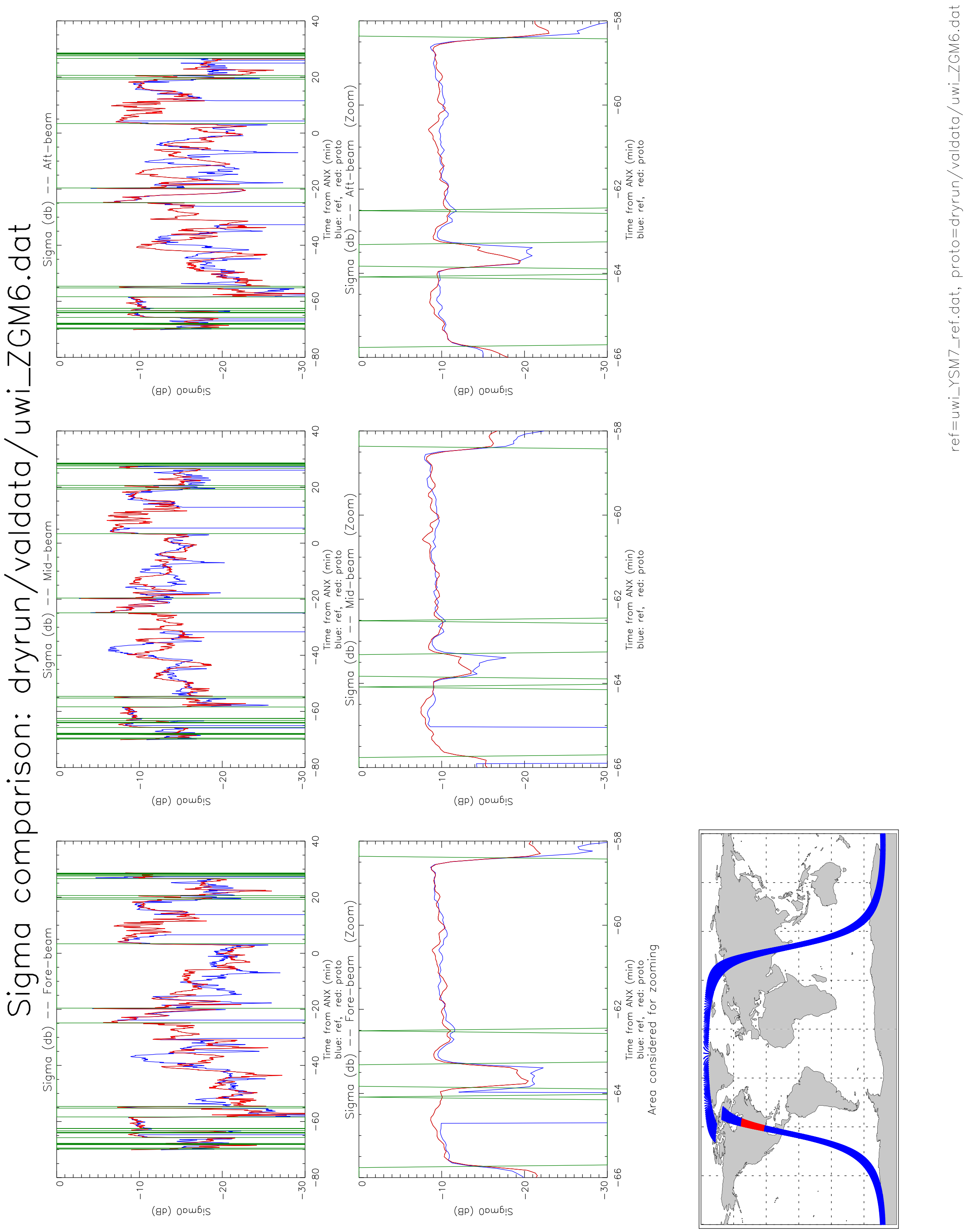


Figure E.15: Report for YSM7/ZGM6

## E.2.7 ZGM7

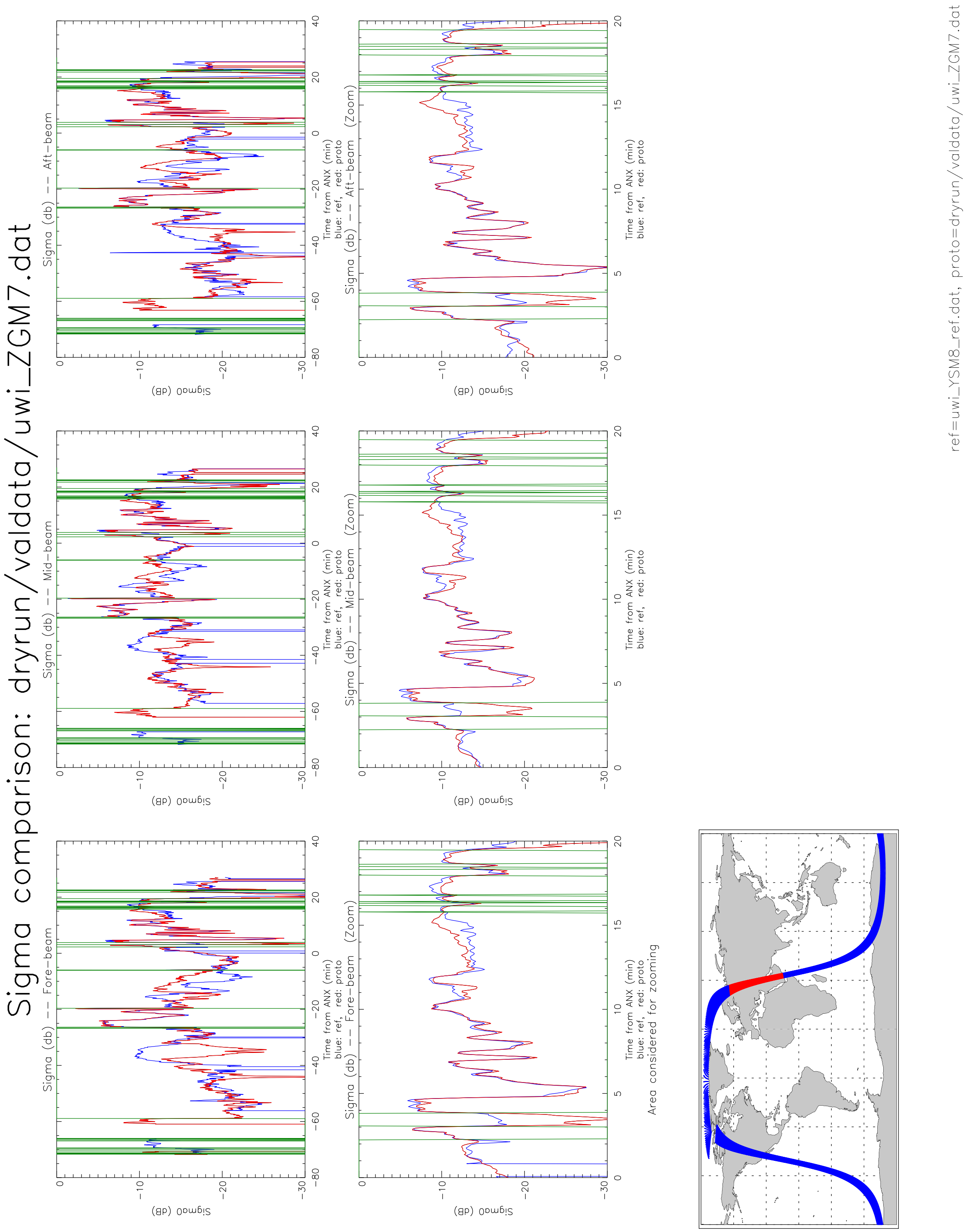


Figure E.16: Report for YSM8/ZGM7

### E.2.8 ZGM8

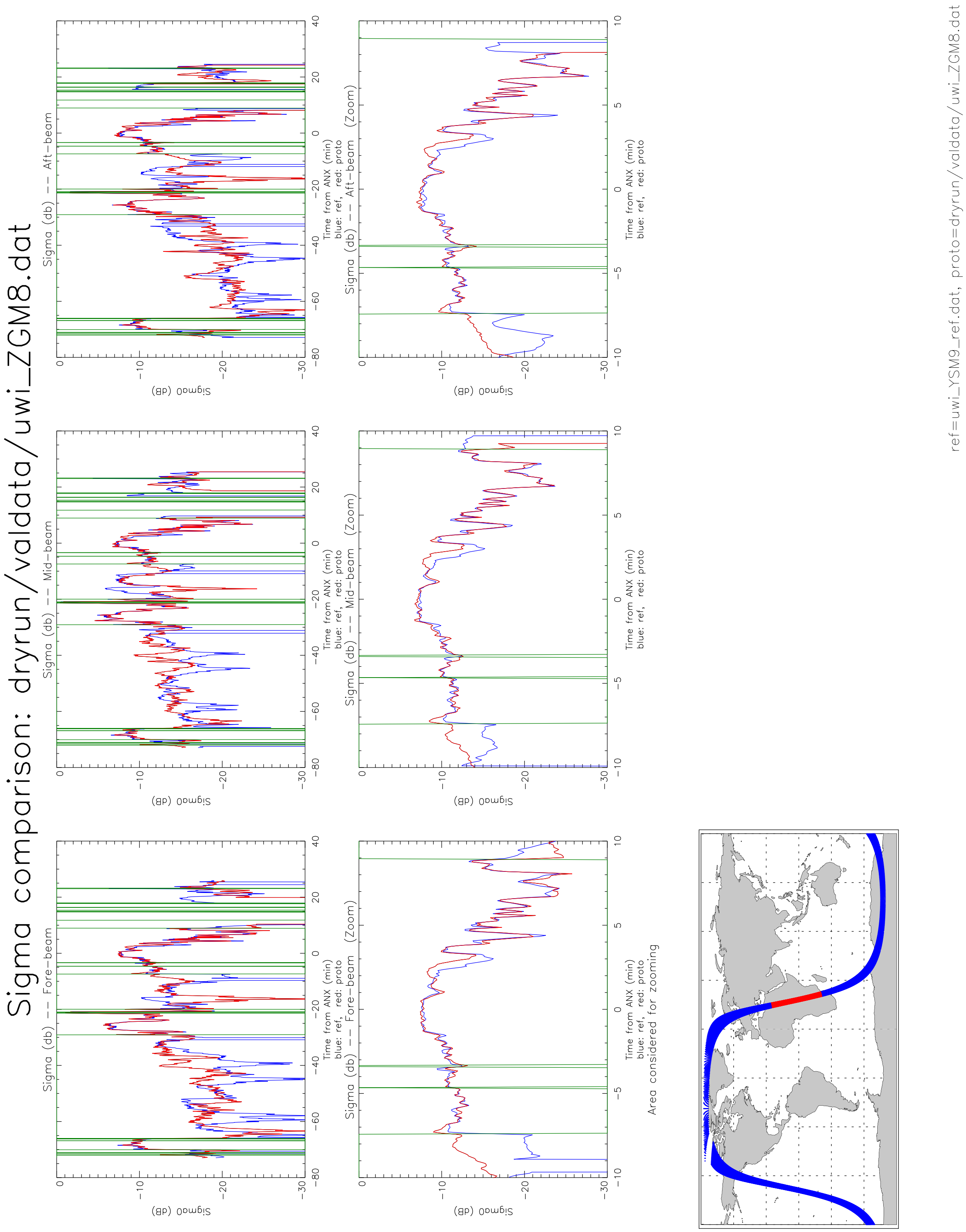


Figure E.17: Report for YSM9/ZGM8